Holism in plant biogeography - improving the representation of, and interactions between, the biosphere, hydrosphere, atmosphere and pedosphere

Dissertation

zur Erlangung des Doktorgrades

der Naturwissenschaften

vorgelegt beim Fachbereich 11 Geowissenschaften / Geographie

der Johann Wolfgang Goethe - Universität

in Frankfurt am Main

von

Liam Jude Langan

aus Dublin, Irland.

Frankfurt am Main (2018)

(D 30)

Vom Fachbereich Geowissenschaften / Geographie der
Johann Wolfgang Goethe-Universität als Dissertation angenommen.

Dekan:

Prof. Dr. Georg Rümpker
Johann Wolfgang Goethe-Universität
Institut für Geowissenschaftenen
Altenhöferallee 1
D-60438 Frankfurt am Main

Gutachter:

Dr. Simon Scheiter
Senckenberg Biodiversität und Klima Forschungszentrum
Senckenberganlage 25
D-60325 Frankfurt am Main

Prof. Dr. Steven Higgins
Universität Bayreuth
Lehrstuhl für Pflanzenökologie, Gebäude NW1
D-95440 Bayreuth

Datum der Disputation:

Summary

The overarching goal of the thesis was to create a holistic predictive framework, a vegetation model, by improving the representations of and interactions between the biosphere, hydrosphere, atmosphere and pedosphere. Vegetation models represent a crucial component of Earth system models since the properties of the land surface, via interactions with the atmosphere, can have extremely large climatic effects. Yet, there remains great uncertainty associated with the dynamics of the vegetated land surface. Various vegetation models have been critiqued for numerous reasons including overly simplistic representations of vegetation, prescribed vegetation, poor representations of diversity, inaccurate representations of competition, non-transparent model calibration, and poor responses to drought. The purpose of the creation of this "next generation" model was to address deficiencies common to current vegetation modelling paradigms.

The representation of the biosphere within this framework was improved via two separate development axes. First, ecological realism was improved by integrating concepts from community assembly theory, co-existence theory, and evolutionary theory. Explicitly, rather than defining teleonomic rules to define plant behaviour the process of natural selection is modelled. By modelling the process of natural selection and its effect on relative fitness, myriad "rules" which continually adapt to biotic and abiotic conditions "come out" as a consequence of the modelled dynamics rather than being "put in". In aDGVM2 (adaptive Dynamic Global Vegetation model 2) communities of plants and their trait values evolve through time, this evolution is constrained by trade-offs between traits. Poorly performing individuals are more likely to die and produce fewer copies of themselves, this results in a filtering of trait values. Further, the community and species' trait values can evolve through successive generations via reproduction, mutation and crossover which we approximate by using a genetic optimisation

algorithm. Thus, a plant community consisting of individuals and species with potentially novel and diverse trait values is assembled iteratively through time.

We tested the assertion that improved integration of concepts from community assembly, evolutionary, and co-existence theory could address limitations of DGVMs in Chapter 2. We demonstrated that such an approach does indeed allow diverse communities of plants to emerge from the modelling framework. We showed that the position of the emergent communities in trait space differed along abiotic gradients and that, in simulations where reproductive isolation was simulated, communities emerged which were composed of multiple co-existing clusters in trait-space. Simulated trait values of co-existing strategies emerging from aDGVM2 were often multimodal, indicative of the emergence of multiple life-history strategies.

Second, to successfully model how natural selection forms a community requires accurate representation of how resource availability affects fitness. In the majority of dynamic global vegetation models (DGVMs) there is no real representation of plant hydraulics with plant water availability being calculated as a simple function of relative soil moisture content and root fractions across a number of soil layers. Worryingly, a number of vegetation models appear to under represent the magnitude of these observed responses to drought. This deficiency was addressed in Chapter 3 by designing a simplified version of the cohesion tension theory of sapwood ascent where elements determining plant conductances are considered in series and a set of trait trade-offs were implemented which influence a plant's hydraulic strategy whereby hydraulic safety trades-off against xylem and leaf conductivity.

Interactions between the biosphere, pedosphere, and hydrosphere can also potentially mediate water resource availability and thus fitness. In the majority of DGVMs the volume of soil explored and explorable by plant roots is fixed globally and usually constrained to a depth not greater than 3m. However we know that soils can have a strong affect on vegetation distributions, that soil depth is not constant globally, and that plants root to variable depths.

In Chapter 4 I explored interactions between soil depth, plant rooting and the emergent properties of communities and highlighted the importance of considering interactions between the biosphere, hydrosphere, pedosphere, and fire across Amazonia. Here I demonstrated that, in addition to fire and precipitation, edaphic constraints on the volume of soil explorable by plant roots (e.g. by shallow soils, lateritic layers, anoxic conditions due to water logging, toxicity resulting from heavy metal concentrations) can affect the process of plant community assembly, alter the mean values of multiple traits in communities, and the trait diversity of communities in Amazonia. Further, such constraints can also alter the probability of a particular biome being simulated. That changes in the volume of soil explorable by plant roots alone can alter the probability of simulating a biome, the highest level of organisation used to categorise vegetation into distinct groups, by ca. 35% highlights the strong importance of considering the role of interactions between plants and edaphic conditions in mediating observed biome distributions. Additionally, this experiment also highlights the effect of allowing increased levels of diversity in this rooting depth on the evolution and assembly of plant communities. That is, given a fixed soil depth, higher diversity in rooting depth can also alter the probability of simulating a particular biome state and multiple, unlinked, emergent traits of plant communities

Chapter 5 represents the partial culmination of the vision detailed in Chapter 1.

Here I examine explicitly interactions between functional diversity, forest biomass storage, forest resilience to drought and climate change. The linkages between biodiversity and ecosystem services have broad global consequences for human well-being. Experimental work on non-woody (grassland) systems has shown that diversity can increase average plot biomass, biomass stability and buffer against ecosystem shocks. Evidence suggests that diversity can influence the rate at which tropical forest biomass accumulates, influence equilibrium tropical forest above ground biomass both positively and negatively, show no apparent signal, increase the modelled resistance of tropical forests to climate change, and influence ecosystem resilience to drought.

Examining whether aDGVM2, with its improved representation of plant hydraulics and soil hydrology, can mimic observed Amazonian tropical forest drought responses we set up a model experiment that mimics the through-fall exclusion experiments run at Tapajos (TNF) and Caxiuana (CAX) national forest sites which revealed that the model was able to reproduce well both the level and rate of biomass loss.

Investigating whether diversity affects biomass response to drought by conducting simulations initialised with different numbers of species showed that sites with lower species richness exhibited more dramatic reductions of biomass following drought, lower pre drought biomass, lower temporal stability in transpiration, and lower amounts of transpiration. Examining the components of functional diversity revealed that functional evenness increases with species richness, that high functional evenness can be associated with a more even distribution of the density with which trait-space is occupied, and that the functional trait composition of high species richness communities differs to that of low species richness communities in our simulations.

Exploration of vegetation development under the IPCC's RCP scenarios 4.5 & 8.5 where climate was forced both with and without CO_2 impacts on plants revealed that, in simulations where only climate forcing was applied, there was a reduction in total biomass stored across Amazonia. The effect of CO_2 fertilisation of plant growth has previously been shown to mitigate the risk of Amazon forest die-back, however, these results reveal that, with an improved representation of the biophysical interactions between CO_2, plant growth and plant responses to changes in water status, even with increasing CO_2 there are large areas of Amazonia where biomass may be reduced. Further, these climate change simulations also revealed that sites with higher functional evenness are more resistant to change and show a lower reduction in biomass. However, we only find significant positive diversity effects when CO_2 fertilises plant growth. The absence of CO_2 fertilised plant growth increases the water stress of plants caused by climate change and overrides any diversity bestowed resistance.

In conclusion, the results presented in this thesis suggests that an individual-based modelling approach that allows functional diversity to evolve within simulations is a plausible and powerful route to improve our capacity to predict how vegetation may shift as our climate changes. That a better understanding of the current distribution of vegetation can be achieved by considering the depth to which plants can and do root and plant hydraulics. That consideration of how constraints on plant rooting and plant hydraulics affect spatial and temporal water availability will further improve the accuracy with which we can predict how vegetation will respond to changing climates. Additionally, that functional diversity has the potential to mediate multiple ecosystem services and processes and can potentially improve the resilience ecosystems to change. Therefore the

conservation of functional diversity and diversity of ecological strategy is crucial. Further, we urgently need to improve our understand of how interactions between biochemical (CO_2 and nutrients) and biophysical (precipitation changes and plant water availability) processes affect plant dynamics as these play an overwhelming role in determining the future of ecosystems.

Zusammenfassung

Das übergeordnete Ziel der Arbeit war es, ganzheitliche, prognostizierbare Rahmenbedingungen für ein Vegetationsmodell zu entwerfen, welches durch eine verbesserte Darstellung von Biosphäre, Hydrosphäre, Atmosphäre und Pedosphäre, sowie deren Wechselwirkungen gekennzeichnet ist. Vegetationsmodelle stellen einen entscheidenden Bestandteil der Erdsystemmodelle dar, denn die Eigenschaften der Landoberfläche und deren Wechselwirkungen mit der Atmosphäre können extreme klimatische Auswirkungen haben. Dennoch bleibt eine Unsicherheit bezüglich der Dynamik der bewachsenen Landoberfläche. Verschiedene Vegetationsmodelle wurden aus unterschiedlichen Gründen kritisiert, unter anderem wegen einer zu vereinfachten Darstellung der Vegetation, einer vorgegebenen Vegetationszusammensetzung, einer schlechten Darstellung der Diversität, einer ungenauen Darstellung des Wettbewerbs, einer intransparenten Modellkalibrierung sowie einer schlechten Reaktion auf Dürre. Die übergeordnete Absicht dieses Modelles der "nächsten Generation" war es, die oben genannten Mängel zu beheben, welche für die gegenwärtigen Vegetationsmodelle typisch sind.

Die Darstellung der Biosphäre wurde im Rahmen dieser Arbeit durch zwei getrennte Entwicklungsachsen verbessert. Erstens wurde der realistische Charakter der Ökologie durch die Integration von Konzepten aus der Artengemeinschafts Entstehungstheorie, der Koexistenztheorie, sowie der Evolutionstheorie verbessert. Anstatt teleonome Regeln zur Definition des Pflanzenverhaltens zu definieren, wird explizit der Prozess der natürlichen Selektion modelliert. Durch die Modellierung des natürlichen Selektionsprozesses und seiner Auswirkungen auf die relative Fitness werden unzählige „Regeln“ „generiert“, die sich ständig an biotische und abiotische Bedingungen anpassen, allerdings als eine Folge der modellierten Dynamik, anstatt vorher „absichtlich“ eingebracht zu werden. In

aDGVM2 (adaptive Dynamic Global Vegetation Model 2) entwickeln sich Pflanzengemeinschaften und ihre Merkmalsausprägungen im Laufe der Zeit. Diese Entwicklung wird durch die Austauschbeziehung zwischen den Merkmalen eingeschränkt. So sterben leistungsunfähige Individuen eher früher und produzieren weniger Nachkommen, was zu einer Filterung der Merkmalsausprägungen führt. Darüber hinaus können sich die Merkmalsausprägungen der Gemeinschaft und der Arten durch Fortpflanzung, Mutation und Crossover über nachfolgende Generationen entwickeln. Dies wiederum approximieren wir mit Hilfe eines genetischen Optimierungsalgorithmus. So wird eine Pflanzengemeinschaft, die aus Individuen und Arten mit potenziell neuen und unterschiedlichen Merkmalsausprägungen besteht, iterativ im Laufe der Zeit aufgebaut.

Wir überprüften die Behauptung, dass eine verbesserte Integration von Konzepten aus der Artengemeinschafts Enstehungstheorie, der Evolutionstheorie und der Koexistenztheorie die Mängel der DGVMs in Kapitel 2 aushebeln könnte. Wir haben gezeigt, dass ein solcher Ansatz unterschiedliche Pflanzengemeinschaften hervorbringt. Wir zeigten weiterhin, dass die Lage der entstandenen Gemeinschaften im Merkmalsraum entlang abiotischer Gradienten unterschiedlich war, und dass in Simulationen, in denen reproduktive Isolation simuliert wurde, Gemeinschaften entstanden, die aus mehreren nebeneinander koexistierenden Clustern im Merkmalsraum bestanden. Simulierte Merkmalsausprägungen koexistierender Strategien, die aus aDGVM2 hervorgehen, waren oft multimodal, was auf die Entstehung mehrerer Lebenszyklusstrategien hinweist.

Zweitens, um erfolgreich modellieren zu können, wie sich natürliche Selektion in einer Gemeinschaft entwickelt, bedarf es einer genauen Darstellung, wie sich

die Ressourcenverfügbarkeit auf die Fitness auswirkt. In den meisten dynamischen globalen Vegetationsmodellen (DGVMs) gibt es keine wirkliche Darstellung der hydraulischen Eigenschaften von Pflanzen (Pflanzenhydraulik), wobei das pflanzenverfügbare Wasser als einfache Funktion der relativen Bodenfeuchte und der Wurzelverteilung über eine Reihe von Bodenschichten berechnet wird. Besorgniserregend ist hierbei, dass eine Reihe von Vegetationsmodellen das Ausmaß dieser beobachteten Reaktionen auf Dürren zu unterschätzen scheinen. Mit dieser Unzulänglichkeit befasst sich Kapitel 3, indem eine vereinfachte Version der Kohäsionstheorie der Wasserleitung entworfen wurde. Hierbei werden Elemente, die die Pflanzenleitfähigkeit bestimmen, in Serie betrachtet, und eine Reihe von Austauschbeziehungen zwischen Merkmale implementiert, die die hydraulische Strategie einer Pflanze beeinflussen, wobei die hydrologische Leitfähigkeit der Kavitationsbeständigkeit gegenübersteht.

Wechselwirkungen zwischen Biosphäre, Pedosphäre und Hydrosphäre können auch die Verfügbarkeit von Wasserressourcen beeinflussen und damit die Fitness. In der Mehrheit der DGVMs ist das Volumen des von Pflanzen durchwurzelten und durchwurzelbaren Bodens global festgelegt und in der Regel auf eine Tiefe von nicht mehr als 3 m begrenzt. Wir wissen jedoch, dass Böden einen starken Einfluss auf die Vegetationsverteilung haben können, dass weiterhin die Bodentiefe global nicht konstant ist, sowie dass verschiedene Pflanzen unterschiedlich tief wurzeln.

In Kapitel 4 untersuchte ich in Amazonien die Wechselwirkungen zwischen Bodentiefe, Wurzelbildung und den entstehenden Eigenschaften von

Gemeinschaften und betonte die Bedeutung der Berücksichtigung von Wechselwirkungen zwischen Biosphäre, Hydrosphäre, Pedosphäre und Feuerauswirkungen. Hier habe ich gezeigt, dass neben Feuer und Niederschlag auch edaphische Einschränkungen des durchwurzelbaren Bodens (z.B. Mächtigkeit des Bodens, verhärtete Schichte wie etwa lateritische Schichten, anoxische Bedingungen durch Wasserabschluss oder Toxizität durch hohe Schwermetallkonzentrationen) die Zusammensetzung von Pflanzengemeinschaften beeinflussen und die Mittelwerte mehrerer Merkmale in Gemeinschaften sowie die Merkmalsvielfalt von Gemeinschaften verändern können. Darüber hinaus können diese Einschränkungen die Wahrscheinlichkeit verändern, dass ein bestimmtes Biom simuliert wird. Die Tatsache, dass Veränderungen im Volumen des von Pflanzen durchwurzelbaren Bodens für sich, die Wahrscheinlichkeit der Simulation eines Bioms um ca. 35% ändert, unterstreicht die große Bedeutung der Berücksichtigung der Rolle von Wechselwirkungen zwischen Pflanzen und edaphischen Bedingungen bei der Vermittlung der beobachteten Biomverteilungen. Hierbei sind Biome die höchste Organisationsebene mit der die Vegetation in verschiedene Gruppen eingeteilt wird ist. Darüber hinaus hebt dieses Experiment auch den Effekt hervor, der sich aus der zunehmenden Vielfalt der Durchwurzelungstiefe auf die Entwicklung und Zusammenstellung von Pflanzengemeinschaften ergibt. Das bedeutet, bei einer festen Bodentiefe kann eine höhere Vielfalt der Durchwurzelungstiefe auch die Wahrscheinlichkeit verändern, das ein Biomzustand, mit mehreren, nicht verknüpft auftretenden Merkmalen von Pflanzengemeinschaften simuliert wird.

Kapitel 5 stellt einen Höhepunkt der in Kapitel 1 beschriebenen Vision dar. Hier untersuchte ich explizit die Wechselwirkungen zwischen funktionaler Vielfalt, Speicherung von Biomasse in Wäldern, sowie die Widerstandsfähigkeit der

Wälder gegenüber Dürre und Klimawandel. Die Verflechtungen zwischen Biodiversität und Ökosystemleistungen haben weitreichende globale Auswirkungen auf das menschliche Wohlbefinden. Experimentelle Arbeiten an nicht holzigen (Grünland-)Systemen haben gezeigt, dass Vielfalt die durchschnittliche Biomasse, die Stabilität der Biomasse und den Puffer gegenüber Ökosystemschocks erhöhen kann. Es gibt Belege dafür, dass Vielfalt die Akkumulationsrate der Tropenwaldbiomasse beeinflussen kann, sowie das Gleichgewicht der oberirdischen Biomasse positiv als auch negativ bzw. nicht sichtbar beeinflussen kann, weiterhin wird die modellierte Widerstandsfähigkeit der Tropenwälder gegenüber dem Klimawandel erhöht, sowie die Resilienz des Ökosystems gegenüber Dürren beeinflusst.

Bei der Untersuchung, ob das aDGVM2 mit seiner verbesserten Darstellung der Pflanzenhydraulik und Bodenhydrologie beobachtete Dürrereaktionen in tropischen Wäldern nachbilden kann, haben wir einen Modellversuch durchgeführt, der die Dürreexperimente an den brasilianischen Nationalparkstandorten Tapajos (TNF) und Caxiuana (CAX) simuliert. Das Modell war in der Lage, sowohl das Niveau als auch die Rate des Biomasseverlustes gut nachzubilden.

Bei der simulierten Untersuchung, die mit unterschiedlichen Artenzahlen durchgeführt wurde, und überprüfen sollte, ob Vielfalt die Reaktion der Biomasse auf Dürren beeinflusst, zeigten sich folgende Ergebnisse. Standorte mit geringerem Artenreichtum zeigten geringere Biomasse vor der Dürre, verloren nach einer Dürre mehr Biomasse, wiesen geringere zeitliche Stabilität bei der Transpiration auf, und zeigten geringere Transpirationsraten. Die Untersuchung der Komponenten der funktionalen Vielfalt ergab, dass erstens die funktionale Gleichmäßigkeit mit dem Artenreichtum zunimmt, zweitens eine hohe

funktionale Gleichmäßigkeit mit einer gleichmäßigeren Verteilung der Dichte verbunden sein kann mit der der Merkmalsraum besetzt ist, und das sich drittens die funktionale Merkmalszusammensetzung von Gemeinschaften mit hohem Artenreichtum von denen mit niedrigem Artenreichtum in unseren Simulationen unterscheidet.

Die Erforschung der Vegetationsentwicklung im Rahmen der RCP-Szenarien 4.5 & 8.5 des IPCC, in denen das Klima sowohl mit als auch ohne CO_2-Einflüsse auf die Pflanzen simuliert wurde, ergab, dass in Simulationen, in denen nur Klimaveränderungen angewendet wurde, die gesamte in Amazonien gespeicherte Biomasse reduziert wurde. In Studien anderer Autoren hat der Effekt der CO_2-Düngung auf das Pflanzenwachstum eine Verringerung des Risikos eines Rückgangs des Amazonaswaldes gezeigt. Meine Ergebnisse zeigen jedoch, dass bei einer verbesserten Darstellung der biophysikalischen Wechselwirkungen zwischen CO_2, Pflanzenwachstum und Pflanzenreaktionen auf Veränderungen des Wasserzustands, selbst bei zunehmender CO_2 Konzentration, in großen Teilen Amazoniens Biomasse reduziert wird. Darüber hinaus haben meine Simulationen auch gezeigt, dass Standorte mit einer höheren funktionalen Gleichmäßigkeit resistenter gegen Veränderungen sind und eine geringere Reduktion der Biomasse aufweisen. Signifikant positive Diversitätseffekte finden wir jedoch nur, wenn CO_2 das Pflanzenwachstum düngt. Das Fehlen von CO_2-gedüngtem Pflanzenwachstum erhöht den durch den Klimawandel verursachten Wasserstress der Pflanzen und setzt jeder Vielfalt entgegen.

Zusammenfassend lässt sich sagen, dass die Ergebnisse, die in dieser Arbeit vorgestellt werden, darauf hindeuten, dass ein individuen-basierter Modellierungsansatz, der es ermöglicht, dass funktionale Vielfalt sich innerhalb

der Simulationen entwickelt, ein plausibler und wirkungsvoller Weg ist, um unsere Fähigkeit zu verbessern Vorhersagen darüber zu treffen, wie sich unsere Vegetation unter einem sich wandelnden Klima verändern kann. Ein besseres Verständnis der aktuellen Vegetationsverteilung kann erreicht werden, indem der Pflanzenhydraulik Beachtung geschenkt wird und die tatsächliche Tiefe berücksichtigt wird, in die Pflanzen wurzeln können bzw. auch tatsächlich wurzeln. Wenn berücksichtigt wird, wie Einschränkungen der Durchwurzelung und der Pflanzenhydraulik die räumliche und zeitliche Wasserverfügbarkeit beeinflussen, wird die Genauigkeit, mit der wir vorhersagen können, wie die Vegetation auf sich ändernde Klimabedingungen reagieren wird, weiter verbessert. Darüber hinaus hat funktionale Vielfalt das Potenzial, mehrere Ökosystemdienstleistungen und -prozesse zu vermitteln und ist in der Lage die Widerstandsfähigkeit der Ökosysteme gegenüber Veränderungen potenziell zu verbessern. Daher ist die Erhaltung der funktionalen Vielfalt und der Vielfalt der ökologischen Strategie von entscheidender Bedeutung. Darüber hinaus müssen wir dringend unser Verständnis verbessern, wie sich biochemische (CO_2 und Nährstoffe) und biophysikalische (Niederschlagsänderungen und Verfügbarkeit von Pflanzenwasser) Prozesse auf die Pflanzendynamik auswirken, da sie eine erhebliche Rolle bei der Gestaltung der Zukunft von Ökosystemen spielen.

Acknowledgements

Dear anybody that should be acknowledged, I have run out of time to write this section properly. I am hopeful you understand.

To my parents Frances and Liam. My learning at home is what has prepared me for academia, not the countless years of school or university. I still spend my time looking out the windows, but, now I get paid for it.

To my girls, Carolin, Polly, and Mimi. Carolin, you have thought me soil science, expanded massively my thinking about the world, and been amazingly understanding of the process of preparing a thesis. I could not wish for a better partner! To all three of you collectively, you have changed my life. While science is still of utmost importance to me, your presence in my life has caused me to step back and reassess the truly important things in life. Your presence in my life has made it blatantly apparent that science, as wonderful as it is, is not the cornerstone of my life, of life in general. That is you.

Polly and Carolin, thanks for the help with the hydraulics figure in Chapter 3. Mimi, you'll get your chance. I can't wait!

To my brother John, you have been my greatest competitor and best counterpart. Growing up with you has prepared me well for the world outside. Our intellectual paths will cross again soon!

To my sister Jane. Dear my little sister Jane. How are you doing? What are you at? Do you like the tree in Chapter 3? There is a bird in the background that I don't think anyone noticed, I snuck it in.. Polly drew the apples on the tree, I don't think anyone noticed that either. Do you wanna build a snowman? Wha' unkie Ger and Pat doin'? Are you doing your work? Are you a Pat How?

To Thomas and Matt. You have been fantastic friends to me through the years. More than that, I have enjoyed and appreciated immensely the scientific exchange we have had. Your thoughts and opinions percolate throughout the words I have written in this thesis.

Finally, to Simon and Steve. You have shown utmost patience with me. Between you both you have thought me modelling and ecology, but, most importantly for me, you have always afforded me the opportunity to explore my own scientific interests. Thank you.

To those I do not mention specifically. I have greatly appreciated your friendship and discourse through the years. As soon as I submit this thing I'll be taking AphukenbBrakE.

Contents

List of Figures

List of Tables

Chapter 1

Introduction

1.1 Predictive plant biogeograpy - dynamic global vegetation models

To understand why the vegetation of the Earth is distributed as it is is the central tenet plant biogeography. To get to such a high level of understanding (Krebs, 2014) requires ecological understanding, i.e. understanding the interactions between individuals in a system, the physical environment, interactions between biological and physical processes, and flows of energy (Odum, 1953). Much theory and many hypotheses have been developed to explain vegetation distributions and ecological patterns and processes, yet, these theories and hypothesis are often unconnected. To quote Krebs (2014) more or less as quoted by Grime (2012), "It is not always easy to see where the pieces fit in ecology, and we will encounter many isolated parts of ecology that are well developed theoretically but are not clearly connected to anything else". To my mind ecology and thus biogeography are missing a unified framework through which theory and hypothesis can be connected. A strange state of affairs given that ecology is supposed to be the

holistic study of the entire system (Odum, 1953; Higgins, 2017). Making such a unified framework predictive would allow the utility of theories and hypothesis to explain some desired phenomena to be assessed (Shipley, 2010), allow a level of objective assessment of how well we understand a system, and importantly, allow prediction of how systems may change (Higgins, 2017). To quote Feynman "What I cannot create, I do not understand" (Hawking, 2001). The best candidate construct within which one could embed such a unified framework is, in my opinion, a vegetation model.

In its simplest form, a vegetation model requires the following components:

1. Input data to provide the abiotic environment and thus a measure of resource available and constraints on plant growth.

2. Rules which define how the birth, growth and death of a plant are governed.

The input data component (e.g. CO_2 concentration, temperature, incoming solar radiation, precipitation, etc.) is provided by Earth system scientists, physicists and meteorologists. The rules which define how the birth, growth and death of a plant is governed by interactions between the abiotic environment, properties intrinsic to a plant and competition between plants are a formalisation, in computer code, of hypotheses associated with the dynamics of the system. Any model code which affects the birth, growth, or death of a plant in a population is a hypothesis, some are explicitly stated (Scheiter & Higgins, 2007), others are convenient constructs used my modellers to approximate complex processes (Fisher *et al.*, 2018). The utility of such models lies not only in their ability to test hypotheses, they can also be used as a tool to generate new hypotheses. Further, they represent a crucial component of earth system models since the properties of the land

surface, via interactions with the atmosphere (e.g. albedo, fire and evapotranspiration), can have extremely large climatic effects (Flato *et al.*, 2013). Yet, there there remains great uncertainty associated with the dynamics of the vegetated land surface. For example, the representation of the land surface scheme within early earth system models has been criticised as being over simplistic whereby vegetation was often prescribed rather than simulated (Flato *et al.*, 2013). More advanced earth system models now employ dynamic global vegetation models (DGVMs) to simulate vegetation dynamics which use ecophysiological principles to model the distribution of plant functional types (PFTs) (Prentice *et al.*, 2007). However, while the use of ecophysiological principles allows for more accurate process representation, there still exists many areas of mismatch between observed and simulated vegetation patterns. For example, many vegetation models fail to predict the distribution and often the presence of the cerrado biome in Brazil (Langan *et al.*, 2017). Such a failure to re-create reality can have multiple causes, e.g. inherent uncertainty in historical and contemporary climate input (Slingo & Palmer, 2011), uncertainty in initial vegetation state (Moncrieff, 2014), or incorrect hypotheses coded into a modelling framework which govern vegetation dynamics. If we are to improve our understanding of the broad drivers of past, present and future vegetation patterns and thus allow for more realistic representations of the interactions between the land surface and other components of the earth system it is imperative that we address such uncertainties associated with DGVMs. This thesis documents the iterative progress we have made in addressing a number of these shortcomings with the current DGVM paradigm.

1.1.1 The representation of diversity within DGVMs

A potentially large shortcoming of PFT based DGVMs is the depauperate way in which plant diversity is represented. The linkages between biodiversity and ecosystem services have broad global consequences for human well-being (Perrings *et al.*, 2011). Experimental work on non-woody (grassland) systems has shown that diversity can increase average plot biomass, biomass stability and buffer against ecosystem shocks (Tilman *et al.*, 1997, 2006; Isbell *et al.*, 2015). Evidence suggests that diversity can influence the rate at which tropical forest biomass accumulates (Huang *et al.*, 2018), influence equilibrium tropical forest above ground biomass both positively and negatively (Poorter *et al.*, 2015), show no apparent signal (Finegan *et al.*, 2015), and increase the modelled resistance of tropical forests to climate change (Sakschewski *et al.*, 2016). Additionally, the functional trait composition of communities has recently been shown to influence ecosystem resilience to drought whereby higher diversity of traits associated with plant hydraulics increases resilience (Anderegg *et al.*, 2018). Evidence is accumulating that diversity, particularly functional diversity, can have real and significant effects on the properties and processes operating in ecosystems and affect the trajectory with which they respond to changes in abiotic conditions. Unfortunately our ability to represent such diversity in vegetation models and explore in greater depth such diversity effects lags dramatically behind our current state of knowledge.

1.1.2 Selecting for performance - the driver of community assembly, adaptive evolution and plant functional diversity distributions

I believe it perhaps useful at this point for the reader and of general relevance to the development of any model which aims to represent natural dynamics, to address here the importance of natural selection. It is surprisingly difficult to find a succinct definition of natural selection. Varying texts refer to it as a process, law, theorem or principal. Its definition is often lumped together with evolution. However, to quote Fischer (1930) "Natural selection is not evolution", although it certainly drives adaptive evolution. The best definition of natural selection I can summon requires paraphrasing both Vincent & Brown (2005) and Shipley (2010): natural selection is an iterative optimisation process whereby "anything" which performs better than other "things" in meeting some criteria or rules increases more in relative abundance than "things" which perform less well. The "things" optimised need not be natural (Shipley, 2010). Within the natural domain this relatively better performance is relative fitness.

Natural selection is the driver of the processes of adaptive evolution and community assembly. For evolution via natural selection to operate the following conditions are requisite (Stearns & Hoekstra, 2000):

1. Individuals must have traits.
2. There must be variability in trait values.
3. Trait values must affect individual fitness.
4. Trait values must be heritable.

A trait can be defined as any characteristic of an organism which is heritable (Garnier *et al.*, 2015). Individual fitness is the number of offspring an individual produces during its lifetime. Relative fitness between individuals is the number of offspring produced by one individual relative to the number produced by another. Traits which affect components of individual fitness, i.e. the growth, reproduction or mortality of an individual, are referred to as functional traits (Garnier *et al.*, 2015). Evolution via natural selection happens when the functional trait values possessed by individuals result in relatively different fitnesses and this differential fitness changes the relative frequency with which the values of functional traits are expressed. Evolution can be deemed to have happened at different scales. A change in the relative frequency of the values of a functional trait within a single species could be classified as evolution of the species. Changes in the relative frequency of the values of a functional trait within a community could be classified as evolution of the community. Within the the field of community ecology, community assembly theory aims to predict the relative abundance of species within a community, given any particular set of abiotic conditions. Functional traits have been incorporated into community assembly theory whereby the performance of a species within a community is estimated based on the values of the functional traits it possesses which ultimately determine its relative abundance (Shipley, 2010). I currently do not appear to possess the intellectual capacity to discern the difference between the evolution of a community and the process of community assembly. Natural selection drives both via increased fitness of individuals which possess trait values which perform relatively better. Both lead to a community of individuals, a community that possesses trait values at differing frequencies. Irrespective of my failing to understand this difference, it is clear that natural selection drives both adaptive evolution and the process of

community assembly.

Taking this definition of natural selection as an iterative optimisation algorithm makes it apparent that the majority of DGVMs employ some form of natural selection. How one however defines or calculates fitness can have repercussions for the trajectory natural selection will take a system of competing "things". Indeed, Smith *et al.* (2001) presents two model versions which represent relative recruitment rates (relative fitness) of different PFTs between time-steps in different ways. The first being based on the proportion of total ground cover a PFT occupies while the second considers the amount of carbon allocated to reproduction. Since ground cover of a PFT is a function of net primary productivity (NPP) as well as PFT specific plant traits (specific leaf area), higher NPP increases relative fitness making NPP the fitness criterion. The second implementation considers more directly allocation to reproduction however all PFTs allocate a constant 10% of NPP to reproductive biomass. Since allocation to reproduction is constant, higher NPP again increases fitness. The utility of such implementations to successfully represent successional dynamics under varying abiotic conditions and disturbance regimes has been demonstrated (Hickler *et al.*, 2004). However, modelling approaches which fail to make some component of accumulated reproductive biomass (seeds or the biomass value itself) the fitness criterion and do not allow differential allocation to reproduction forgo the opportunity to investigate how fundamental trade-offs between the partitioning of available growth between plant compartments such as those responsible for improved resource acquisition, storage of acquired resources and reproduction result in the diverse set of plant life history strategies we see in the world around us (Wenk & Falster, 2015), how such trade-offs may affect successional dynamics and the process of plant community assembly (Huston & Smith, 1987; Bond & Keeley, 2005; Scheiter

et al., 2013), and lead to the co-existence of diverse sets of plant life history strategies (Falster *et al.*, 2017). Further, any teleonomic rules applied to model living organisms which choose to maximise anything other than fitness may produce the correct answer but not by virtue of the accuracy of the rules derived and applied in general, rather, the chosen rule coincides with how natural selection has shaped multiple trait values into "ecological strategies" across the fitness landscape. Such approaches often choose rules which maximise life span, reproductive output, or, as is almost exclusively the case in DGVMs, to maximise growth rate (Lacointe, 2000). However, the use of such rules is limited for a number of reasons. Trade-offs between traits and the presence of multiple limiting resources may allow that many ecological strategies are capable of producing equal fitness (Tilman & Pacala, 1993; Falster *et al.*, 2017). Thus, to model a diverse community, each functional strategy would require its own rule. To derive one rule for particular abiotic conditions, while attractive, is tantamount to assuming that evolution is universally convergent and that evolutionary and abiotic history plays no role (Moncrieff *et al.*, 2014*a*). Fitness is relative, thus, any rule to represent a functional strategy is dependent on the other functional strategies present in a community. Addition or removal of functional strategies, the frequency of addition or removal as well as the order with which functional strategies are added or removed are often highly dependent on chance events (Shipley, 2010) and can all potentially change the "rules" of the game. Paramaterising such rules would be impossible.

There are however simple rules I believe to be the universal, or to borrow from mathematical terminology, invariant, which govern the formation of any natural community which I formulate in terms of traits:

1. Natural selection operates on all traits of the individual.

2. The summed benefits and costs of particular trait values across all traits determines individual fitness.

3. Differential relative fitness through generations forms communities.

By modelling the process of natural selection and its affect on relative fitness, myriad "rules" which continually adapt to biotic and abiotic conditions "come out" as a consequence of the modelled dynamics rather then being "put in". We adopt this approach with aDGVM2 whereby the community of plants and their trait values evolve through time, this evolution is constrained by trade-offs between traits. Poorly performing individuals are more likely to die and produce fewer copies of themselves, this results in a filtering of trait values. Further, the community and species' trait values can evolve through successive generations via reproduction, mutation and crossover which we approximate by using a genetic optimisation algorithm. Thus, a plant community consisting of individuals and species with potentially novel and diverse trait values is assembled iteratively through time.

1.1.3 On the linkages between the biosphere, hydrosphere and pedosphere

To successfully model how natural selection forms a community depends not only on the choice of fitness measure but also on the ability to accurately represent how resource availability affects fitness. Any parametrisation chosen to represent plant resource uptake is effectively a hypothesis about how the process works. Often such hypotheses within DGVMs are not explicitly tested and while they may provide reasonable approximations of reality under some circumstances, their application to others can lead to incorrect results. An example

of such a hypothesis relates to the way water availability is calculated in the vast majority of DGVMs. Commonly individual water availability is calculated based on the fraction of roots in a particular soil layer, e.g. Scheiter & Higgins (2009). Testing this approach with aDGVM2, where traits control the allocation of growth between roots, leaves, stems, storage and reproductive tissues, lead to the surprising result that the fittest allocation strategy was one which minimised allocation to roots. Since water availability of an individual is dependent only on the placement of roots within the soil profile rather than both the placement of roots and the mass available to do the work of transporting water there is only a cost to allocating carbon to roots, no benefit, and thus natural selection correctly assembles communities which minimised allocation to roots. The emergent "optimum" allocation strategy when the function of root mass is ignored is the one closest to zero. Further, natural selection will always assemble a community which minimises allocation to roots irrespective of the amount of water available as a resource, thus, such an implementation is incapable of simulating observed root to shoot ratios across resource gradients when applied within aDGVM2 (Mokany *et al.*, 2006).

During the course of my research it became apparent that, while the trait based modelling approach developed in chapters 2 and 3 certainly represented an improvement in the way models represent functional trait variation, competition, and thus the biosphere. This was not a panacea which allowed us to accurately model the distribution of plant traits, biomes, biomass, tree cover, etc.. Something, or some things were blatantly missing. Two candidate solutions presented themselves as being most relevant.

First, as highlighted above, in the majority of DGVMs there is no real representation of plant hydraulics with plant water availability being calculated as a simple function of relative soil moisture content and root fractions across a number of

soil layers. Experiments where precipitation has been artificiality reduced to examine the response of tropical forests to drought have demonstrated dramatic reductions in tree biomass with the highest mortality rates exhibited by large trees (Nepstad *et al.*, 2007; da Costa *et al.*, 2010). Worryingly, a number vegetation models appear to under represent the magnitude of these observed responses to drought (Galbraith *et al.*, 2010; Powell *et al.*, 2013). However, progress at understanding drought induced vegetation responses in vegetation models is improving rapidly (see McDowell *et al.*, 2013*a*). To meet this challenge and avoid the logically flawed method above we implemented a simplified version of the cohesion tension theory adopted by Sperry *et al.* (1998) where elements determining plant conductances are considered in series and implement a set of trait trade-offs which influence a plant's hydraulic strategy whereby hydraulic safety trades-off against xylem and leaf conductivity (Markesteijn *et al.*, 2011). This implementation makes root mass functional by allowing that the conductances of the soil-root and root compartments be modified by root biomass (Hickler *et al.*, 2006). Further, by considering more explicitly the interface between the soil and root we can simulate more accurately how interactions between water and the physical properties of the soil affect overall plant performance (Sperry *et al.*, 2016) and thus allow for an improved representation of the interface between the biosphere, hydrosphere and pedosphere.

Second, the modelled dynamics of resource amount through space and time must be as accurate as possible. A further component of plant water availability is the soil volume available to hold water from which a plant can then extract it. In the majority of DGVMs this volume is typically constrained by a assuming a soil depth not greater than 3m (Ostle *et al.*, 2009). This is just one example of a representation of plant-soil interactions this is at odds with pedological and plant

ecological knowledge, knowledge we have possessed since before DGVMs were ever conceived. Indeed, Darwin (1972) refers repeatedly throughout his book to the effect both climate and soils can have on selection strength. Walter (1986) begins his book by introducing the dual importance of soils and climate in mediating vegetation distributions. We know that soil depth is not constant globally and can be much greater than the 2-3m assumed by modellers (Walter & Breckle, 1986). We further know that plants root to variable depths which can exceed 60m (Kleidon & Heimann, 1998; Schenk & Jackson, 2002*a*). Such discrepancies between observed and modelled soil and rooting depths can have implications for plant water availability and the exchange of moisture between the land surface and atmosphere (Ostle *et al.*, 2009; Kleidon & Heimann, 1998).

It would be folly to assume that vegetation model developers and users are unaware or ignore the importance of soil properties in mediating vegetation distributions, carbon storage (both above and below ground) and fluxes between the atmosphere and the land surface. Rather, two constraints have and continue to limit an improved representation of plant-soil interactions. The first is a data limitation since models require such data as input. Yet, although the spatial sampling of soil depth data is improving rapidly, returned depths in global data-sets are typically not deeper than 3.5 meters (Batjes, 2009), far short of observed soil or plant rooting depths (Walter & Breckle, 1986; Schenk & Jackson, 2002*a*). While such data may not accurately represent the maximum soil depths available for plant root exploration it would however give enough information to highlight areas where vegetation models currently assume deeper soil than observed.

This leads us to a second constraint on improving plant-soil interactions in DGVMs. As highlighted above and elaborated on in Chapter 2, standard DGVMs require paramaterisation. That is, to deviate from standard rooting depths would

require that the root profile distribution for each plant functional type (PFT), at each new possible rooting depth, under varying precipitation regimes be re-paramaterised. In contrast, because of the representation of the process of community assembly via natural selection within aDGVM2, a plant population evolves iteratively whereby plants with below ground traits which allow better overall performance enjoy higher reproductive success and pass more seeds into future generations. This feature of aDGVM2 essentially allows us to forgoe the difficult task of model paramaterisation and test theory in novel ways. Chapter 4 takes advantage of this novel feature to explore how interactions between climate, fire and the soil depth available to plant roots affect biome and trait distributions across Amazonia.

Ecology is the study of the interactions between all individuals in a system, the physical environment, interactions between biological and physical processes and the flows of energy between spheres (Odum, 1953). To accurately model the biosphere requires more than an improved representation of biological processes, it is crucial to also improve the representations of and interactions between the atmosphere, hydrosphere, pedosphere and biosphere. Chapter 2 of this thesis addresses some limitations of contemporary DGVMs, particularly those associated with the biosphere and demonstrates how one can move beyond the limited representation of diversity in DGVMs.

Chapter 3 is a technical description of aDGVM2, the realisation of the goal of building such in model from Chapter 2. Within this description however lies the brunt of the work done during this thesis. There would be no thesis without a working model. Chapter 3 documents all model components which address inadequacies in the representation of diversity, presents novel solutions to represent light competition, address conceptual flaws such as the commonly

adopted method to calculate water availability, details the improved representation of the interaction between the hydrosphere and pedosphere via the inclusion of percolation of water through the soil and the improved representation of plant hydraulics and plant interactions with the atmosphere, hydrosphere and pedosphere. Much of the work done building this model has not resulted in publications and will be forever subsumed into Chapter 3, I however view the production of a working model as the most important output of this thesis, an output which has been and will continue to be used to understand the world beyond the scope of the chapters contained herein.

Chapter 4 represents the first application of the model detailed in Chapter 3 and demonstrates how such a modelling approach, which effectively parametrises itself, can be used to explore interactions between soil depth, plant rooting and the emergent properties of communities. It thus highlights the importance of considering interactions between the biosphere, hydrosphere, pedosphere, and fire. It however falls short of highlighting the interactions between diversity and ecosystem properties and processes.

Chapter 5 represents the partial culmination of the vision detailed in Chapter 1. Here we examine explicitly interactions between functional diversity, forest biomass storage, forest resilience to drought and climate change. In so doing it deepens our understanding of the role that functional diversity can play in mediating ecosystem processes and properties. It further demonstrates that improvements in the representation of and linkages between the biosphere, hydrosphere, atmosphere and pedosphere can indeed allow us to better "create" and thus "understand" the distribution of vegetation we see around us.

1.2 Aims

The aims of this thesis can be summarised as follows:

1. The aim of Chapter 2 was to review deficiencies in vegetation modelling, derive a modelling road-map through which such deficiencies could be addressed, and demonstrate the initial potential of such a modelling approach.

2. Chapter 3 documents the realisation of the road-map set out in Chapter 2. It is a technical description of the product developed during my work which has provided the tool to perform the simulations in the subsequent chapters presented here and has already been used to successfully publish a further three papers.

3. The aim of Chapter 4 was to highlight the importance of considering plant hydraulics and interactions between plant traits, biomass, biome distributions and the pedosphere.

4. The aim of Chapter 5 was to investigate interactions between functional trait diversity, drought, ecosystem properties and climate change.

1.3 Overview

Chapter 1 gives a general overview of the current state of vegetation modelling and highlights the necessity to improve the way we represent multiple components of such models in order to achieve a more holistic representation of the vegetated land surface.

Chapter 2 discusses in detail deficiencies associated with current DGVM paradigms, develops a road-map towards a new modelling approach through

which such deficiencies can be addressed and demonstrates the initial potential of such an approach.

Chapter 3 is a technical description and realisation of the new modelling approach premièred in Chapter 2 but extended to include new sub-modules which describe soil hydrology, plant hydraulics, and grass architecture.

Chapter 4 demonstrates the application of this new modelling approach and highlights the additional importance of considering both plant hydraulics and soil properties.

Chapter 5 examines the relationships between functional trait diversity, ecosystem stability and resilience, and climate change.

Chapter 6 synthesises the findings of the previous chapters and provides suggestions for further ways in which DGVMs could be improved.

Chapter 2

Next generation dynamic global vegetation models: learning from community ecology

Simon Scheiter, Liam Langan and Steven I. Higgins * †

2.1 Introduction

A grand challenge in plant ecology is to understand how climate and vegetation interact to define the past, current and future distribution of vegetation. In principle, this challenge could be addressed by modelling the rate at which individual plants grow, reproduce and die and how these rates are influenced by the plant's traits and the abiotic and biotic environment. A variety of conceptual constructs and associated research programs have been developed and used to address this

*This chapter is published in the journal *New Phytologist* as 'Scheiter *et al.* (2013) Next generation dynamic global vegetation models: learning from community ecology'

†Author contributions: S.S. and S.H. wrote the manuscript and designed the study with contributions from L.L.. S.S. conducted simulations and analysed simulation results with contributions from L.L.. L.L. conceived the addition of reproductive isolation which was coded by S.S..

challenge. One of these research programs is the DGVM (Prentice *et al.*, 2007) program, while another is community ecology (Keddy, 1992; Weiher & Keddy, 1995*a*,*b*; Shipley *et al.*, 2006).

DGVMs use ecophysiological principles to model the distribution of plant functional types (Prentice *et al.*, 2007). DGVMs are motivated by two quite different goals. First, these are models for articulating and developing our understanding of the factors that influence past, current and future distribution of vegetation at regional to global scales (Prentice *et al.*, 2007). Second, DGVMs have been developed to serve as a component of earth system models, that is, they provide a dynamic representation of the land-surface energy budget and an accounting system for components of global carbon and water budgets (Bonan, 2008).

DGVMs have been used successfully to address a range of questions in applied and theoretical ecology. For example, DGVMs showed that large areas of the world would be forested in the absence of fire (Bond & Keeley, 2005) and that the absence of angiosperms would dramatically reduce the area covered by evergreen forests because high transpiration rates of angiosperms promote local precipitation which in turn maintains rainforests (Boyce & Lee, 2010). As DGVMs only require climate and soil data to run simulations, they allow us to simulate past and future vegetation. For example, Scheiter *et al.* (2012) explored the role of fire for C_4 grass expansion in the late Miocene, Prentice *et al.* (2011) investigated how vegetation cover and carbon stocks changed after the last ice age and Kuemmerle *et al.* (2012) modelled the potential habitat of the European bison during the Holocene. A large number of studies have used DGVMs to explore the impacts of climate change on the carbon cycle and biome patterns (e.g. Cramer *et al.* (2001)) and models have recently been extended to investigate how landuse influences the carbon cycle (Bondeau *et al.*, 2007). DGVMs have been linked with

general circulation models (GCMs) to create fully coupled biosphere-atmosphere models. Such fully coupled models are important tools for the analysis of both the impacts of climate on vegetation and how these changes in vegetation cover influence climate via changes in albedo, leaf area index and water fluxes (Raddatz *et al.*, 2007; Brovkin *et al.*, 2009). Despite the fact that DGVMs have allowed vegetation ecologists and earth system scientists to address a range of important questions, the applicability of DGVMs is limited by two major weaknesses. The first relates to how these models use plant functional types (PFTs) to represent vegetation. DGVMs typically use a small set of plant attributes to define a limited number of static plant functional types. The second common weakness is that DGVMs poorly represent competition (Fisher *et al.*, 2010; Quillet *et al.*, 2010) essentially because competition is modelled at the PFT level and not at the individual plant level (Clark *et al.*, 2010, 2011*a*). Both weaknesses cast doubt on the ability of DGVMs to model how changes in climate might force switches in vegetation structure.

These deficiencies of the DGVM approach are, in turn, the explicit focus of community ecology (Keddy, 1992; Weiher & Keddy, 1995*b*,*a*) and coexistence theory (Chesson, 2000). Community assembly models aim at understanding how properties of plants, often referred to as functional traits, influence the assembly of plant communities at a site. The community assembly program involves two intimately linked activities (Weiher & Keddy, 1995*a*). First, a minimum set of traits that can be used to predict the composition of an ecological community at a site is identified (Keddy, 1992). Second, the series of environmental filters that act on these traits to determine the community assembly process is identified. For example, Valk (1981) found that life span, propagule longevity and propagule

establishment were traits that determined how flooding (the environmental filter) determines which species may establish in a wetland. A weakness of this approach is that it generally describes observed vegetation patterns by using statistical models (regression models, statistical mechanics models or Bayesian multilevel models) rather than process-based, mechanistic models (Webb *et al.*, 2010; Gotzenberger *et al.*, 2012).

Coexistence theory, aims to explain community structure using heuristic models and empirical analyses (Warner & Chesson, 1985; Tilman, 1988; Chesson, 2000; Clark *et al.*, 2010). Such models describe the mechanisms that allow coexistence of species by focusing on niche differentiation, trade-offs between plant traits and storage effects. However, coexistence theory still struggles to explain the paradox of high diversity (Hutchinson, 1961), an issue which Clark, in a series of studies, suggests can be resolved by considering individual level variation and trade-offs in a high-dimensional trait space (Clark *et al.*, 2004, 2010).

The aim of this paper is to review deficiencies in the DGVM program and to provide a viewpoint on how DGVMs need to be improved to address these deficiencies. We articulate this viewpoint by first describing a conceptual scheme of how next generation DGVMs could be structured. We then describe our implementation of such a DGVM and provide examples of model behaviour that highlight how this new model differs from the current generation of DGVMs. We conclude by discussing how this approach could foster more intimate collaboration between dynamic global vegetation modellers and the broader community of ecologists and evolutionary biologists.

2.2 Description

2.2.1 Deficiencies of DGVM Modelling

1. Hidden calibration of plant functional types

DGVMs model the behaviour of plant functional types (PFTs). Plant functional types provide a means to use a finite set of parameters to aggregate traits of individual plants with similar ecological behaviour (Diaz & Cabido, 1997; Lavorel *et al.*, 1997; Kattge *et al.*, 2011). These parameters should aggregate several sources of variability in these traits, including between individual variation, between population variation due to local adaptation, between species variability as well as variability due to the statistical uncertainty associated with measuring and estimating these parameters. In practise many of these sources of variability are not quantified in DGVMs and most models define PFTs using point estimates of parameters that describe plant traits (Prentice *et al.*, 2007). Such an aggregation implies a loss of information and obscures aspects of plant behaviour and variation in behaviour that is known to influence the likelihood of coexistence (Clark *et al.*, 2011*b*). An additional concern is that the parameter value used in a model to describe a trait is often not a maximum likelihood estimate of the parameter, but rather a permissible value and modellers tend to choose (whether consciously or sub-consciously) a permissible value that enhances model performance. Hence, trait values are often hidden model tuning parameters and simulation results may well be biased by this hidden calibration process. Furthermore, trait values are generally selected such that models perform well for ambient environmental conditions simply because most benchmarking data sets are derived from ambient conditions. However, this assumes that trait values

used to parametrise PFTs were valid under past environmental conditions and will still be valid under future conditions (Clark & Gelfand, 2006).

To illustrate some of these parametrisation issues we ran the aDGVM (Scheiter & Higgins, 2009) where (1) each individual tree had the same point estimates for traits and (2) values of four selected traits were drawn from normal distributions with means defined by the point estimates and standard deviations covering a feasible range of values (Fig. 2.1). As one would expect there is more variability between the output of replicate simulations when using variable traits, but more significant is that there is a systematic bias where variable trait simulations project higher mean biomasses than fixed trait simulations (Fig. 2.1). The latter effect is because, by selecting a range of trait combinations one increases the chance that trait combinations that allow individuals to grow larger and produce more biomass are simulated. Fisher *et al.* (2010) used a similar approach to explore model uncertainties in the JULES-ED model. They conducted a sensitivity analysis where five model parameters related to demography and competition were selected by using a Latin Hypercube exploration of the trait space. This study showed that simulated biomass for different parameter combinations was highly variable under ambient conditions and variability in biomass projections increased further in forward projections. While the practise of using permissible parameter estimates for defining plant functional types in DGVMs might have been understandable in the past, we now have excellent databases (e.g. TRY database, Kattge *et al.* (2011)) that allow us to generate more objective estimates of trait values and methods to inversely parametrise DGVMs by using these trait databases as prior information (Hartig *et al.*, 2012).

A special case of hidden calibration of DGVMs relates to bioclimatic limits (Haxeltine and Prentice, 1996)(Haxeltine & Prentice, 1996). Many DGVMs use bioclimatic limits to constrain the range of environmental conditions where modelled PFTs can grow (e.g. BIOME3, Haxeltine & Prentice (1996) or LPJ, Sitch *et al.* (2003)). Bioclimatic limits are based on empirically observed limits of PFTs, however, these empirical rules have no formal physiological basis. For example, Sitch *et al.* (2003) assumes that the minimum coldest-month temperature for survival of the tropical herbaceous PFT (C_4 photosynthesis) and the maximum coldest-month temperature for establishment of temperate herbaceous PFT (C_3 photosynthesis) occurs at 15.5 °C. However, these threshold temperatures are influenced by the CO_2 concentration (Ehleringer *et al.*, 1997). Similarly, a cold tolerance limit might be due to a failure of vegetative growth or the failure of a reproductive process (Bykova *et al.*, 2012). The lack of explicit physiological justifications for the bioclimatic limits in many DGVMs means that bioclimatic limits are in effect calibration parameters that force PFTs to grow in the "correct" climate region. Ideally these bioclimatic limits should be explicitly linked to physiological processes or removed from DGVMs.

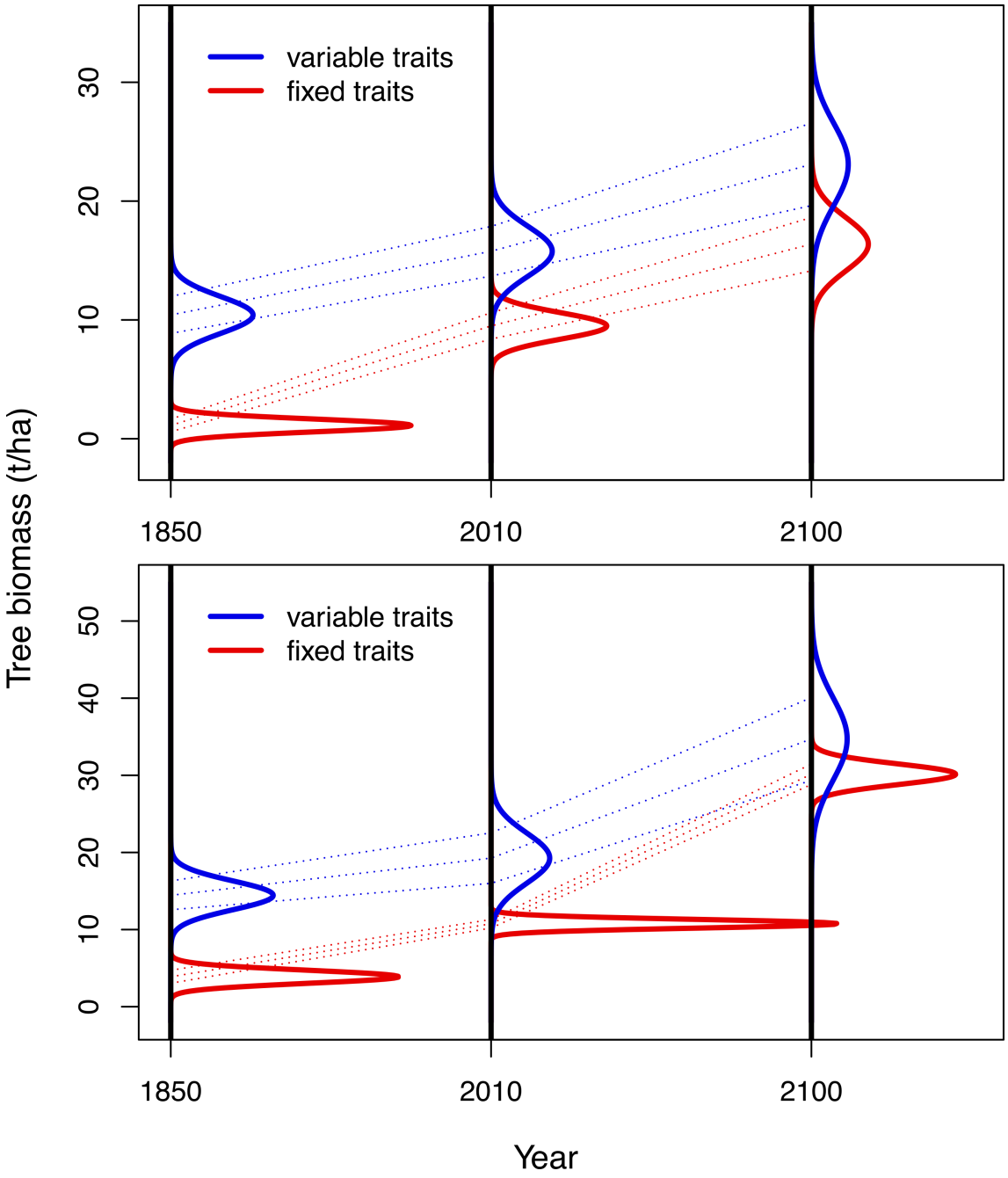

FIGURE 2.1: Sensitivity analysis of tree biomass to fixed traits or randomly selected traits in the aDGVM (Scheiter & Higgins, 2009) for two savanna study sites in South Africa. 'Fixed traits' indicates that the four traits SLA, light extinction in canopy, canopy radius to tree height ratio and carbon allocation to stem biomass are constant and equal for all trees whereas 'variable traits' indicates that trait values were selected randomly for each tree. Mean and standard deviations are 10 +/- 3.2 for SLA, 0.37 +/- 0.13 for light extinction in canopy and 0.37 +/- 0.13 for canopy radius to tree height ratio. Carbon allocation to stem biomass was increased or decreased by a random number between 0 and 0.3, therefore carbon allocation to root biomass was decreased or increased by the same amount. The mean values were used for the 'fixed trait' simulations. Density distributions were generated by 100 replicate simulations.

2. Depauperate functional diversity

A second problem associated with the parametrisation of functional types relates to the question of how many species or what level of functional diversity do we need to sustain ecosystem function, both in real ecosystems (Hooper *et al.*, 2005, 2012) and in modelled ecosystems. An illustrative example of this issue is the Amazon dieback phenomenon. Cox *et al.* (2004) projected a collapse of the Amazon rainforests under future climate conditions due to anticipated decreases in precipitation. These simulations project a widespread loss of the 'broadleaved evergreen tree' PFT and its replacement by C_4 grasses and bare soil (Cox *et al.*, 2004). These changes imply a transition from the forest biome to savanna and grassland biomes. Repeating Cox et al. 2004's simulation experiments with different DGVMs showed that the magnitude of dieback is sensitive to the model used (Huntingford *et al.*, 2008; Sitch *et al.*, 2008; Galbraith *et al.*, 2010) suggesting that the simulated collapse might be an artefact of the fact that rainforests are typically represented by a single PFT (e.g. 'broadleaved evergreen tree') in DGVMs. More specifically, Galbraith *et al.* (2010) found that much of this variability can be attributed to differences in temperature sensitivity in different models and Poulter *et al.* (2010) highlights the importance of parameters describing vegetation dynamics such as establishment rates or rooting depth. In reality one might expect that phenotypic plasticity, local adaptation and shifts in the tree community structure, for instance shifts to more drought-tolerant forest tree types, may buffer the impacts of decreasing precipitation and thereby avoid a catastrophic dieback of the Amazon rainforest. Such compositional shifts have been reported for tropical forests in Ghana, where long-term drought increased the abundance of drought-tolerant deciduous trees and these changes were associated with increases in the total biomass stocks (Fauset *et al.*, 2012). Analogously, increasing

functional diversity in DGVMs by increasing the number of PFTs and increasing trait diversity by allowing trait values of vegetation to be dynamic may avoid a modelled collapse of the Amazon.

3. Competition

Competition does influence a variety of ecological processes that have consequences for community assembly and the distribution of biomes. For example, Clark *et al.* (2011*a*), in an analysis of temperate forest species show that the effects of competition on growth rates and mortality risk exceed the effects of climate, while Bond & Midgley (2012) argue that the atmospheric CO_2 concentration determines the outcome of grass and tree competition in subtropical regions, and thereby the continental scale distribution of savanna, forest and grassland biomes (Higgins & Scheiter, 2012). DGVMs differ considerably in how they represent competition between functional types. One approach, often used to simulate competition for space, is to assume that the best performing PFT is able to occupy open space and ultimately dominate the vegetation stand. Such models often use net primary productivity as a measure of performance (e.g. BIOME3, Haxeltine & Prentice (1996)) and the outcome is typically that one PFT dominates. When modelling competition more explicitly there are two broad approaches that have been adopted in DGVMs. One approach is to use Lotka-Volterra type differential equation models where competition coefficients are used to describe competition between functional types. This approach has been adopted for instance by TRIFFID (Cox, 2001), JSBACH (Raddatz *et al.*, 2007) and CTEM (Arora & Boer, 2006). The disadvantage of this approach is that the number of competition parameters increases as a square of the number of PFTs. Moreover such competition coefficients do not describe the mechanism of competition but rather the aggregated

outcome of competitive interactions. This makes them a poor choice for projecting how competitive hierarchies might change in novel ecological settings, for instance under conditions of elevated CO_2. Additionally, such competition coefficients are difficult to directly measure in field experiments and inverse model parametrisation techniques are required (Freckleton & Watkinson, 2000; Higgins *et al.*, 2010).

An alternative is to model the impact of each individual plant or each PFT on the resource pool which, in turn, influences the growth of other individual plants or PFTs. For example, many DGVMs use a bucket model for soil hydrology (e.g. the aDGVM, Scheiter and Higgins 2009, LPJ, Sitch et al. 2003, LPJ-GUESS, Smith et al. 2001). In such models, each PFT extracts water from the bucket based on the PFTs rooting depth, transpirational demand, drought tolerance and soil water availability. The water extracted by each PFT influences the water available to other PFTs and thereby ensures that only PFTs adapted to the local site conditions persist. In such models the focus is therefore on modelling the ecosystem engineering and ecosystem modulating impacts of plants on their environment which feeds back to influence the performance of competitors (Jones *et al.*, 1994; Linder *et al.*, 2012). A further advantage of modelling competition via the resource pool is that, in contrast to Lotka-Volterra models, the number of parameters increases linearly with the number of PFTs. Competition models of this kind are also consistent with the aims of earth system modellers, which are in part interested in the engineering and modulating effects of vegetation on the climate system (e.g. Boyce and Lee, 2010) and how the effects feed back and influence the conditions that determine vegetation distribution (Cox *et al.*, 2000; Brovkin *et al.*, 2009). Modelling competition as an engineering feedback additionally provides a

natural way to model priority effects, for instance the successional shifts in temperate forest (Hickler *et al.*, 2012) or that forests are fire excluding ecosystems that prevent the invasion of C_4-grasslands and savannas (Higgins & Scheiter, 2012; Scheiter *et al.*, 2012).

4. Phylogenetic biome conservatism

A poorly understood, but potentially far-reaching limitation of current DGVMs is that they assume that convergent evolution is pervasive. Specifically, DGVMs assume that the same climate in different phylogenetic contexts will yield the same evolutionary responses, and that these evolutionary responses are manifest in the traits that define the plant functional types. This convergence assumption is now being questioned by several lines of evidence. For instance, savannas are convergent in structure, yet how climate and fire interact differs between continents with the consequence that each continents' savannas are expected to respond qualitatively differently to climate change (Lehmann *et al.*, 2014). A similar example comes from grasslands, where Buis *et al.* (2009) showed that compositional differences in the forb communities of South Africa and North America ensured that forb above ground net primary productivity responded differently to environmental drivers in these two regions. Interestingly the above ground net primary productivity of the grasses did in this study respond similarly to environmental drivers. More directly, Banin *et al.* (2012) have shown that the architecture of the worlds tropical forests differ from one another not only due to bioclimatic factors, but also due to a continent effect, which is a proxy for evolutionary history.

Such phylogenetic niche conservatism has been demonstrated at local and regional scales (Losos *et al.*, 2003; Ackerly *et al.*, 2006; Silvertown *et al.*, 2006). A

more recent study of more than 11,000 plant species from across the Southern Hemisphere suggests that phylogenetic biome conservatism is widespread. This study found that only 3.6% of speciation events involved daughter species being associated with a new biome, suggesting that many lineages have a limited capacity to adapt to new biomes. These findings imply that the assembly of biomes is highly constrained by the phylogenetic history (Crisp *et al.*, 2009). A counter example suggests that conservatism is not pervasive. Simon *et al.* (2009) found that most of the fire-adapted lineages of the Cerrado have sister lineages in fire-free forests ecosystems suggesting that the assembly of the Cerrado biome involved the convergent evolution of fire-adapted trees from several different tropical forest tree lineages rather than dispersal of fire-adapted lineages. Crisp *et al.* (2009)'s synthesis and the contradictory results of Simon *et al.* (2009) suggest that we still have a lot to learn about the situations in which phylogenetic conservatism constrains evolutionary convergence. The message for DGVMs is, however, clear. Phylogenetic history potentially constrains how ecosystems respond to environmental forcing and we should for example not expect each of the worlds tropical forests to respond in the same way to environmental forcing (Banin *et al.*, 2012).

2.2.2 Next generation DGVMs

We argue that the next generation of DGVMs should implement ideas derived from coexistence theory (Chesson, 2000) and community assembly theory (Keddy, 1992; Webb *et al.*, 2010) into the process-based paradigm of dynamic global vegetation modelling. Yet, we wish to emphasise that while we can learn a lot from community ecology and coexistence theory, we should also appreciate that these disciplines do not have the same aims as dynamic global vegetation

modelling. Community ecology primarily seeks to understand which traits determine fitness in which environmental settings. Much of this understanding can be gained using statistical methods (Webb *et al.*, 2010; Shipley, 2010; Swenson & Weiser, 2010). Coexistence theory generally uses heuristic models to understand which processes and environmental settings promote coexistence (Chesson, 2000). Dynamic global vegetation models, on the other hand, seek to represent and understand the interplay between climate and vegetation. In the paragraphs that follow we describe a conceptual scheme for a next-generation DGVM that is illustrated in Fig. 2.2.

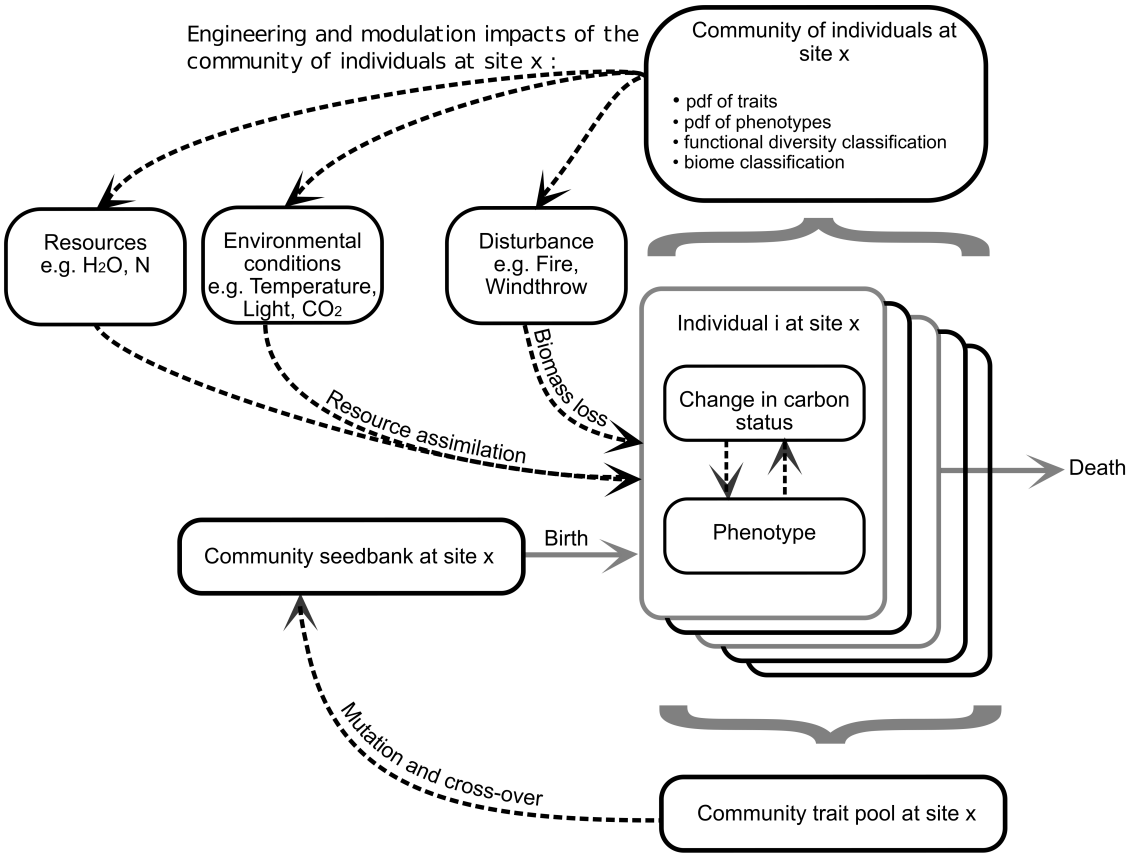

FIGURE 2.2: Conceptual modelling framework for a next generation DGVM as outlined in the section "Next Generation DGVMs". Individuals are characterised by their traits which influence their carbon status and phenotype. All individuals at a site form the community, which influences resources, environmental conditions and disturbances via engineering and modulating impacts. These conditions interact to influence growth of the individuals. Individuals can add their traits to the community trait pool. Cross-over and mutation of the community trait pool yield the community seed bank.

We propose that the key challenge for DGVMs is to move away from the fixed-PFT paradigm towards a more flexible trait-based approach which allows communities to be assembled based on how plants with different trait combinations perform under a given set of environmental conditions. The primary object in such a model is the individual. An individual-based approach (DeAngelis & Mooij, 2005) allows a simulation run to consider many individual plants, each of which can potentially have a unique set of trait values (see Fig. 2.3 for traits

of an individual plant that one could simulate in DGVMs). In this model structure the traits describe how the rates of resource assimilation, growth, carbon allocation and respiration are influenced by the environment; these rates in turn determine the carbon balance and the state variables that define the phenotype of each individual plant (Fig. 2.2). Individuals with inappropriate trait values and poor carbon balance die, whereas individuals with sufficient carbon gain, and trait values that allow seed production, reproduce. This model structure allows for variance in how plants respond to variable environmental conditions which has been shown to promote species coexistence (Clark *et al.*, 2004, 2010).

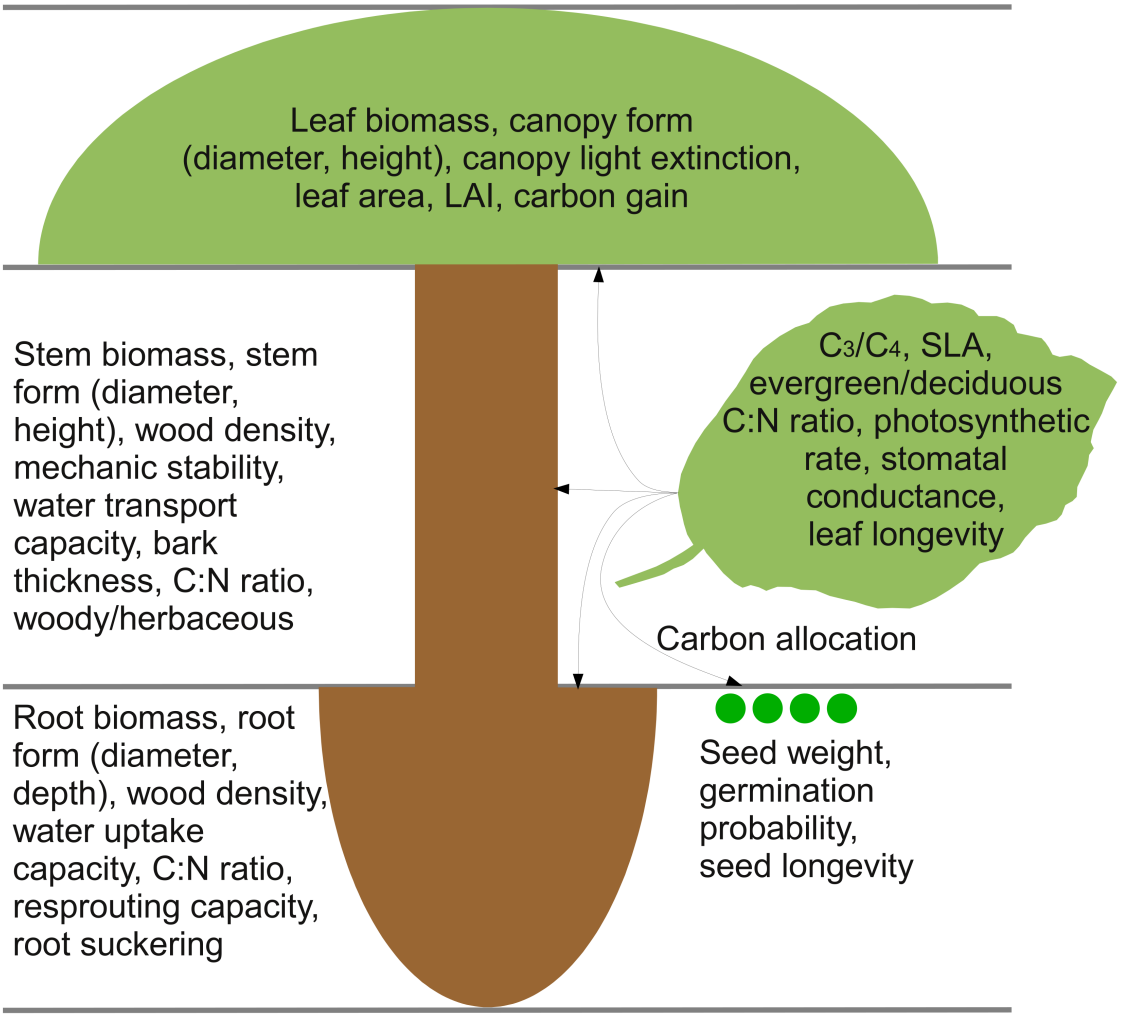

FIGURE 2.3: Traits and state variables of a single plant in a next generation DGVM. Arrows represent allocation of carbon produced by leaves to different biomass compartments of the plant.

Reproduction is a key element in next generation DGVMs, since reproduction transfers traits from one generation to the next (inheritance), allows transfer of traits between reproductive individuals (cross-over) and allows novel trait values to enter through mutation. There are many ways these processes could be modelled. A realistic modelling of these evolutionary processes (for instance how dispersal, pollination processes or reproductive biology influences gene flow) is not warranted, rather we require an effective algorithm that rapidly generates

and selects for individual trait combinations that are adapted to the abiotic and biotic environment at a site. A pragmatic approach, which we follow, is to use a genetic optimisation algorithm to manage the transfer of traits between generations. Genetic optimisation algorithms are general purpose optimisation routines that use the concepts of re-combination and mutation to efficiently find quasi-optimal solutions to optimisation problems (e.g. differential evolution, Storn and Price, 1997). In the context of DGVMs, the vectors that describe trait values of each reproducing individual are added to the community trait pool. Traits are mutated and recombined to produce a community seed bank of seeds which can potentially germinate (Fig. 2.4). Trait filtering occurs through the reproduction and mortality functions; trait combinations that do not produce offspring do not contribute their traits to the next generation, whereas those that produce many seeds dominate the community trait pool.

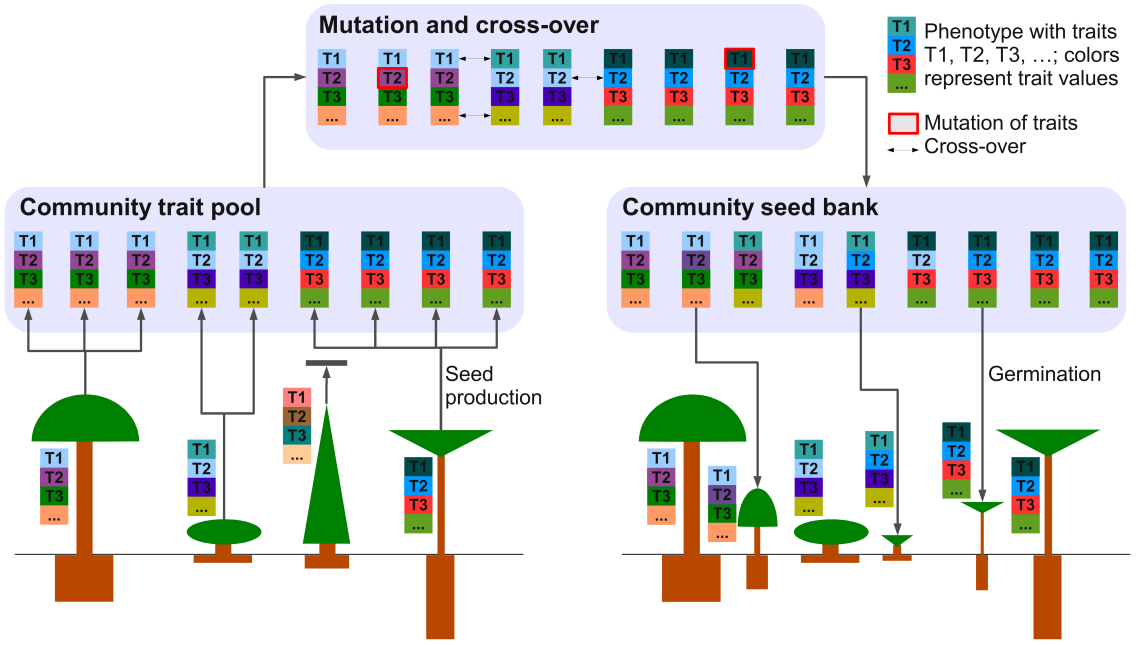

FIGURE 2.4: Seed bank model in a next generation DGVM. Each plant is characterised by a unique trait combination. Reproducing individuals add their seeds to the community trait pool. In the community trait pool, mutation and cross-over of seeds generate new trait combinations which constitute the community seed bank. Randomly selected seeds can germinate which means that they are added to the plant community as seedlings.

What emerges from trait filtering is a community of individuals at a site. The information on this community can be summarised in various ways; as a probability density function (pdf) of traits, a pdf of phenotypes, the phenotype can be used to classify individuals as belonging to a specific functional type, or the phenotypes at a site can be used to assign a site to a biome type (Fig. 2.2). The properties of individuals can additionally be used to calculate changes in resource availability (e.g. soil water, light environment) and environmental conditions (e.g. surface temperature). Hence, competitive effects are simulated by modelling the engineering and modulating effects of plants on their environment which feeds back to influence plant growth (Fig. 2.2).

The community of individuals at a site additionally determines disturbance

regimes (Fig. 2.2). While DGVMs have in recent years made great strides in improving the representation of fire and disturbance (e.g. Thonicke et al., 2010), the individual-based approach we propose emphasises the possibility to link traits and phenotypes to fuel properties and to the response of individual plants to fire (Pausas *et al.*, 2004; Pausas & Verdú, 2008). One example of this link is the invasion of Norway spruce in northern Europe in the late-Holocene where it has been shown that the associated changes in the community structure had more impacts on fire regimes than climatic changes (Ohlson *et al.*, 2011). Analogously, individual level variance in the plant phenotype defines the value of vegetation to herbivores and how vegetation structure will respond to herbivory (Scheiter & Higgins, 2012).

The promiscuous nature of the way such a genetic algorithm (Fig. 2.4) simulates reproduction has two major side effects. First, the trait "evolution" such a model simulates cannot be compared to the trait evolution evolutionary biologists study. This is because the genetic algorithm will rapidly find optimal solutions to the "evolutionary" problems the modelled environment poses. However, reproduction could be constrained to individuals with similar traits or individuals with the same 'species label'. This would restrict gene flow and thereby simulate reproductive isolation. The second side effect is that the rampant and unconstrained evolution of trait combinations is likely to produce Darwinian demons (Law, 1979), individuals that simultaneously maximise all functions that contribute to fitness. Darwinian demons do not exist in the real world because allocation of resources, for instance, to reproduction ensures that fewer resources are available for other functions such as growth and survival. Identifying such trade-offs is one of the major activities of life-history theory and of the growing literature on functional plant traits (e.g. Reich et al., 1997; Enquist, 2002; Wright et al., 2004;

Shipley et al., 2006; Westoby and Wright, 2006; Chave et al., 2009). Process-based vegetation models that explicitly consider trade-offs between traits are, however, rare (Kleidon and Mooney, 2000; Marks and Lechowicz, 2006; Reu et al., 2011; Pavlick et al., 2013).

The major task for the developer of the kind of DGVM we are proposing is to conceptualise and parametrise life-history trade-offs. We envisage that there are three major types of trade-offs that need to be considered. The first are mass conservation trade-offs - the amount of resource allocated to candidate functions must sum to one. The consequences of these trade-offs manifest themselves naturally as part of the model's dynamic. For example, allocating more carbon to bark might protect a tree from fire damage, but this might compromise its ability to grow tall and compete for light (Gignoux *et al.*, 1997). The second kind of trade-offs are engineering trade-offs - certain plant structures or architectures are not mechanically feasible. For example, a minimum stem diameter is required to ensure the mechanical stability of a stem of a given height (Niklas, 1994). Similarly a critical sapwood area is need to supply foliage with water (Shinozaki *et al.*, 1964). These first two kinds of trade-offs can be addressed respectively by having a sound accounting system in the model and by using established principles of engineering. The third kind of trade-offs are more diffuse to define and difficult to deal with. We will refer to them as empirical trade-offs. Empirical trade-offs are due to processes not explicitly simulated by the model. For example, Shipley *et al.* (2006) argued that the trade-off between leaf photosynthetic rates and leaf longevity is a consequence of cell anatomy. Yet, DGVMs do not explicitly model cell anatomy, meaning that this trade-off cannot emerge as a result of the model's internal dynamics. We are forced to parametrise this trade-off using empirically defined functions. We might use the empirical functions identified by Wright *et al.*

(2004) to describe the trade-off between photosynthetic rate and leaf longevity and refrain from attempting to model the mechanisms that Shipley *et al.* (2006) proposed. The problem of which processes to model empirically and which to model mechanistically is of course a pervasive problem in any kind of modelling endeavour.

2.2.3 The aDGVM2: a trait-based dynamic vegetation model

We now turn to the question, can we implement a model of the kind narrated in the previous section? In this section we describe how we modify an existing DGVM (the aDGVM, Scheiter and Higgins, 2009) to realise aspects of the conceptual scheme illustrated in Fig. 2.2. The aDGVM2 is individual-based which means that it simulates growth, reproduction and mortality of each individual plant and that it keeps track of state variables such as biomass, height and leaf area index of each individual plant. In addition, each plant is characterised by an individual and potentially unique set of traits describing plant type (grass or tree), leaf characteristics, leaf phenology, carbon allocation to different plant compartments, allometry of plant architecture, re-sprouting response to fire, reproduction and mortality (Fig. 2.2). Each plant is tagged with a "species label". These "species" differ in trait values used for the model initialisation. Growth, reproduction and mortality of plants are influenced by both the plant specific trait combination and the environmental conditions.

Plant traits are linked by trade-offs to constrain overall plant performance. Mass conservation trade-offs regulate allocation to roots, stems, leaves, bark, storage and reproduction. Engineering trade-offs regulate plant architecture (Niklas & Spatz, 2010), while empirical functions define, for example, trade-offs between

specific leaf area (SLA) and leaf longevity (Reich *et al.*, 1997) or between SLA and the capacity of a plant to extract water from the soil. The aDGVM2 simulates soil water competition and light competition via impacts of each individual plant on the resource base. Water uptake of single plants is defined by the fraction of root biomass in different soil layers, the moisture content of these soil layers and by the plant's capacity to extract water from the soil. The light available to a target plant is influenced by the height of neighbouring plants. Light availability and water availability influence the photosynthetic rate and thereby, via carbon status, the reproduction and mortality rates of each individual plant. Nutrient competition was not considered in this model version, even though it is important (Tilman, 1988).

Reproduction follows the scheme described in Fig. 2.4. Specifically, plants that allocate enough carbon to reproduction can produce seeds. Seeds of the same species label can exchange trait values thereby allowing recombination of the community trait pool. Mutation adds new trait values to the community trait pool. Randomly selected seeds are drawn from the resulting community trait pool and are added to the plant population as seedlings. By simulating inheritance, mutation and crossover, the model generates a large variety of different trait combinations and iteratively, via mortality and reproduction, assembles a plant community that is adapted to and influences the environmental conditions, resource availability and the disturbance regime at a study site.

2.3 Results

The following paragraphs describe simulation runs that illustrate major features of the aDGVM2. The environmental space in all simulation experiments is defined to be close to a savanna-forest boundary (9 °N and 10 °E, 1000mm MAP). A first simulation run is designed to illustrate how the assembled communities are influenced by rainfall and CO_2. Simulations are conducted for ambient and elevated CO_2 concentrations (380ppm and 700ppm). Additionally, we scale precipitation to generate a rainfall gradient (400mm, 1000mm and 1500mm). Simulations are conducted with and without reproductive isolation, that is with and without the restriction of trait exchange to individuals of the same "species". A principal component analysis (PCA) shows that at the end of a 2000 year simulation run, the communities in different scenarios occupy different regions of the trait space (Fig. 2.5) and are clearly arranged along the rainfall and the CO_2 axes. These simulation runs additionally highlight the importance of simulating reproductive isolation. When reproductive isolation is not simulated then the aDGVM2 simulates essentially one strategy per simulation scenario and simulated individuals are clustered in the trait space (Fig. 2.5A). In contrast, when reproductive isolation is simulated and reproduction is restricted to individuals of the same "species", coexisting strategies emerge, and the individuals belonging to different "species" occupy distinct regions of the trait space (e.g. the yellow and green strategies in Fig. 2.5B).

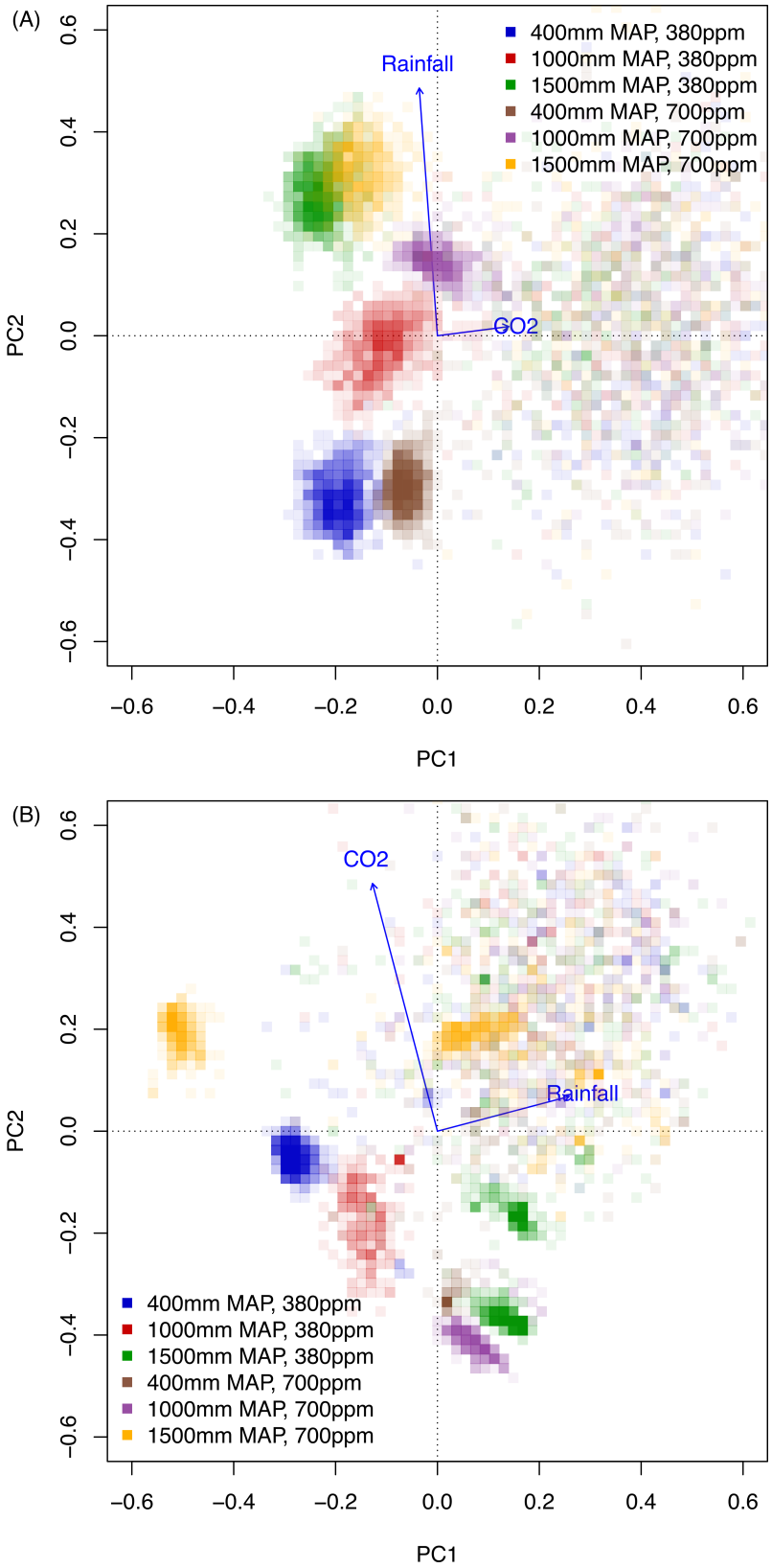

FIGURE 2.5: Principal component analysis (PCA) showing that simulated communities respond to the environmental conditions. Simulations were conducted for a rainfall gradient and for ambient and elevated CO_2 concentrations. Simulations were conducted without reproductive isolation between individuals (trait exchange between all 'species', panel A) and with reproductive isolation (trait exchange restricted to individuals of the same 'species', panel B). Saturation of different colours represents the number of plants within a region of the trait space. We ordinated a trait by site table.

A second simulation run illustrates how trait values and plant communities at a site develop over time. The simulation starts by allowing fires to occur. After approximately 1000 iterations, the assembled community is relatively stable and mean trait values reach a plateau (Fig. 2.6A). In the second simulation phase (iteration 2001 to 4000) fire suppression is introduced. Following the release from fire induced selection pressure, carbon allocation to roots increases, which improves water uptake potential and wood density increases, which reduces the risk of mortality as a result of mechanical instability (Fig. 2.6A). Therefore, carbon allocation to bark, which protects trees against fire, decreases. Fig. 2.6A shows the mean trait value of all individuals in a simulation whereas Fig. 2.6B shows the frequency of different trait values. Hence, increases in mean wood density (Fig. 2.6A) can be attributed to increasing abundances of 'species' with high wood density (Fig. 2.6B). When the system is exposed to fire the community trait diversity (measured as the total distance between all trait combinations) is, after an initial transient phase, low (Fig. 2.6C). When fire is suppressed, trait diversity increases. This shift in trait diversity in response to fire agrees with Pausas and Verdu (2008) who found that trait dispersion was lower in Mediterranean shrubland communities subject to higher fire frequencies.

The distributions of simulated trait values are often multi-modal (Fig. 2.6B), suggesting that the aDGVM2 simulates different life history strategies that can persist and coexist under the given environmental conditions. In the example simulation (same as in Fig. 2.6), four dominant strategies persist (Fig. 2.7). These coexisting strategies are consistent with colonisation-competition trade-off models of species coexistence theory. The strategy plotted in blue is the better coloniser as it starts growing early in the growing season (Fig. 2.6A), has shallow roots

(Fig. 2.7B), is fast growing (low wood density, Fig. 2.6C), allocates a high proportion of the carbon gain to reproduction (Fig. 2.6D) and produces smaller seeds (Fig. 2.6E). In contrast, the strategy plotted in yellow is the better competitor because it has deeper roots (Fig. 2.6B), higher wood density (Fig. 2.6C) and produces heavier seeds (Fig. 2.6E). Accordingly, the tallest trees in the simulated population stem from the yellow strategy (Fig. 2.6F).

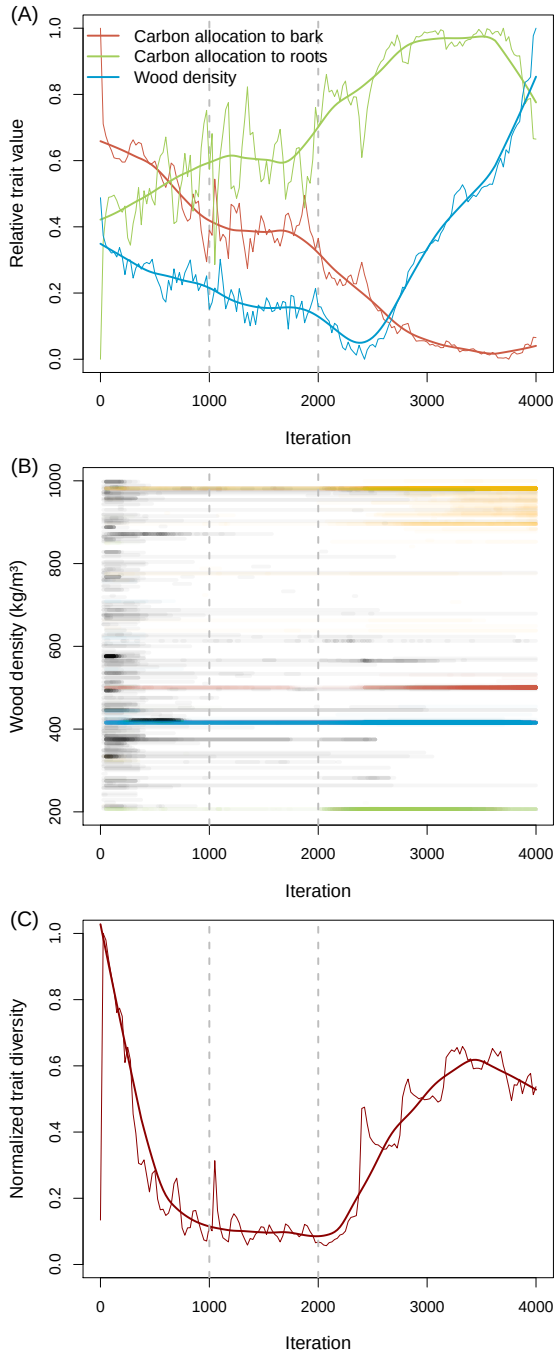

FIGURE 2.6: Trait evolution and trait diversity simulated by the aDGVM2. Panel A shows how mean trait values of all simulated trees evolve. We selected three traits for this plot. Panel B shows in detail how wood density of trees evolves. The aDGVM2 simulates, in the specific simulation run, four dominant coexisting strategies, represented by different colours. Grey colour represent strategies that are only present in low abundances, saturation of colours indicates the number of individuals with different trait values. Panel C shows the evolution of community trait diversity (calculated as the euclidean distance between the normalised trait values of all trees). The first simulation period (iteration 0 to 2000) was conducted in presence of fire, after which fire was suppressed.

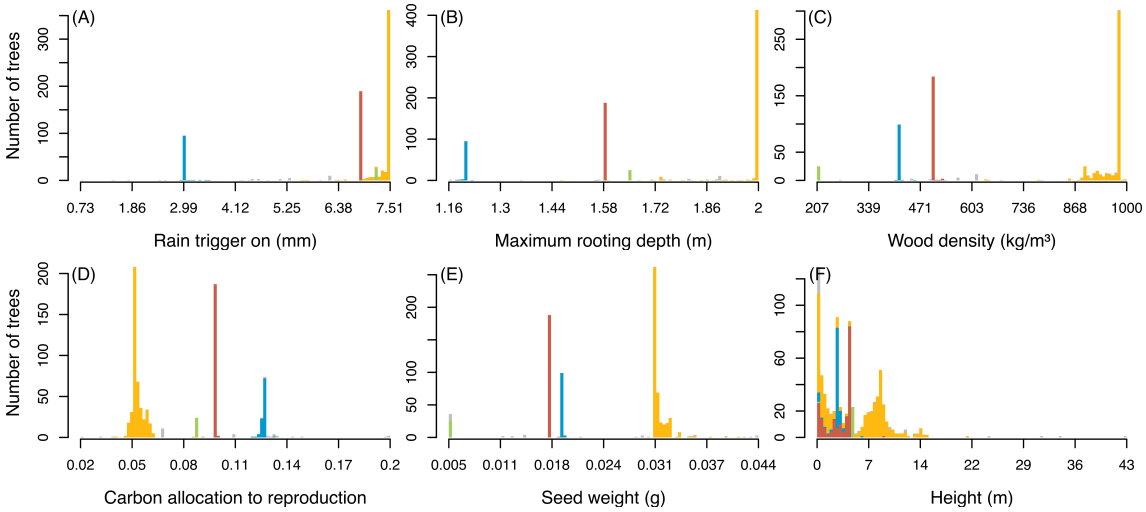

FIGURE 2.7: Histograms of selected plant traits after a 4000 year simulation. The aDGVM2 simulates, in the specific simulation run (same as in Fig. 2.6), four different co-existing strategies, represented by different colours. Grey bars represent other strategies that are only present in low abundances. The 'rain trigger on' trait in panel A describes the value of a running average of precipitation where trees move from the dormant to the metabolic state.

2.4 Discussion

In this paper we review limitations of dynamic global vegetation models and argue that many of these limitations could be addressed by integrating concepts from community assembly (Keddy, 1992; Weiher & Keddy, 1995*a*,*b*) and plant coexistence theory (Chesson, 2000). More specifically, we propose an approach which models individuals, each of which can potentially have a unique suite of trait values, and uses environmental forcing to drive community assembly through trait filtering and selection.

The approach we outline has several advantages. First, it redefines the process of model parametrisation and calibration and thereby avoids hidden model calibration. The trait values that individual plants adopt are not parametrised but

emerge from the model dynamics. Environmental conditions and resources influence the fitness of individual plants, thereby filtering which trait combinations dominate and coexist. This is particularly important when environmental conditions change. When using this approach, the model parametrisation process switches emphasis from defining trait values to defining functions that describe trade-offs between traits. This approach reduces the dimensionality of the parametrisation process while increasing the functional diversity the model represents. For example, in a conventional approach, maximum plant height can be defined as a PFT specific constant. Should one want to simulate 100 functional types, one would require 100 maximum height estimates. In the new approach, the parametrisation process is no longer estimating the maximum height of each PFT, but rather defining the mechanical limits to plant height. One only needs the few parameters that define how height scales with other components of plant architecture such as stem diameter and wood density (Niklas, 1994; Niklas & Spatz, 2010). However, trait filtering only yields useful results if appropriate filters act on the phenotypes. This filtering process includes not just the abiotic forcing variables but also includes how vegetation at a site influences resource availability, environmental conditions and disturbance regimes. Hence, the success of the approach is largely dependent on the ability to model resource competition and the engineering and modulating effects that plants have on their environments. There is a substantial literature on mechanisms that promote the coexistence of plants (e.g. Chesson, 2000) and on modern statistical methods to test which coexistence mechanisms are involved in a specific community (Angert *et al.*, 2009; Clark *et al.*, 2010). Yet, few of these mechanisms are explicitly included in DGVMs. The aDGVM2 considers competition for soil water and light at the individual level and allows for the emergence and coexistence of several life history

strategies. However, we readily concede that more sophisticated concepts are warranted. In particular, how to represent in the model structure (Fig. 2.2) how individuals and species partition environmental variation (Angert *et al.*, 2009; Clark *et al.*, 2010) remains to be explored.

An individual and trait-based approach allows the number of plant functional types in the model to equal the number of modelled individuals (e.g. Pavlick et al., 2013). The consequences of increasing functional diversity are potentially far reaching. For example, it has been proposed that productivity can be higher in highly plastic communities with large phenotypic and niche diversity, compared to communities where many individuals adopt an optimal trait combination (Norberg *et al.*, 2001). Further, several studies have shown that ecosystem services are a function of both species diversity and functional diversity (Hooper *et al.*, 2012).

Having a model that potentially has thousands of functional types also means that how we represent and interpret model output differs. For example, the classification of simulation output into PFTs or biome types is now a post-hoc analysis which can be tailored to the aims of the study or to the benchmarking products available. This classification means that modellers can use available trait data (e.g. Kattge et al., 2011) more effectively because the model generates similar trait data. Developing such classification schemes serves to identify the traits required to differentiate between PFTs, both in models and in reality.

The aDGVM2 does however pose some computational issues. Being individual-based it has, in principle, higher computational demands than PFT and cohort based models. However, in the context of the computational demands of a full

earth system model the demands are not prohibitive. For example, global simulations with the fully coupled earth system model MPI-ESM1 at a standard resolution used for the CMIP5 (Coupled Models Intercomparison Project Phase 5) simulations take approximately 360 CPU hours per simulation year (R. Schnur, pers. comm.). Running the aDGVM2 at the same resolution (6222 land grid points) would take less than two CPU hours per simulation year. The speed at which the modelled plant community converges to a climatically defined state will, however, depend on the number of modelled individuals, the mutation rate and the algorithm used for trait recombination. Experimentation will be needed to find the right compromise between rapid convergence of the assembled community and computational efficiency.

DGVMs assume that convergent evolution is pervasive, that is they assume that functional diversity is defined by a series of labile traits that, given the same selective pressures, will converge to the same ecological optimum. This assumption is highly questionable (Crisp *et al.*, 2009; Buis *et al.*, 2009; Banin *et al.*, 2012) and the consequences of making this assumption are still poorly understood. As a starting point for investigating this issue with DGVMs one should conduct carefully designed sensitivity analyses that explore how the community assembly process is influenced by different ways of initialising, parameterising and constraining functional diversity and by different parameters to describe mutation and crossover.

In conclusion we believe that this paper has illustrated that it is possible to construct a dynamic global vegetation model that deals with functional diversity in a fundamentally different way and in a way that is consistent with theories of plant community assembly and with theories of plant coexistence. We anticipate that pursuing such next generation DGVMs will provide opportunities for fruitful

collaboration between research communities that focus on plant functional traits, plant competition, plant allometry, plant physiology, systems ecology and earth system science and to improve our understanding of how climate and vegetation interact to define the past, current and future distribution of vegetation.

Chapter 3

aDGVM2 Model Description

Liam Langan, Steven I. Higgins and Simon Scheiter * †

*This chapter is published as an appendix to 'Langan et al. (2017) Climate-biomes, pedo-biomes or pyro-biomes: which world view explains the tropical forest-savanna boundary in South America?' in the *Journal of Biogeography*

†Author contributions: aDGVM2 was conceived by S.H. and S.S. and the initial implementation was written by S.S.. Model description text written by S.S. and L.L., text based on submodels shared between aDGVM1 and aDGVM2 is identical to that published in the aDGVM1 model description (Scheiter & Higgins, 2009). L.L. and S.H. redesigned plant hydraulics submodels and L.L. implemented the designed hydraulics submodels. L.L. redesigned the soil hydrology submodel. L.L. conceived the reproductive isolation functionality which was coded by S.S.. S.H. and L.L. redesigned and implemented grass architecture submodules. L.L. and S.S. designed the semi-spatial light competition functionality which was implemented by S.S.. S.H. and L.L. redesigned carbon allocation and leaf phenology submodules. L.L. modified plant recruitment and plant mortality submodels.

3.1 Introduction and modelling concepts

This document provides a description of aDGVM2 (adaptive dynamic global vegetation model, version 2). Scheiter *et al.* (2013) detailed the motivation for the development of this model as well as the novel features of aDGVM2. The following paragraphs summarize important features of aDGVM2.

DGVMs commonly define vegetation using a limited number of plant function types (PFTs) and use point estimates for plant trait values (Scheiter *et al.*, 2013; Sakschewski *et al.*, 2015) (Fig. 3.1). Collapsing observed variability in plant traits in this way may limit the potential of these models to explore past, present and future vegetation dynamics. Further, the way in which competition is represented in many DGVMs has been criticised (Fisher *et al.*, 2010; Scheiter *et al.*, 2013) as competition is simulated at the PFT level rather than at the individual level where competitive processes operate (Clark *et al.*, 2011*a*). aDGVM2 is an individual-based dynamic vegetation model where the growth, reproduction and mortality of individual plants is simulated. A novel feature of aDGVM2 is that each plant can have a specific and potentially unique combination of trait values that influence how a plant performs under given biotic and abiotic conditions. This implementation allows that the level where competitive and selective processes operate within our modelling framework moves from the level of the PFT or plant cohort to the level of the individual and trait.

The community of plants and their trait values evolve through time, this evolution is constrained by trade-offs between traits. Poorly performing individuals are continually removed from the plant population by mortality which results in a filtering of trait values. Further, the community and species' trait values can evolve through successive generations via reproduction, mutation and crossover

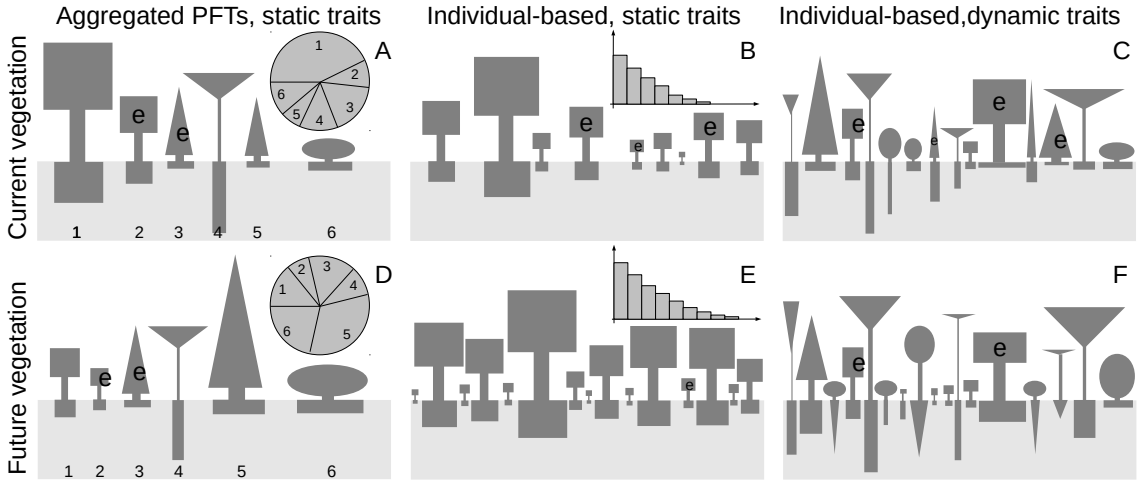

FIGURE 3.1: Conceptual model of representation of vegetation in DGVMs. (A) The model simulates six individuals where each individual represents a functional type. The number of individuals and their parameters are fixed. The dominant vegetation is defined by the relative abundance of the functional types. (B) The model is individual-based and each individual can differ in size or biomass while all individuals of one functional type have a similar trait combination. The dominant vegetation is defined by biomass and density of different functional types. (C) The model is individual-based and each individual has a unique combination of traits. Individuals can differ both in size or biomass and in trait values. The dominant vegetation is defined by the relative abundance of individuals. Panels (D), (E) and (F) depict how climate change influences vegetation. (D) The relative abundances of the functional types change. (E) The number of trees, biomasses and the height structure are modified. (F) Tree number, tree community and traits of individuals can be modified. The 'e' indicates an evergreen functional type.

which we approximate by using a genetic optimisation algorithm (GOA, Eq. 3.75). Additionally, we simulate reproductive isolation in the model by assigning individuals a 'species label' and restricting reproduction to individuals with the same species label. Previous simulations showed that reproductive isolation increases the likelihood that multiple coexisting plant strategies emerge from simulations (Scheiter *et al.*, 2013). Thus, a plant community consisting of individuals and species with potentially novel and diverse trait values is assembled iteratively through time.

Modelling how plants respond to drought has proven to be a major challenge for earth system models and improving the representation of plant hydraulics

may allow us to better predict how a changing climate will influence vegetation (Sperry & Love, 2015). To meet this challenge we implemented a simplified version of the cohesion tension theory adopted by Sperry *et al.* (1998) where elements determining plant conductances are considered in series and implement a set of trait trade-offs which influence a plant's hydraulic strategy whereby hydraulic safety trades-off against xylem and leaf conductivity (Markesteijn *et al.*, 2011).

One of the main aims of vegetation models is to investigate how climate and vegetation interact and define the historical, current and potential future distributions of vegetation. A second is to provide a dynamic representation of the land-surface as a component of earth system models (Scheiter *et al.*, 2013). By moving away from the paradigm of fixed-trait PFTs and improving the way we represent plant competition, hydraulics, community assembly, trait diversity and processes associated with co-existence we aim to iterate towards a more holistic representation of vegetation dynamics, improve our understanding of how biotic and abiotic interactions shape vegetation patterns and better elucidate how current patterns of vegetation will respond to climate change.

3.2 Input data

To simulate vegetation we use site specific soil and climate data as input data. Topsoil texture data were obtained from a global 5×5 minute data set of selected soil characteristics (Nachtergaele *et al.*, 2012). Saturated water content (θ_{swc}), saturated hydraulic conductivity (K_{sat}), saturation suction (ϕ_{soil}), a parameter which influences the rate with which conductance declines as soil dries (r), and the residual content of the soil (rc), were then classified based on these soil texture data (Table 3.1). As in Scheiter & Higgins (2009), climate data were obtained from

New *et al.* (2002)'s global 10×10 minute data set of mean monthly surface climate data. We used precipitation (given by the mean value r_m and the coefficient of variance r_{cv}), wet-day frequency w_f, days with frost d_f, mean temperature $\bar{T}$, diurnal temperature range T_Δ, relative humidity h_s, sunshine percentage p_s, wind speed u_{ref} and elevation Z from this data set (Table 3.2).

These input data are used to calculate the secondary atmospheric characteristics, radiation, photosynthesis and evapotranspiration of study sites. We follow Allen *et al.* (1998)'s guidelines to calculate atmospheric pressure P, minimum and maximum temperature T_{min} and T_{max}, day temperature T, average saturation vapor pressure e^A, saturation vapor pressure e^S, slope of the vapor pressure curve s, vapor pressure deficit h_{vpd}, psychrometric constant γ, density of air ρ_{air}, photosynthetic active radiation Q_p and the net radiation Q_0 (Table 3.2). The rainfall algorithm (New *et al.*, 2002) generates a time series of daily rainfall F_i for each year from the parameters r_m and r_{cv}.

Characteristics of the input data from the database and other variables characterising the environment are summarized in Table 3.2.

3.3 Model description

3.3.1 Leaf physiology

The following sections describe how we estimate the daily leaf-level photosynthetic and respiration rates of study sites from temperature, relative humidity, atmospheric pressure, wind speed and photosynthetically active radiation. We link sub-models for photosynthesis and for stomatal conductance.

Photosynthesis sub-model

We follow Collatz *et al.* (1991, 1992)'s implementation of the Farquhar *et al.* (1980) model of leaf photosynthesis to calculate the (bio-physical) gross and net photosynthetic rates A_0^b and A_n^b (units μmol $m^{-2}s^{-1}$). Maximum light saturated rate of photosynthesis A_{max} is fixed to 30 μmol $m^{-2}s^{-1}$ (Larcher, 2003). The maximum light saturated rate of photosynthesis A_{max} is used to estimate the maximum carboxylation rate V_{max} (μmol $m^{-2}s^{-1}$) as

$$V_{max} = 2^{0.1(T-25)} A_{max} \cdot A_S \frac{1}{\left(1 + e^{0.3(13-T)}\right)\left(1 + e^{0.3(T-36)}\right)}, \tag{3.1}$$

where T is the (leaf) temperature (Collatz *et al.*, 1992) and A_S is a global scaling factor for both C_3 and C_4 photosynthesis (Collatz *et al.*, 1992).

For calculating the biophysical rate of photosynthesis we prescribe the internal CO_2 partial pressure, c_i, using simplifying assumptions. For C_3 plants, c_i is taken to be 70% of atmospheric partial pressure (Woodward *et al.*, 1995). For C_4 plants, c_i represents the bundle sheath value. There is no consensus on how to chose c_i for C_4 plants and we estimated c_i to be eight times the atmospheric partial pressure of CO_2 even though in our simulations, C_4 photosynthesis is not sensitive to the bundle sheath value as photosynthesis is not CO_2 limited, see section (3.3.1) for how c_i is estimated by linking it to a diffusion gradient model of photosynthesis. The CO_2 compensation point is defined as

$$\Gamma_* = \frac{O_i}{2\tau}, \tag{3.2}$$

where τ describes the partitioning of RuBP to the carboxylase or oxygenase reactions of Rubisco and O_i is the inter-cellular partial pressure of oxygen (assumed

to be 21 kPa). Further, K_c is the Michaelis constant for CO_2 and K_o is the O_2 inhibition constant. We use the function

$$f_{25}(T) = K_{25} \cdot Q_{10}^{\frac{T-25}{10}}, \tag{3.3}$$

to describe the response of K_c, K_o and τ to temperature T. Here, K_{25} and Q_{10} are empirically determined parameters specific for K_c, K_o and τ (see Table 3.5).

The gross rate of photosynthesis A_0 is calculated, following Collatz *et al.* (1991) for C_3 plants and Collatz *et al.* (1992) for C_4 plants, as the minimum of three potentially limiting assimilation rates. The Rubisco limited assimilation rate J_c is defined as

$$J_c = \frac{V_{max} \cdot (c_i - \Gamma_*)}{c_i + K_c(1 + O_i/K_o)}, \tag{3.4}$$

$$J_c = V_{max}, \tag{3.5}$$

for C_3 and C_4 respectively. When light is limiting, the efficiency of CO_2 fixation is limited by the quantum yield. The light limited assimilation rate J_e is defined as

$$J_e = a \cdot \alpha \cdot Q_0 \cdot \left(\frac{c_i - \Gamma_*}{c_i + 2\Gamma_*} \right), \tag{3.6}$$

$$J_e = a \cdot \alpha \cdot Q_0, \tag{3.7}$$

for C_3 and C_4 respectively. Here Q_0 is the incident quantum flux density (μmol $m^{-2}s^{-1}$) that a leaf receives, a is the leaf absorptance and α is the intrinsic quantum yield of photosynthesis (see Table 3.5). When light and Rubisco do not limit the assimilation rate, then it is assumed that the capacity for the export of the

products of photosynthesis is limiting for C_3 plants. This transport limited assimilation rate J_s is approximated as

$$J_s = \frac{V_{max}}{2}. \tag{3.8}$$

For C_4 plants, when light and Rubisco are not limiting it is assumed that CO_2 concentrations limit the assimilation rate. This CO_2 limited rate J_p is approximated as

$$J_p = \frac{\kappa \cdot c_i}{P}, \tag{3.9}$$

(Woodward & Smith, 1994). The term κ is the empirically defined initial slope of the response of CO_2 to photosynthesis (units μmol m^{-2} s^{-1}) and P is the atmospheric pressure (Pa). In summary, the gross rate of (bio-physical) photosynthesis A_0^b is

$$A_0^b = \min(J_c, J_e, J_s), \tag{3.10}$$

$$A_0^b = \min(J_c, J_e, J_p), \tag{3.11}$$

for C_3 plants and for C_4 plants. The net rate of (bio-physical) photosynthesis A_n^b is

$$A_n^b = A_0^b - R_{mLs}, \tag{3.12}$$

where

$$R_{mLs} = r \cdot V_{max}, \tag{3.13}$$

is the single leaf maintenance respiration rate. Here, r is a proportion assumed to be 0.015 for C_3-photosynthesis and 0.025 for C_4-photosynthesis (Collatz *et al.*, 1991, 1992) and V_{max} is the maximum carboxylation rate from Equation (3.1). All

parameters and variables for section (3.3.1) are summarized in Table 3.5.

Stomatal conductance sub-model

The CO_2 assimilation rate is coupled to stomatal conductance using Ball *et al.* (1987)'s empirical model. The model relates the response of stomatal conductance g_s (μmol $m^{-2}s^{-1}$) to the net rate of CO_2 uptake A_n:

$$g_s = m\frac{A_n \cdot h_s \cdot P}{c_s} + b. \tag{3.14}$$

The terms m and b are empirically derived parameters (see Table 3.6), h_s is the relative humidity (expressed as unitless ratio), P is the atmospheric pressure (Pa) and c_s is the partial pressure of CO_2 at the leaf surface, calculated as

$$c_s = c_a - \frac{1.4 \cdot A_n \cdot P}{g_b}. \tag{3.15}$$

Here, c_a is the atmospheric partial pressure of CO_2 (Pa) and g_b is the leaf boundary layer conductance, estimated as

$$g_b = 0.271 \cdot 10^6 \sqrt{\frac{u(z)}{D_L}}, \tag{3.16}$$

where, $u(z)$ is the wind speed (ms^{-1}) at height z (m) above the ground and D_L is the characteristic leaf dimension (Jones, 1992). We calculate the wind speed $u(z)$ from the reference wind speed u_{ref} (m s^{-1}), measured at height z_{ref} (m) above the ground as

$$u(z) = u_{ref}\frac{\ln(z - z_d) - \ln(z_0)}{\ln(z_{ref} - z_d) - \ln(z_0)}. \tag{3.17}$$

Here, z_d is the displacement height (m) and z_0 is the roughness length (m) (Jones, 1992). Both z_0 and z_d are functions of the aerodynamic properties of the vegetation and following Jones (1992) we simply assume $z_d = 0.86 \cdot \bar{H}$ and $z_0 = 0.06 \cdot \bar{H}$. For these purposes we assume mean vegetation height $\bar{H}$ is 1.5m. The reference height z_{ref} is 10 m and the wind speed u_{ref} is read from a database. Variables in section (3.3.1) are summarized in Table 3.6.

Linking photosynthesis and stomatal conductance

The leaf photosynthesis and conductance sub-models are interdependent. The photosynthesis model requires estimates of c_i, which is determined by stomatal conductance. The stomatal model, in turn requires estimates of A_n, which also depends on c_i. The system of equations is closed by noting that A_n can also be defined in terms of the CO_2 diffusion gradient

$$A_n^d = \frac{g_s \cdot (c_s - c_i)}{1.6 \cdot P}. \tag{3.18}$$

When solving for A_n we iteratively seek the value of c_i that satisfies both Equation (3.18) and the equations

$$A_n^b = \min(J_c, J_e, J_s) - R_{mLs}, \tag{3.19}$$

$$A_n^b = \min(J_c, J_e, J_p) - R_{mLs}, \tag{3.20}$$

for C_3 and C_4 plants given by Equations (3.10) or (3.11) and (3.12), hence, we solve the equation

$$c_i^* = \min_{c_i > 0} \left| A_n^b - A_n^d \right|. \tag{3.21}$$

3.3.2 Single plant biomass pools

aDGVM2 is individual-based and simulates the dynamics of trees and grasses. Each plant consists of different compartments; we simulate biomass pools for leaves B_l, stem B_s, bark B_b, root B_r, reproduction B_p and storage B_t. Leaf biomass is required for photosynthetic carbon gain, stem biomass creates the structure required to capture light efficiently, bark biomass protects vegetation against fire, root biomass is required for water uptake, reproduction biomass is used for seed production and storage biomass is required for leaf flush after dormancy and for re-sprouting after fire. For grasses, we simply assume that $B_s = B_b = 0$. More details of the functions of the different compartments are provided in the following sections. We further simulate dead leaf biomass which accumulates when plants move from the metabolic to the dormant state. The dead leaf biomass pool is required to calculate the fire intensity (see section 3.3.13).

3.3.3 Tree architecture

Canopy architecture

Plant height H is calculated as

$$H = \mathrm{e}^{\frac{\log(B_s)+b_1}{b_2}}, \tag{3.22}$$

where B_s is the stem biomass. The parameters b_1 and b_2 describe the relation between aboveground biomass and plant height and they are subject to change as defined by the GOA (Table 3.3 provides trait value ranges). Plant height and aboveground biomass are used to calculate the stem diameter. We assume that

the stem is a cylinder with homogeneous wood density ρ_{wood}. Wood density is calculated as a function of P_{50}, the matric potential at which a 50% loss of xylem conductivity occurs (see section 3.3.6).

The inner stem diameter, that is the stem diameter excluding bark is given as

$$D_i = 2\sqrt{\frac{B_s}{\pi \cdot \rho_{wood} \cdot H}}, \tag{3.23}$$

the overall stem diameter including the bark is given as

$$D_s = 2 \cdot \sqrt{\frac{B_s + 2 \cdot B_b}{\pi \cdot \rho_{wood} \cdot H}}. \tag{3.24}$$

Here we simply assume that the bark density is $\rho_{wood}/2$. The difference between the diameters D_i and D_s defines the bark thickness as $0.5 \cdot (D_s - D_i)$ which influences the fire sensitivity of plants (see 3.3.13).

Based on the equation used by Strigul *et al.* (2008), tree stem diameter is used to calculate the canopy radius r_c at height z above the ground by using the equation

$$r_c(z) = C_1 \cdot D_i \left(1 - \left(\frac{z}{H}\right)^{C_2}\right). \tag{3.25}$$

Here, C_1 is the ratio between the canopy radius at the ground ($z = 0$) and stem diameter and C_2 defines the shape of the canopy, thus, $C_2 = 1$ defines a cone shaped canopy, $C_2 > 1$ defines a more cylinder shaped canopy and $C_2 < 1$ defines a copped canopy. The parameter C_1 is fixed at 10.0 and parameter C_2 is a trait defined by the GOA (Table 3.3). Canopy area at the ground, $D_c(0)$, has a minimum value of 0.2m^2. Canopy area at height z above the ground is then given by

$$D_c(z) = r_c(z)^2 \cdot \pi. \tag{3.26}$$

where tree leaf area index L_{tree} (LAI) is calculated as

$$L_{tree} = \frac{B_l \cdot A_{SL}}{D_c(0)}. \tag{3.27}$$

Here, B_l is the leaf biomass, $D_c(0)$ is the canopy area at the ground and A_{SL} is the specific leaf area (SLA).

Stem architecture

Equations (3.22) and (3.24) describe how plant height and stem diameter are obtained from biomass. These equations use three traits to describe plant allometry, b_1, b_2 and ρ_{wood}. These parameters describe whether plants grow preferentially in height which implies low stem diameters or whether they grow preferentially in diameter which implies low plant height. These differences in stem architecture imply a trade-off between water transport capacity, light availability and mechanic stability. Thus, a tall stem with small diameter implies high light availability and an advantage in light competition, however, it is mechanically unstable and does potentially not allow to transport the amounts of water required by the plant. In contrast, plants with high stem diameters are mechanically stable and not susceptible breakage however, they are generally smaller and potentially shaded by other plants.

To be mechanically stable, plant height H, stem diameter D_s and wood density

ρ_{wood} must fulfil a stability condition. Following Niklas & Spatz (2010) we calculate the critical buckling height (in m) as

$$H_{crit} = 0.79 \left(\frac{11.852 \cdot \rho + 37}{9.81} \cdot \rho_{wood} \right)^{\frac{1}{3}} D_s^{\frac{2}{3}}. \tag{3.28}$$

When the plant height exceeds the critical height H_{crit}, then the mortality probability of the plant increases (see section 3.3.12). Section (3.3.6) describes the hydraulic trade-offs associated with tree architecture.

3.3.4 Grass architecture

Grass architecture in DGVMs has received little attention. Here we implement a novel grass architecture scheme where leaf width L_w (mm) is calculated using Craine et al.'s (2013) constraint line and is a function of P_{50}, the matric potential where 50% loss of xylem conductivity occurs,

$$L_w = 1.25 \cdot P_{50} + 22.5. \tag{3.29}$$

We then use the relationship between leaf tissue density L_{TD} and P_{50} in Tucker et al. (2011) to calculate L_{TD} (in g mm^{-3})

$$L_{TD} = (-0.025 \cdot P_{50} + 0.294) \cdot 0.001. \tag{3.30}$$

Leaf volume L_v (mm^3) is calculated as

$$L_v = \frac{0.7 \cdot 1000 \cdot B_l}{L_{TD}}. \tag{3.31}$$

We assume a leaf thickness L_t of 0.1 (mm) and calculate total leaf length L_{LT} (m) as

$$L_{LT} = \frac{L_v}{L_t \cdot L_w}. \tag{3.32}$$

Grass leaf area $L_{A^{grass}}$ (m^2) is

$$L_{A^{grass}} = \frac{L_w}{1000} \cdot L_{LT}. \tag{3.33}$$

Grass specific leaf area $A_{SL_{grass}}$ (m^2 kg^{-1}) is calculated by setting B_l to 1 kg. Canopy diameter D_{grass} (m) is assumed to be a function of root biomass

$$D_{grass} = 0.5 + 1.5 \cdot \frac{B_r}{B_r + 0.250}. \tag{3.34}$$

Grass canopy area D_c (m^2) is assumed to have a maximum of $1m^2$ and is calculated as

$$D_c = \min\left(1, \pi \cdot \left(\frac{D_{grass}}{2}\right)^2\right), \tag{3.35}$$

making grass leaf area index L_{grass} (LAI)

$$L_{grass} = \frac{L_{A^{grass}}}{D_c}. \tag{3.36}$$

3.3.5 Light availability and light competition

Light availability of an unshaded plant is described using Beer's law, that is

$$Q_0 = \int_0^L e^{-\omega L}\, dL = \frac{1}{\omega} \cdot \left(1 - e^{-\omega L}\right), \tag{3.37}$$

where L is an individual's leaf area index and the parameter ω describes the light extinction in the canopy, we assume higher density leaves result in higher light

extinction and calculate ω as a function of specific leaf area

$$\omega = 0.3 + \frac{A_{SL^{max}}}{A_{SL^{max}} \cdot A_{SL}}. \tag{3.38}$$

where the maximum permissible SLA ($A_{SL^{max}}$) is 32.67 (m^2kg^{-1}) which corresponds to the maximum value of P_{50} allowed, see section (3.3.6).

To simulate light competition, we assume that plants are arranged on an equidistant rectangular grid. The size of a grid-cell is dependant on the plot area and the number of individuals we simulate. Light availability of a target plant is influenced by eight neighbours. When the canopy height of the target plant H_t^c is less then the canopy height of a neighbour plant, H_n^c, the neighbour has a canopy area greater than the size of a grid-cell on our equidistant grid, here $2.77m^2$, and the neighbour has an LAI greater than 0.1 then light availability of the target plant is reduced and calculated as

$$Q_t = Q_0 \cdot \mu \cdot \left(1 - \frac{H_t^c}{H_n^c}\right)^{L \cdot min\left(1, \frac{D_c(0)}{25}\right)}. \tag{3.39}$$

Here, $\mu = 0.5$, describes the maximum impact of a neighbour plant on the light environment of the target plant, L is the leaf area index of a neighbour plant and 25 is the point at which a neighbours canopy area at the ground, $D_c(0)$, is greater than the summed area of it's own grid-cell and the 8 surrounding grid-cells given the number of simulated individuals is 3600 and the plot size is $10{,}000m^2$. Thus, the light availability of an individual is influenced by it's height relative to it's neighbours as well as the leaf area index and canopy area of it's neighbours. This procedure is repeated for the eight neighbours of a plant. The canopy height is defined as

$$H^c = H \cdot \sqrt[C_1]{0.5}, \tag{3.40}$$

to account for different canopy forms. The canopy height of more cylinder shaped canopies is almost the plant height while the canopy height of more copped canopies is less than the plant height.

3.3.6 Root architecture and water competition

In the model we assume that for both trees and grasses the distribution of roots in the soil is described by the function

$$R_F(z) = R_n \left(1 - \left(\frac{z}{R_m}\right)^{R_1}\right)^{R_2}, \tag{3.41}$$

where $R_F(z)$ is the fraction of roots at depth z, R_m is the maximum rooting depth of the plant, R_1 and R_2 describe the root form and R_n is a scaling factor that ensures that

$$\int_0^{R_m} R_F(z)\, dz = 1. \tag{3.42}$$

This function allows us to simulate various root forms. The parameters R_1, R_2 and R_m are traits defined by the GOA (Table 3.3). In the model we do not directly use Equation (3.41) to describe the root form. We rather assume that roots in different soil layers are represented by cylinders. The proportion of roots R_{Fi} in soil layer i ($i = 1, 2, \ldots n$, where n is the number of soil layers is calculated by using Equation (3.41)) is,

$$R_{Fi} = R_F(D_i). \tag{3.43}$$

Here, D_i is in the average depth of soil layer i. The actual root fractions in soil layer i is then defined as

$$R^*_{Fi} = R_n \cdot R_{Fi} \cdot T_i, \tag{3.44}$$

where T_i is the thickness of the soil layer i and R_n is a scaling factor that ensures that

$$\sum_{i=1}^{n} R_{Fi}^{*} = 1. \tag{3.45}$$

Plant Hydraulic Strategies - safety versus efficiency trade-offs

The plant water availability sub-models are crucial for modelling vegetation dynamics as well as predicting how vegetation formations may change in response to climate change. Vegetation models typically calculate plant water availability as a function of relative soil moisture content and root fractions across a number of soil layers, typically to a depth not greater than 3m (Ostle *et al.*, 2009). In many areas of the world, observed plant rooting depths exceed those used in vegetation models; this discrepancy between observed and modelled rooting depths can have implications for plant water availability (Ostle *et al.*, 2009). Experiments where precipitation has been artificiality reduced to examine the response of tropical forests to drought have demonstrated dramatic reductions in tree biomass with the highest mortality rates exhibited by large trees (Nepstad *et al.*, 2007; da Costa *et al.*, 2010). Worryingly, a number vegetation models appear to under represent the magnitude of these observed responses to drought (Galbraith *et al.*, 2010; Powell *et al.*, 2013). However, progress at understanding drought induced vegetation responses in vegetation models is improving rapidly (see McDowell *et al.*, 2013*a*). The accurate representation of plant water relations requires sub-models of plant hydraulics.

Modelling plant water transport though the soil-plant-atmosphere hydraulic continuum requires consideration of multiple plant compartments (Hickler *et al.*,

2006). Implementations of the cohesion-tension theory of plant water ascent using an Ohm's law analogy have been shown to mimic important plant hydrological phenomena (Tyree, 1997; Sperry *et al.*, 1998). We implement a simplified version of the cohesion tension theory adopted by Sperry *et al.* (1998) where elements determining plant conductances are considered in series. In order to properly constrain emergent plant hydraulic strategies in aDGVM2 we consider the conductances of the following hydraulic elements; soil-root, root, sapwood and leaf. We implement a set of trait trade-offs which define a plant's hydraulic strategy in which hydraulic safety trades-off against xylem and leaf conductivity (Markesteijn *et al.*, 2011). We detail this implementation below.

The matric potential at which a 50% loss of xylem conductivity occurs, P_{50}, is a key trait regulating plant hydraulic strategies. In aDGVM2, P_{50}, is a plant trait defined by the GOA (Table 3.3) with values ranging from -3.0 to -0.2 MPa. We use the empirical relationships described in Markesteijn *et al.* (2011) to describe relationships between P_{50}, wood density (ρ_{wood}), leaf dry matter content (L_{DMC}), sapwood conductivity (k_{sw}) and leaf conductivity (k_{leaf}). We calculate ρ_{wood} as

$$\rho_{wood} = 0.259 + (-0.05921 \cdot P_{50}) \cdot 10^3 \cdot 1.55, \tag{3.46}$$

where 10^3 and 1.55 convert to ρ_{wood} to kg m^{-3}. L_{DMC} (g g^{-1}) is calculated as

$$L_{DMC} = 0.224 + (-0.041 \cdot P_{50}). \tag{3.47}$$

L_{DMC} in turn defines tree specific leaf area $A_{SL_{tree}}$ (m^2 kg^{-1})

$$A_{SL_{tree}} = \frac{1}{L_{DMC} \cdot L_T}, \tag{3.48}$$

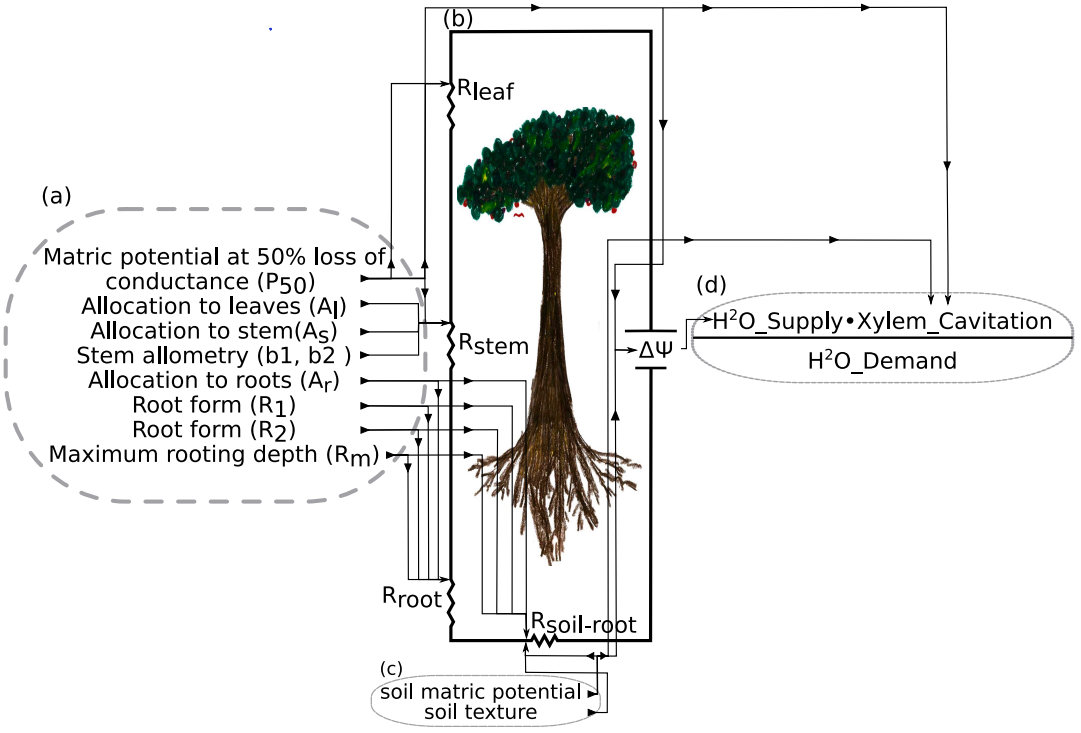

FIGURE 3.2: (a) Traits which can evolve and influence plant hydraulics in (b) and (d), (b) Ohm's law analogy of plant transpiration, $\Delta\Psi$ is the water potential difference between soil and leaf driving water flow while soil-root, root, stem, and leaf resistances mediate flow rates, (c) soil properties influencing (b) and (d), (d) Plant water availability G_w (eq.3.54) is determined by the quotient of water supply E_{canopy}, which is modified by xylem cavitation G, and water demand E_p^t.

L_T (mm) is tree leaf thickness, we assumed tree leaf thickness increases as a function of P_{50} where,

$$L_T = \frac{0.0224 - (0.041 \cdot P_{50})}{0.224 - (0.041 \cdot P_{50})}. \tag{3.49}$$

Sapwood conductivity k_{sw} (kg s^{-1} m^{-1} MPa^{-1}) is calculated as

$$k_{sw} = \frac{581.85 + (90.07 \cdot P_{50} \cdot 18)}{10^3} \cdot \frac{A_{sw}}{H}, \tag{3.50}$$

where H (m) is plant height and sapwood area A_{sw} (m^2) is calculated following Meinzer *et al.* (2001) as

$$A_{sw} = \frac{1.582 \cdot D_s^{1.764}}{10^4}, \tag{3.51}$$

where D_s is stem diameter. Leaf conductivity k_{leaf} (kg s^{-1} m^{-1}) is calculated as

$$k_{leaf} = \frac{61.993 + (7.758 \cdot P_{50} \cdot 18 \cdot 0.001)}{10^3} \cdot A_{leaf}, \tag{3.52}$$

where A_{leaf} is leaf area (m^2) and is calculated as

$$A_{leaf} = D_c(0) \cdot L. \tag{3.53}$$

Here, $D_c(0)$ is the canopy area at the ground and L is leaf area index.

Water transport

We calculate plant water availability, G_w, as follows

$$G_w = \min\left(1, \frac{E_{canopy} \cdot G}{E_t^p}\right), \tag{3.54}$$

where E_t^p is a plant's evapotranspiration calculated using Eq. (3.83) and E_{canopy} is the amount of water which can be extracted from the soil and transported through an individual for the purpose of transpiration,

$$E_{canopy} = \frac{\Delta\Psi}{(R_{sw} + R_{leaf} + R_{root} + R_{soil-root}) \cdot \eta}. \tag{3.55}$$

The viscosity of water, η, is taken to be 1.00. R_{sw} and R_{leaf} are sapwood and leaf resistivity while R_{root_i} and $R_{soil-root_i}$ are the root and soil to root resistances of

the i^{th} soil layer. For grasses, R_{sw} is omitted. The potential difference driving transpiration, $\Delta\Psi$ (MPa), is calculated as

$$\Delta\Psi = P_{50} - \frac{H \cdot \rho_{water} \cdot g}{10^6} - \Psi_{soil}, \tag{3.56}$$

here H is plant height, ρ_{water} is the density of water (999.97 kg m^3), g is acceleration due to gravity (9.8 m s^{-2}) and 10^{-6} scales to MPa. Ψ_{soil} is the average soil matric potential an individual experiences across it's root profile and is calculated as

$$\Psi_{soil} = \sum_{i=1}^{n} \Psi_{soil_i} \cdot R_{Fi}. \tag{3.57}$$

The soil matric potential of the i^{th} soil layer, Ψ_{soil_i}, is calculated following Verhoef & Egea (2014) as

$$\Psi_{soil_i} = \frac{-\phi_{soil} \cdot es^{-r}}{100}, \tag{3.58}$$

where es is the effective saturation of the soil

$$es = \frac{\theta_i - rc}{\theta_{swc} - rc}, \tag{3.59}$$

θ_i is the soil water content in soil layer i, rc is the residual content (Rawls *et al.*, 1982), θ_{swc} (Saxton & Rawls, 2006) is the saturated water content. Saturation suction, ϕ_{soil} (Clapp & Hornberger, 1978), r (Boone *et al.*, 2004), rc and θ_{swc} are soil texture specific parameters, see Table 3.1.

We calculate R_{sw} as

$$R_{sw} = \frac{1}{k_{sw}}, \tag{3.60}$$

and R_{leaf} as

$$R_{leaf} = \frac{1}{k_{leaf}}, \tag{3.61}$$

where k_{sw} and k_{leaf} are sapwood and leaf conductivity as defined in Equations (3.50) and (3.52).

Root resistance across a plant's root profile R_{root} is calculated by summing the resistances across all soil layers and is calculated following Hickler *et al.* (2006)

$$R_{root} = \sum_{i=1}^{n} R_{root_i}, \tag{3.62}$$

where

$$R_{root_i} = \frac{1}{k_{root_i}}, \tag{3.63}$$

k_{root_i} (kg kg^{-1} s^{-1} MPa^{-1}) is calculated as a function of fine root biomass B_{Fr}. We assume that 20% and 90% of total root biomass is fine root biomass for trees and grasses respectively and we calculate conductance as

$$k_{root_i} = 0.0004 \cdot B_{Fr} \cdot R_{Fi}, \tag{3.64}$$

where R_{Fi} is the proportion of an individual's root biomass in soil layer i. Soil to root resistance $R_{soil-root}$ (m^2 MPa s kg^{-1}) is calculated by summing the resistances across the all soil layers and is calculated following Fisher *et al.* (2007)

$$R_{soil-root} = \sum_{i=1}^{n} R_{soil-root_i}, \tag{3.65}$$

and

$$R_{soil-root_i} = \log\left(\frac{\sqrt{\frac{1}{L_i \cdot \pi}}/r}{2 \cdot \pi \cdot L_i \cdot K_{soil_i} \cdot g}\right), \tag{3.66}$$

where L_i is the root length (m) in the i^{th} soil layer, r is the root radius (m) which is set to 0.0005m (Williams *et al.*, 2001). K_{soil_i} is soil hydraulic conductivity of the i^{th} soil layer and is calculated using Eq. (3.82). Again following Fisher *et al.* (2007),

we calculate root length L_i for the i^{th} soil layer as

$$L_i = \frac{B_{Fr} \cdot R_{Fi} \cdot 1000}{\rho_{root} \cdot \pi \cdot r^2}, \tag{3.67}$$

where ρ_{root} is the density of root material (g m^{-3}). We assume root material density is the same as wood density ρ_{wood}.

In aDGVM2 it is assumed that xylem vulnerability to cavitation regulates transpiration by reducing canopy water supply, we thus scale plant water supply by a measure of xylem cavitation G,

$$G = 1 - \frac{1}{1 + e^{a(\Psi_{soil} - P_{50_{root}})}}, \tag{3.68}$$

where a is an empirically defined parameter which determines the slope of the G curve and is currently set to 5. $P_{50_{root}}$ defines the point at which 50% of conductance is lost

$$P_{50_{root}} = P_{50} + 0.2 + (H \cdot \rho_{water} \cdot g) \cdot 10^{-6}, \tag{3.69}$$

where H is plant height, ρ_{water} is the density of water (999.97 kg m^3), g is acceleration due to gravity (9.8 m s^{-2}) and 10^{-6} scales to MPa. Roots usually cavitate at less negative matric potentials than stems, we thus add 0.2 MPa to P_{50} to account for this.

3.3.7 Carbon balance

Leaf level photosynthetic rates A_0 are scaled to the canopy level by using the plant's light and water availability. Light competition is described by a parameter Q_t (see section 3.3.5, water stress is described by a parameter G_w (see section 3.3.6). The canopy photosynthetic rate is then given by

$$A = Q_t \cdot G_w \cdot D_c(0) \cdot A_0. \tag{3.70}$$

Respiration is simulated as in aDGVM (Scheiter & Higgins, 2009) and we do not provide all details here. The respiration model separates between growth and maintenance respiration. Growth respiration is a fixed fraction of the photosynthetic carbon gain, maintenance respiration is defined by biomass, C:N ratios and temperature and it is calculated separately for each biomass pool. In the model it is assumed that bark has the maintenance costs as stem biomass, reproduction biomass has the maintenance costs as leaf biomass and storage has the maintenance costs as root biomass.

When plants are in the metabolic state, then the net carbon balance is given by

$$\Delta C = A - R_g - R_m, \tag{3.71}$$

where A is the water and light limited canopy photosynthetic rate, R_g is the growth respiration and R_m is maintenance respiration. When plants are in the dormant state, they do not have a photosynthetic carbon gain and they are only affected by maintenance respiration and turnover.

Turnover, that is the permanent mortality of leaf biomass, is a function of SLA and leaf biomass. Each day, leaf biomass is reduced by a value

$$B_{turnover} = \frac{1}{29664 \cdot (A_{SL} \cdot 10)^{-0.909}} \cdot B_l. \tag{3.72}$$

This function creates a tradeoff; leaves with high SLA ensure high photosynthetic rates while longevity is short. In contrast, leaves with low SLA have lower photosynthetic rates but higher longevity (Figure 3.3). Hence, the total photosynthesis of a leaf over it's lifespan can be similar for leaves with high and low SLA.

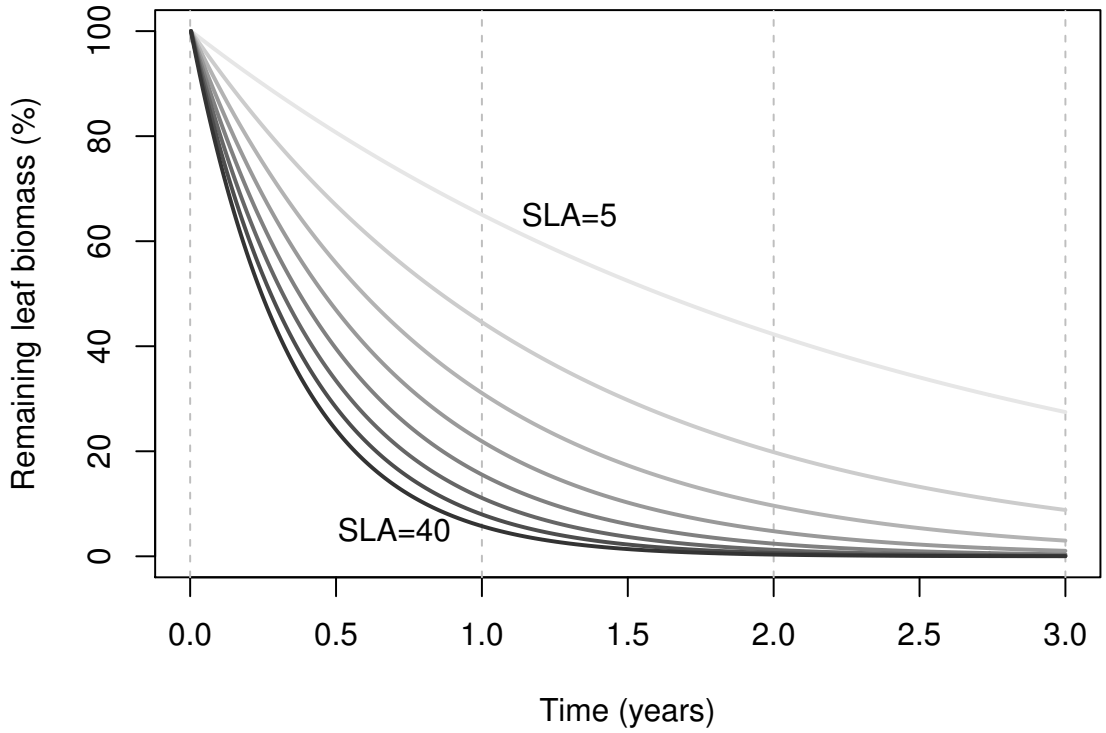

FIGURE 3.3: Leaf turnover as a function of SLA.

3.3.8 Carbon allocation

The carbon gained by photosynthesis ΔC needs to be allocated to the different biomass pools of the plant (leaf, stem, bark, roots, storage, reproduction, Figure 3.4). Although there are complex models that describe carbon allocation based on the environmental conditions and deficits of the plants (Tilman, 1988; Friedlingstein *et al.*, 1999), we use a simple carbon allocation scheme in aDGVM2. We assume that carbon allocation to different biomass pools is given by fixed parameters A_p, where p indicates one of the biomass pools. All A_p must sum to one. The parameters A_p differ between single plants and they are adjusted by the GOA (Table 3.3). This allocation rule implies a mass balance trade-off as an increase of allocation to one pool implies a decrease of allocation to at least one other pool. Allocation to leaf is assumed to be dynamic and a function the plant's leaf area index

$$A_{leaf}^{dyn} = \frac{A_{leaf}}{1 + \mathrm{e}^{c_1(L-c_2)}}, \tag{3.73}$$

where c_1 and c_2 are constants (c_1=3, c_2=7). This dynamic allocation function ensures that carbon allocation to leaves and leaf growth is high when plants move from the dormant to the metabolic state (see section *"Leaf phenology"*) or after fire has removed leaf biomass and that allocation to leaves decreases when the leaf area index approaches seven. For higher LAI, additional leaf biomass does not increase carbon gain substantially because Q_0 (Eq. 3.37) saturates. For trees we assume that as the difference between A_{leaf} and A_{leaf}^{dyn} is added to carbon allocation to stem A_s while for grasses this difference is distributed evenly across all plant compartments. We further assume that the individual's storage biomass pool size can not be larger than the root biomass pool and storage for trees and grasses cannot exceed 0.5 and 50 kg respectively, hence when $B_{storage} > B_{root}$ then

$A_{storage} = 0$. This is to prevent excessively large storage pools from accumulating and allow dynamic allocation to the other carbon pools.

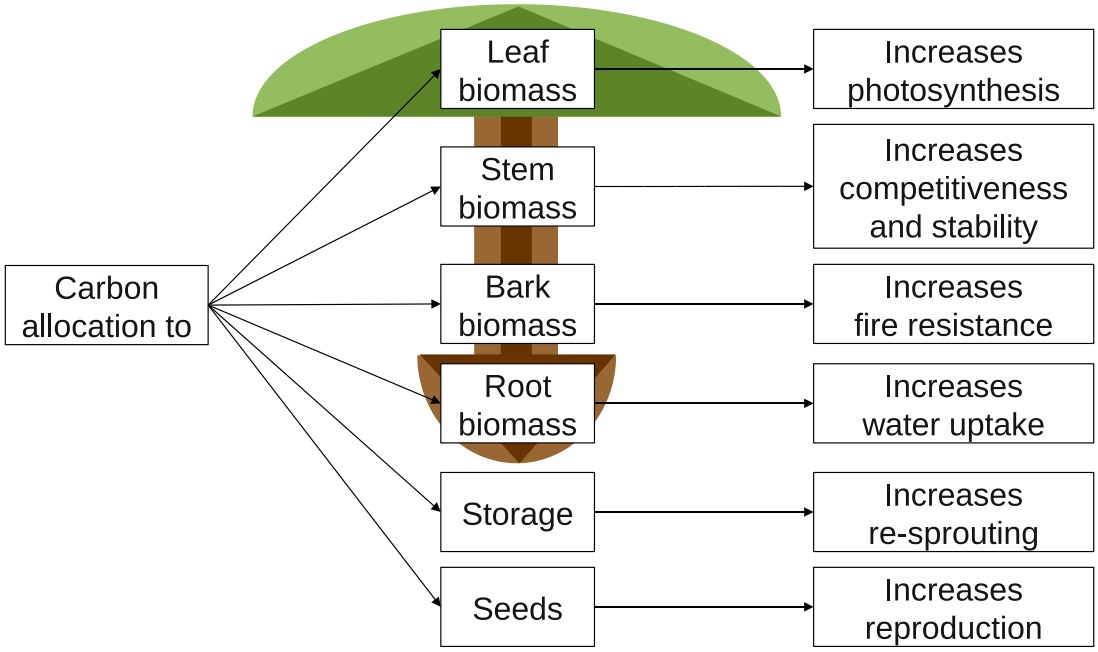

FIGURE 3.4: Biomass pools of single plants and benefits of carbon allocation to the biomass pools.

3.3.9 Leaf phenology

Four phenology strategies are considered. Deciduous (soil matric potential triggered leaf flush and abscission), deciduous (light triggered leaf flush and abscission), evergreen (soil matric potential triggered leaf flush) and evergreen (light triggered leaf flush). Whether a plant is evergreen or deciduous is described by a trait P_E which is defined by the GOA (Table 3.3). Whether a plant's leaf flush is governed by soil matric potential or light is described by a trait P_S which is modified by the GOA (Table 3.3).

A cost of cavitation is implemented whereby, if Ψ_{soil} (integrated over the plant's rooting profile, Equation 3.57) is more or less negative than P_{50} a cavitation

counter C_{cav} is incremented or decreased. If this counter exceeds 30 then an unscheduled abscission event occurs. During an unscheduled abscission event 2% of leaf and root biomass is lost, this loss of biomass occurs daily until either biomass approaches zero or C_{cav} is less than 30.

Deciduous trees abscise leaves according to the light or Ψ_{soil} triggers. During such a scheduled abscission we assume that a constant proportion (we assume 30%) of leaf biomass is transferred to storage and the remainder is lost to leaf litter. For both evergreen and deciduous strategies, when leaf flush occurs (in accordance with the light or Ψ_{soil} triggers) carbon in the storage pool is used. When plants flush their leaves, a fraction A_{TL} of the storage biomass is allocated to leaf biomass to enable photosynthesis. The parameter A_{TL} is a trait and defined by the GOA (Table 3.3). The carbon cost of this reallocation is assumed to be 35%, i.e. the growth respiration cost.

For soil moisture triggered plants, when soil matric potential falls below a threshold T_{rd} for 7 days, then the plant moves into the dormant state. For light triggered plants, when light availability falls below a threshold T_{ld} for 7 days the plant moves into the dormant state. For deciduous strategies this leads to leaf abscission while for evergreen strategies it sets a phenology trigger to the off state. When soil matric potential across the rooting zone exceeds T_{rd} for 7 days or when light availability exceeds T_{lu} for 7 days, then leaf flush from storage is initiated and deciduous plants move from the dormant to the metabolic state. The parameter T_{rd} is constrained to be less negative than an individual's P_{50}. The parameters T_{rd}, T_{ld} and T_{ru} are traits defined by the GOA (Table 3.3).

3.3.10 Reproduction, inheritance, mutation, and cross-over

One major feature of aDGVM2 is that each plant is characterised by an individual combination of trait values (Table 3.3). This trait combination is passed to the offspring of the plant. Additionally, trait combinations can be modified by mutation and cross-over. The model iteratively generates various trait combinations but only a limited set of these trait combinations can survive and reproduce under the given environmental conditions. Hence, the model iteratively assembles a set of trait combinations (or a plant community) that is optimally adapted to the environment (Fig. 3.5). The following paragraphs describe these processes in more detail.

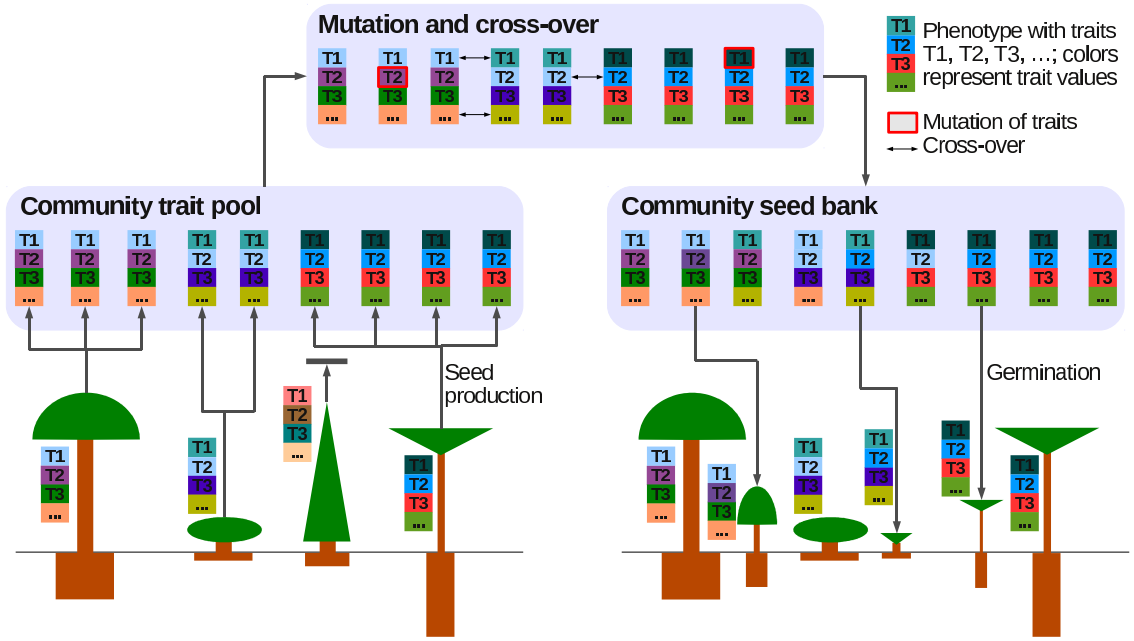

FIGURE 3.5: Scheme of the seed bank model. Plants produce seeds which are modified in the seed bank by mutation and cross-over (Scheiter *et al.*, 2013).

The number of seeds produced by each plant ϕ is defined by the biomass in the reproduction pool B_P and by the seed weight W,

$$\phi = \left\lfloor \frac{B_P}{W} \right\rfloor, \tag{3.74}$$

where $\lfloor x \rfloor$ describes the integer value of x. The biomass ϕW is removed from the reproduction biomass pool B_P. The seed bank collects the seeds of all plants. Seeds store the trait combination of the parent plant. For reasons of model performance, we assume that a plant can add a maximum of 200 seeds into the seed bank; our seed bank, of size 720,000 can then store up to 3600 seeds with different trait combinations for trees and grasses respectively.

In the model we allow mutation and cross-over to modify the trait values of the seeds. We assume that $\mathbf{T}_i = (T_{i1}, T_{i2}, \ldots, T_{in})$ is the trait combination of a seed i, that is a vector with the n trait values. Here, the vector $\mathbf{T}_i$ only contains traits which are subjected to the modification; these are the traits given in Table 3.3.

Mutation

Mutation means that trait values can randomly fluctuate. Mutation is defined by two parameters, (1) the mutation probability m_p and (2) the mutation rate m_r. The mutation probability a is pre-defined model parameter set to 0.01. For each trait of each seed, a random number between 0 and 1 is calculated, when this random number between is less than m_p then mutation will occur. When a trait value of a seed mutates, then a random number m_j in the interval between $1 - m_r$ and $1 + m_r$ is drawn for each trait in $\mathbf{T}$ and the new trait value T_j^* is obtained by multiplying old trait values with m_j, that is, $T_j^* = m_j \cdot T_j$. The mutation rate m_r is a pre-defined model parameter set to 0.05

Cross-over

The cross-over algorithm used in aDGVM2 is based on the genetic optimisation algorithm DEoptim (Price *et al.*, 2005) as implemented in R (R Development Core Team, 2008; Mullen *et al.*, 2009). The basic concept of the cross-over algorithm is to recombine trait combinations $\mathbf{T}_i$ to obtain a new set of trait combinations $\mathbf{T}_i^*$. Cross-over is restricted to seeds possessing the same species label. New trait combinations $\mathbf{T}_i^*$ are generated by using the original trait values $\mathbf{T}_i$ and values from a randomly drawn seed $\mathbf{T}_{random}$ which has the same species index. For each seed and each trait, crossover happens when a random number between 0 and 1 is less than the crossover probability C_p which is a fixed parameter set to 0.5. When cross-over occurs, then the new trait combination $\mathbf{T}_i^*$ is calculated as

$$\mathbf{T}_i^* = \mathbf{T}_i + c_f \cdot (\mathbf{T}_{random} - \mathbf{T}_i)\,, \tag{3.75}$$

where c_f is a random number between 0 and 1 that is drawn for each trait of each seed. The cross-over routines in aDGVM2 ensure that trait values of a new seed are within the range of trait values of a plant's species.

3.3.11 Plant recruitment

Once per year, new recruits are added to the plant population. As the plant population size N_{max} is fixed in the model, only a limited number of recruits can be added to the plant population. The probability of a grass or tree seed being drawn from the population of seeds is equal. The trait combination of a recruit is given by randomly selecting a seed from the seed bank. The availability of light to and

weight of a seed can affect it's germination probability (Denslow, 1987) (Pearson *et al.*, 2002). We thus calculate seed germination probability P_{germ} as

$$P_{germ} = (W + 0.04) - \left[0.15 \cdot \min\left(1, \frac{C_{gap}}{C_{eff}}\right)\right] \tag{3.76}$$

where W is the seed weight and C_{gap} is the summed canopy area at the ground of neighbouring trees, see section 3.3.5, and C_{eff} is a constant set to 50 which affects the degree to which canopy closure alters germination probability.

3.3.12 Plant mortality

Once per year, plant mortality is simulated. There are several potential reasons for plant mortality, (1) negative carbon balance, (2) insufficient height growth and (3) mechanic instability.

Negative carbon balance

A plant is removed from the plant population when it has a negative carbon balance ΔC (Equation 3.71) and when a random number between zero and one is less than the mortality probability M_C.

No height growth

A tree is removed from the plant population when it's height is below a threshold level of $M_B = 5$cm after 2 years. This rule removes trait combinations that cannot grow under the given environmental conditions.

Mechanic instability

We assume that mechanic instability of tree stems can lead to buckling and plant mortality Marks & Lechowicz (2006). The probability for mortality as a result of mechanic instability P_i is defined as

$$P_i = \max\left(M_I\left(\frac{H}{H_{crit}} - 1\right)\right). \tag{3.77}$$

where H_{crit} is the critical buckling height (eq. 3.28), H is the plant height and M_I is a mortality parameter, Table 3.4. When a random number between zero and one is less than P_i then a tree is removed from the plant population.

3.3.13 Grass fire and tree topkill

The fire model used in aDGVM2 is similar to the fire model used in aDGVM (Scheiter & Higgins, 2009). By using fuel moisture θ_F, fuel biomass B_F and wind speed u_{ref} we calculate the potential fire intensity following Higgins *et al.* (2008) as

$$I(B_F, \theta_F) = hB_F \frac{\arctan(u_{ref}) \cdot c \cdot f(B_F, a_w)}{Q_m \cdot \theta_F + Q_v(1 - \theta_F)}. \tag{3.78}$$

Here, Q_m and Q_v are heats of preignition of moisture and fuel, c is regression parameter and h is the heat yield of fuel consumed. Further,

$$f(B_F, a_w) = \frac{B_F}{B_F + a_w} \tag{3.79}$$

is a sigmoidal function defined by a regression parameter a_w.

For a fire to occur on a particular day, the matric potential of the first soil layer must be less than -1.5 (MPa), precipitation must be less than 5 (mm), a random

number between 0 and 1 must be less than P_{fire} where P_{fire} is calculated as

$$P_{fire} = 0.003 \cdot \max\left(0.01, \frac{\sum_{i=1}^{n} D_{c,i}(0)}{8000}\right). \tag{3.80}$$

These conditions implicitly ensure that fuel is dry enough to carry fire. We assume that fire probability is higher in more open vegetation stands with low tree cover and that fire probability decreases as tree cover increases, here $D_{c,i}(0)$ is the canopy area at the ground of the ith tree.

Fire removes the total aboveground grass biomass, the total dead aboveground biomass and it can cause topkill, that is, damage of aboveground tree biomass. For fire to spread the fire intensity must exceed a minimum of 300 (kJ s^{-1}m^{-1}). Following Higgins *et al.* (2000) the probability of topkill is an empirically derived function of fire intensity I and tree height H,

$$P_{topkill}(H, I) = \frac{D_i}{D_s} \cdot \frac{\exp(D_1 - D_2 \cdot \ln(H) + D_3 \cdot \sqrt{I})}{1 + \exp(D_1 - D_2 \cdot \ln(H) + D_3 \cdot \sqrt{I})}, \tag{3.81}$$

where D_i and D_s are the stem diameters excluding and including bark and D_1, D_2 and D_3 are regression parameters. By the multiplication with the stem diameters we simulate that bark protects vegetation against fire. This effect is supported by empirical evidence from Brazilian Cerrados (Higgins *et al.*, 2008; Hoffmann *et al.*, 2009, 2012), yet it is weak in other savanna areas. Topkilled trees loose their aboveground biomass, however, storage biomass A_T allows them to re-sprout and to recover from the disturbance. To re-sprout, plants allocate fractions A_{TS} and A_{TL} of the storage biomass to stem and leaf biomass. The fractions A_{TS} and A_{TL} are traits and defined by the GOA.

3.3.14 Water balance

To describe the soil water balance, we use a multi-layer tipping bucket model of soil moisture, similar to the model used in aDGVM (Scheiter & Higgins, 2009). In aDGVM2, rainfall is tipped from one layer into the next deeper layer when the soil moisture content exceeds the saturated water content θ_{swc}. Percolation between soil layers is calculated following Campbell (1974) using the equation

$$K_{actual_i} = K_{sat} \cdot \left(\frac{\theta_i}{\theta_{swc}} \right)^{2r+2} \tag{3.82}$$

where K_{actual_i} is the non-saturated hydraulic conductivity of soil layer i, K_{sat} is saturated hydraulic conductivity, θ_i is the actual soil moisture content of soil layer i, θ_{swc} is the saturated soil moisture content while r determines the rate at which percolation decreases as soil dries. The parameters K_{sat}, θ_{swc} and r are related to soil texture, Table 3.1. The amount of water percolating from one soil layer to the next is calculated daily.

A plant's evapotranspiration is calculated using the Penman-Monteith equation (Jones, 1992; Allen *et al.*, 1998),

$$E_t^p = \frac{s \cdot Q_0 + 86400 \cdot \rho_{air} \cdot c_p \cdot h_{vpd} \cdot g_b^c}{\lambda \left(s + \gamma \left(1 + \frac{g_b^c}{g_s^c} \right) \right)}. \tag{3.83}$$

Here s is the slope of vapour pressure curve, Q_0 is the net radiation, ρ_{air} is the density of air, c_p is the specific heat of moist air, h_{vpd} is the saturation vapour pressure deficit, g_b^c is the canopy boundary layer conductance from eq. (3.16), λ is the latent heat of air, γ is the psychrometric constant and g_s^c is the canopy stomatal conductance from eq. (3.14). As in Scheiter & Higgins (2009), Allen *et al.* (1998)'s detailed guide to the computation of the components of E_t^p is used.

TABLE 3.1: Soil properties. θ_{swc}: saturated water content; K_{sat}: saturated hydraulic conductivity; ϕ_{soil}: Saturation suction; r: shape parameter describing how percolation decreases as soil dries; rc: residual soil water content.

Soil Code HWSD	θ_{swc} ($m^3\ m^{-3}$)	K_{sat} ($m\ hr^{-1}$)	ϕ_{soil} (m)	r	rc ($m^3\ m^{-3}$)
1	0.50	0.00133	0.405	12.13	0.020
2	0.52	0.0037	0.49	10.21	0.035
3	0.52	0.0037	0.49	10.21	0.041
4	0.51	0.0057	0.356	8.16	0.027
5	0.48	0.0043	0.63	8.16	0.015
6	0.48	0.022	0.63	3.63	0.068
7	0.48	0.0161	0.786	5.42	0.075
8	0.44	0.0014	0.153	9.39	0.040
9	0.46	0.0155	0.478	6.10	0.109
10	0.43	0.0113	0.356	6.77	0.056
11	0.45	0.0503	0.218	4.73	0.090
12	0.46	0.0967	0.09	4.32	0.090
13	0.46	0.1081	0.121	3.91	0.121
Nachtergaele *et al.* (2012)	Saxton & Rawls (2006)	Saxton & Rawls (2006)	Clapp & Hornberger (1978)	Boone *et al.* (2004)	Rawls *et al.* (1982)

TABLE 3.2: Input data from databases and secondary environmental variables. Secondary environmental variables are calculated as in Scheiter & Higgins (2009). "variable" indicates that this parameter is a modelled variable.

Name	Description	Value	Units
T_Δ	Daily temperature range	database	°C
$\bar{T}$	Mean day temperature	database	°C
w_f	Wet day frequency	database	frequency
r_m	Mean value of rain	database	$mm/_{month}$
r_{cv}	Coefficient of variance of rain	database	%
p_s	Percentage of sunshine per day	database	%
h_s	Relative humidity	database	%
d_f	Frost days per month	database	$days/_{month}$
u_{ref}	Reference wind speed	database	$m/_s$
Z	Elevation	database	m
P	Atmospheric partial pressure	variable	Pa
T	Day temperature	variable	°C
T_{min}	Minimum temperature	variable	°C
T_{max}	Maximum temperature	variable	°C
s	Slope of vapor pressure curve	variable	$kPa/_C$
γ	Psychrometric constant	variable	$kPa/_C$
e^A	Actual vapor pressure	variable	kPa
e^S	Saturation vapor pressure	variable	kPa
ρ_{air}	Density of air	variable	g/m^3
h_{vpd}	Saturation vapor pressure deficit	variable	kPa
Q_p	Photosynthetically active radiation	variable	$^-mol/m^2s$
Q_0	Net radiation	variable	$^-mol/m^2s$
F_i	Simulated precipitation at day i	variable	mm

TABLE 3.3: Plant traits modified by the genetic optimisation algorithm. The columns 'Min' and 'Max' define the minimum and maximum possible trait values used for the genetic optimization algorithm for trees and C_4 grasses.

Name	Description	Trees		C_4 Grasses	
		Min	Max	Min	Max
P_{50}	Matric potential at 50% loss of conductance	-3	-0.2	-3	-0.2
A_R	Allocation to roots	0.2	0.4	0.2	0.8
A_L	Allocation to leaves	0.35	0.5	0.25	0.5
A_S	Allocation to stem	0.25	0.35	0	0
A_B	Allocation to bark	0	0.05	0	0
A_T	Allocation to storage	0.1	0.4	0	0.4
A_P	Allocation to reproduction	0.05	0.2	0.01	0.2
P_S	Phenology (rain/summergreen, evergreen)	0	1	0	1
P_E	Phenology (deciduous or evergreen)	0	1	0	0
T_{rd}	Rain threshold for plant dormancy	-3	-0.2	-3	-0.2
T_{lu}	Light threshold for plant activity	6	14	6	14
T_{ld}	Light threshold for plant dormancy	6	14	6	14
b_1	Parameter for height calculation	2.4	2.8	na	na
b_2	Parameter for height calculation	0.4	0.5	na	na
R_1	Parameter for the root form	0.01	10	0.01	10
R_2	Parameter for the root form	-1	20	1	20
R_m	Maximum rooting depth	1.0	10.0	1.0	1.0
W	Seed weight	0.001	0.05	0.001	0.05
C_2	Parameter for the canopy form	21	25	20	60
A_{TS}	Storage to stem allocation after fire	0.2	0.4	0	0
A_{TL}	Storage to leaf allocation	0.6	0.9	0	1.0

TABLE 3.4: Plant traits not modified by the genetic optimisation algorithm.

Name	Description	Trees	C_4 Grasses	Reference
M_C	Mortality: negative carbon balance	0.2	0.4	tuning parameter
M_B	Mortality: low height	0.05	na	tuning parameter
M_I	Mortality: mechanic instability	10	na	tuning parameter
T_C	Topkill parameter	4.3	0	Higgins *et al.* (2000)
T_H	Topkill parameter	5.003	0	Higgins *et al.* (2000)
T_I	Topkill parameter	0.004408	0	Higgins *et al.* (2000)
M	Ball Berry constant	9.0	4.0	Ball *et al.* (1987)
B	Ball Berry constant	0.01	0.04	Ball *et al.* (1987)
R_m	Maintenance respiration constant	0.015	0.025	Collatz *et al.* (1991, 1992)
R_g	Growth respiration constant	0.35	0.35	Arora (2003)
R_l	Respiration constant, leaves	0.01	0.01	Scheiter & Higgins (2009)
R_s	Respiration constant, stem	0.01	0.01	Scheiter & Higgins (2009)
R_r	Respiration constant, roots	0.01	0.01	Scheiter & Higgins (2009)
R_n	Respiration constant	0.281	0.281	Arora (2003)
v_l	C:N ratio leaves	120	120	Scheiter & Higgins (2009)
v_s	C:N ratio stem	150	120	Scheiter & Higgins (2009)
v_r	C:N ratio roots	60	120	Scheiter & Higgins (2009)
C_1	Parameter for the canopy form	10.0	na	following Strigul *et al.* (2008)

TABLE 3.5: Photosynthesis sub-model.

Name	Description	Value C_3	Value C_4	Units
A_{max}	Maximum light saturated photosynthesis	variable	variable	$^{-}mol/m^2s$
A_0	Gross photosynthetic rate	variable	variable	$^{-}mol/m^2s$
A_n	Net photosynthetic rate	variable	variable	$^{-}mol/m^2s$
A_0^b	Gross photosynthesis (bio-physical)	variable	variable	$^{-}mol/m^2s$
A_n^b	Net photosynthesis (bio-physical)	variable	variable	$^{-}mol/m^2s$
A_n^d	Net photosynthesis (diffusion)	variable	variable	$^{-}mol/m^2s$
V_{max}	Maximum carboxylation rate	variable	variable	$^{-}mol/m^2s$
A_R	Scaling factor for C_4 photosynthesis	1	39/90	unitless
A_S	Scaling factor for V_{max}	2	2	unitless
R_{mLs}	Constant leaf level respiration rate	0.82	1.36	$^{-}mol/m^2s$
c_a	Atmospheric partial pressure of CO_2	38.1	38.1	Pa
c_i	Internal CO_2 pressure (C_3 only)	$0.7c_a$	—	Pa
c_i	Bundle sheath value (C_4 only)	—	$8c_a$	Pa
K_c	Michaelis constant for CO_2	variable	variable	Pa
K_o	O_2 inhibition constant	variable	variable	Pa
τ	Fraction of RuBP to reaction of rubisco	variable	variable	prop
$f_{25}(T)$	Temperature function for K_c, K_o, τ	variable	variable	unitless
K_{25,K_c}	Constant for f_{25} for K_c	30	140	Pa
Q_{10,K_c}	Constant for f_{25} for K_c	2.1	2.1	Pa
K_{25,K_o}	Constant for f_{25} for K_o	30	34	Pa
Q_{10,K_o}	Constant for f_{25} for K_o	1.2	1.2	Pa
$K_{25,\tau}$	Constant for f_{25} for τ	2600	2600	Pa
$Q_{10,\tau}$	Constant for f_{25} for τ	0.57	0.67	Pa
O_i	Intercellular partial pressure of oxygen	21	21	kPa
Γ_*	CO_2 compensation point	variable	variable	Pa
J_c	Rubisco limited assimilation rate	variable	variable	$^{-}mol/m^2s$
J_e	Light limited assimilation rate	variable	variable	$^{-}mol/m^2s$
J_s	Transport limited assimilation rate for C_3	variable	—	$^{-}mol/m^2s$
J_p	CO_2 limited assimilation rate for C_4	—	variable	$^{-}mol/m^2s$
a	Leaf absorbtance of incident flux	0.86	0.80	unitless
α	Intrinsic quantum yield of photosynthesis	0.08	0.067	unitless
κ	Initial slope of response of CO_2	—	$0.7{\cdot}10^6$	$^{-}mol/m^2s$
V_{max}^c	Initial estimation for V_{max}	0.8	0.4	$^{-}mol/m^2s$
r	Respiration as fraction of V_{max}	0.015	0.025	prop
c_p	Specific heat of moist air	$1.013{\cdot}10^{-3}$	$1.013{\cdot}10^{-3}$	MJ/kgdegC
λ	Latent heat of air	2.45	2.45	MJ/kg

TABLE 3.6: Stomatal conductance sub-model.

Name	Description	Value C_3	Value C_4	Units
g_s	Leaf level stomatal conductance	variable	variable	$^{-}mol/m^2s$
m	Empirical parameter for g_s	9	4	unitless
b	Empirical parameter for g_s	0.01	0.04	$^{-}mol/m^2s$
g_b	Leaf level boundary layer conductance	variable	variable	m
c_s	Partial pressure of CO_2 at leaf surface	variable	variable	Pa
D_L	Characteristic leaf dimension	0.02	0.005	m
$\bar{H}$	Mean vegetation height	1.5	1.5	m
$u(z)$	Wind at height z from ground level	variable	variable	m/s
z_d	Displacement height	$0.86\bar{H}$	$0.86\bar{H}$	m
z_0	Roughness length	$0.06\bar{H}$	$0.06\bar{H}$	m
z_{ref}	Reference height	10	10	m

Chapter 4

Climate-biomes, pedo-biomes or pyro-biomes: which world view explains the tropical forest - savanna boundary in South America?

Liam Langan, Steven I. Higgins and Simon Scheiter * †

4.1 Introduction

The current distribution of forest within the tropics is well explained by Walter's (1986) zonal biome concept, however, it remains poorly understood why

*This chapter is published in the *Journal of Biogeography* as 'Langan et al. (2017) Climate-biomes, pedo-biomes or pyro-biomes: which world view explains the tropical forest-savanna boundary in South America?'

†Author contributions: All authors conceived and designed the study. aDGVM2 was conceived by S.H. and S.S., and the initial implementation was written by S.S.. L.L. and S.H. redesigned hydraulics submodels and L.L. implemented the designed hydraulics submodels with help from S.S.. L.L. performed the simulations and led the data analyses and writing. All authors contributed to the data analyses and writing.

the position of the forest-savanna biome boundary, in a domain defined by rainfall and temperature, differs in South America, Africa and Australia (Lehmann *et al.*, 2014). Tropical savannas occupy 20% of the land surface (Lehmann *et al.*, 2011) and predicting how these areas respond to our changing climate is therefore important. Unfortunately, dynamic global vegetation models (DGVMs) often under-predict the distribution of the savanna biome (Baudena *et al.* (2015) and references therein). Two hypotheses may explain the between continent variation in the position of the savanna-forest boundary: first, unique evolutionary histories may constrain micro-evolutionary processes and may set the development of vegetation on unique evolutionary trajectories (Moncrieff *et al.*, 2016); second, additional environmental variables may explain the differences between continents.

Empirical field studies suggest that the position of the forest-savanna boundary in South America is mediated by fire (Hoffmann *et al.*, 2012). Furthermore, Bond *et al.* (2005) show in a modelling study that across vast areas of Africa fire plays a crucial role in mediating both biomass and tree cover, however, they also highlight difficulties in explaining the boundary between the rainforest and savanna in mesic South America. Veenendaal *et al.* (2015) and Lloyd *et al.* (2015) question the role fire plays in mediating biome boundaries.

Indeed, there is good agreement that some of the most important variates influencing vegetation along the gradient from arid to humid climates *sensu* Walter & Breckle (1986) are associated with soil (Eiten, 1972, 1982; Huntley, 1982). Huntley & Morris (1982) argue that water availability exerts the largest effect and assert that water and nutrient availability throughout the year determine where the change from forest to savanna occurs. Huntley & Morris (1982) further argue that water availability determines the height and structure of savanna vegetation while nutrient status influences composition. Veenendaal *et al.* (2015) show

the importance of the interacting effects of soil nutrient status, evaporation deficit and stored soil water in determining tropical woody vegetation cover. Lloyd *et al.* (2015) highlight the interacting effects of precipitation, soil water storage capacity and potassium on stand-level canopy area. Edaphic controls can be multifaceted; constraints on the depth to which plants can and do root can occur due to high aluminium concentrations, lack of soil or the presence of hard lateritic layers. Lateritic layers can retard root penetration and result in both waterlogging and reductions in deep soil water recharge. However, how fire, soil nutrient status and constraints on plant rooting depth interact to influence forest-savanna transitions remains unclear.

Climate change has necessitated the development of methodologies for projecting how the global distribution of vegetation formations may develop. This has selected for process based modelling systems, exemplified by Dynamic Global Vegetation Models [DGVMs, Prentice *et al.* (2007)]. The effect of constraints on plant rooting depth on vegetation dynamics is rarely considered in DGVMs (Kleidon & Heimann, 1998). Yet, such constraints can play a key role in determining the success of particular plant strategies as they can influence the total amount of water available to plants. We use aDGVM2 (Scheiter *et al.*, 2013) to explore how constraints on plant rooting depth affect vegetation formations in tropical South America. The aDGVM2 modelling concept and its initial application were described in Scheiter *et al.* (2013). aDGVM2 combines elements of traditional DGVMs (Prentice *et al.*, 2007) in a new architecture where traits are properties of modelled individual plants and trait values evolve via a simulated selection process. Hence, the model deals with the parametrisation of plant functional types differently to conventional DGVMs. Trait values are not prescribed to individuals or to plant functional types but rather evolve during simulations (Fig. 4.1). This

trait evolution is constrained by trade-offs between traits.

aDGVM2 is well suited to studying the effects of fire and spatially variable constraints on plant water availability on the forest-savanna boundary. First, it is individual-based which allows it to model the impacts of biotic and abiotic conditions on individual plants (e.g. fire and stem mortality, Fig. 4.1). Second, light competition is modelled in a spatially explicit way; plant light acquisition is affected by neighbours' height, leaf area index and canopy area (Fig. 4.1). Third, plant water uptake is a function of root biomass in multiple soil layers and therefore allows the consideration of how constraints on plant rooting can affect water availability. Fourth, plant hydrology is represented by the cohesion-tension theory (Tyree, 1997; Sperry *et al.*, 1998) with resistances calculated for roots, stems and leaves. In the model, trait trade-offs ensure that plant hydraulic safety trades-off against efficiency (Markesteijn *et al.*, 2011). This representation ensures that multiple plant traits influence individuals' hydraulic performance, creating a selective environment whereby co-ordination of multiple traits can improve individuals' hydraulic status. These, together with the simulated trait evolution within aDGVM2, provide new opportunities to examine how climate, constraints on plant rooting depth and fire interact to control the distribution of plant functional types and biome boundaries.

Reliably predicting plant responses to changing conditions is a major challenge for biogeography. We argue that understanding how constraints on plant rooting depth mediates plant traits and vegetation distributions will help elucidate how plants will respond to changing conditions. In this study we examine the extent to which constraints on plant rooting depth, fire and precipitation interactively determine the position of the forest-savanna boundary in South America. Specifically, we ask: (1) Do constraints on plant available water, associated with

constraints on plant rooting depth, influence the position of the savanna-forest boundary? (2) Is the position of this boundary influenced by fire? (3) Do these constraints and fire interact to shape community structure?

4.2 Materials and methods

4.2.1 aDGVM2

aDGVM2 is designed to allow us to move away from the paradigm of fixed-trait plant function types (PFTs, Fig. 3.1) as adopted in the original version of aDGVM (Scheiter & Higgins, 2009) and other DGVMs. This requires improvements in the representation of plant competition, hydraulics and community assembly (Scheiter *et al.* (2013), Chapter 2). Scheiter *et al.* (2013) (Chapter 2) describe the modelling concept and provide results that illustrate aDGVM2 functionality. Chapter 3 provides a full model description. Below we summarise important features of aDGVM2.

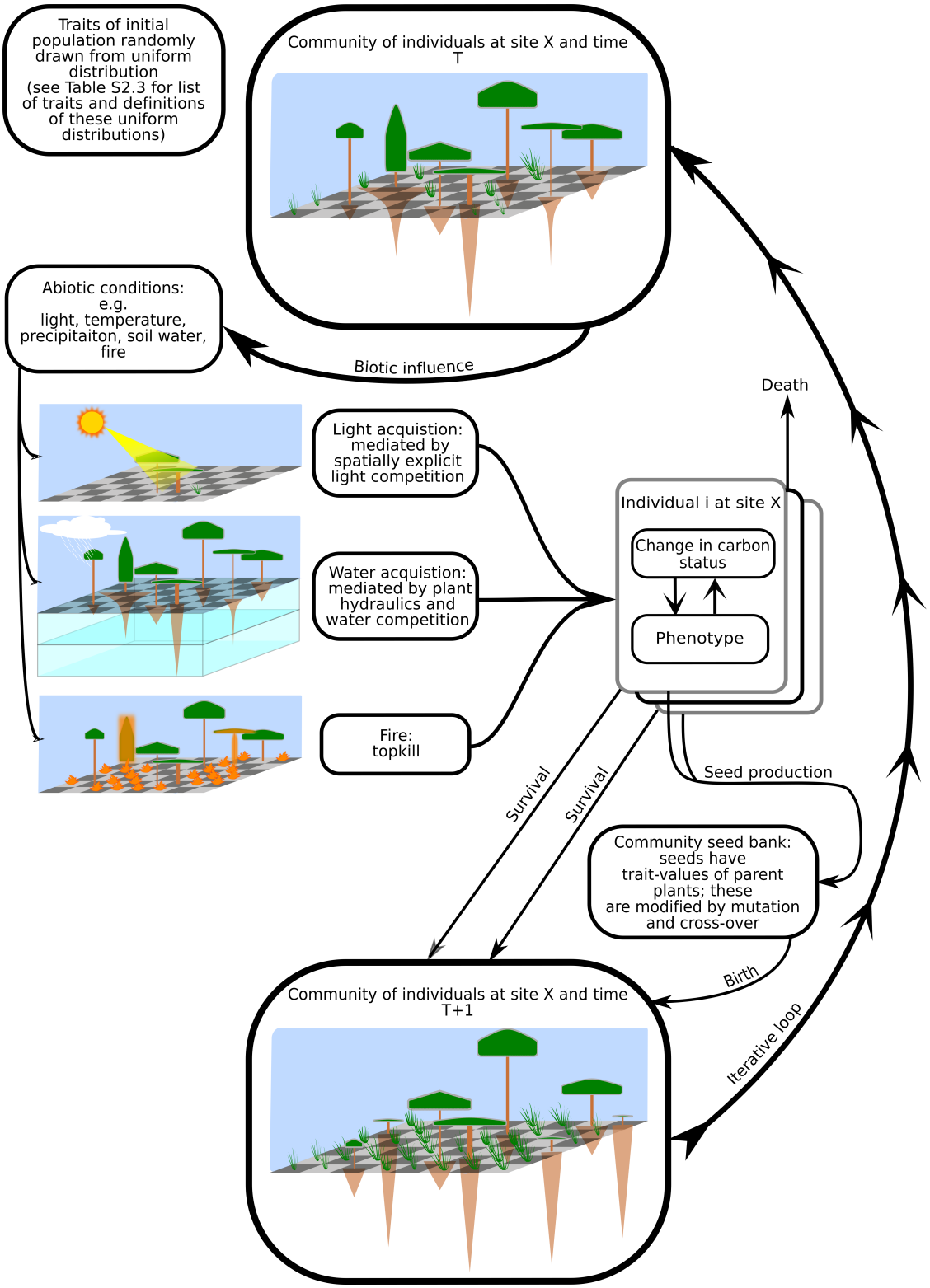

FIGURE 4.1: Conceptual model of aDGVM2 depicting the iterative process through which a community of plants assembles.

The model is individual and trait based (Fig. 4.1). Each plant has a potentially unique set of trait values (all 23 traits that are subject to selection are listed in Table 3.3). An initial plant population is generated whereby each plant's traits are randomly assigned by drawing a uniform random number between the bounds listed in Table 3.3. The bounds (Table 3.3) ensure that each trait is constrained to a plausible range. The performance of an individual with a particular combination of trait values is constrained by trade-offs between traits, abiotic conditions and competition (Fig. 3.1). For example, light competition is simulated by considering how the light acquisition of an individual can be influenced by the height, leaf area index and canopy area of its neighbours. Water competition and plant hydraulics (see section "Plant hydraulics" (4.2.1) below and Fig. 3.2) affect individual's water availability. An individual's photosynthetic carbon gain is scaled by water availability. Disturbance via fire can cause topkill in trees and consumes all above-ground grass biomass. The probability of a tree being topkilled is influenced by its height and bark thickness (section "Grass fire and tree topkill" (3.3.13) in Chapter 3). Height and bark thickness of a tree are determined by its traits and its cumulative carbon status. Resource competition (light and water) and fire interactively shape the plant community by affecting individuals' carbon status as well as the availability of light and soil water. The probability of individual mortality increases with decreasing carbon status. The number of seeds produced by an individual is determined by the amount of total carbon gain allocated to seed production and by seed weight. These values are plant traits. Seeds possess their parent's trait values as modified by mutation and cross-over (Fig. 4.1). Seeds are added to the community seed bank. The subsequent plant population is composed of surviving individuals and newly germinated individuals drawn randomly from the community seed bank. This process of community assembly

and trait selection is iterative, this allows constant adaptation and evolution of plant communities and their trait values (Fig. 4.1).

Plant hydraulics

Sperry & Love (2015) argue that modelling how plants respond to drought is a major challenge for vegetation models that can be addressed by improving their representation of plant hydraulics. Simulating plant water transport though the soil-plant-atmosphere hydraulic continuum requires consideration of multiple plant elements (Hickler *et al.*, 2006). Specifically, the cohesion-tension theory of plant water ascent can be implemented using an Ohm's law analogy (Tyree, 1997; Sperry *et al.*, 1998). We implement a simplified version of the cohesion-tension theory adopted by Sperry *et al.* (1998), where elements determining plant resistances are considered in series (Fig. 3.2b). We calculate plant water availability (G_w, Fig. 3.2d) as the quotient of water supply and water demand as

$$G_w = \min\left(1, \frac{E_{canopy} \cdot G}{E_t^p}\right), \tag{4.1}$$

where E_t^p is canopy water demand, water supply is determined by E_{canopy}, a plant's ability to transport water to the canopy (Eq. 4.2), and G determines the proportion of conductance lost due to xylem cavitation (Eq. 2.67). E_{canopy} is influenced by multiple plant traits (Fig. 3.2a) which affect the resistances of the following hydraulic elements: xylem (R_{sw}), leaf (R_{leaf}), root (R_{root}) and soil-root ($R_{soil-root}$, Fig. 3.2b, Eq. 4.2); as well as soil properties (Fig. 3.2c) and $\Delta\Psi$, the potential difference driving transpiration (Eq. 3.56), such that

$$E_{canopy} = \frac{\Delta\Psi}{(R_{sw} + R_{leaf} + R_{root} + R_{soil-root})}. \tag{4.2}$$

In Eqn. 4.1, G is a function of the difference between soil matric potential experienced by an individual across its rooting profile and P_{50}, the matric potential at 50% loss of conductance. P_{50} is a plant trait which evolves in the model and affects overall plant hydraulic performance whereby more negative P_{50} values lead to increased cavitation resistance. We use empirical relationships in Markesteijn *et al.* (2011) to allow cavitation resistance to trade-off against hydraulic efficiency, whereby increased resistance to cavitation results in higher leaf and stem resistances (Eqns. 3.52, 3.50, 3.61 & 3.60).

Root traits affect individuals' ability to access water across multiple soil layers (Fig. 3.2a). Root and soil-root resistances are calculated based on the shape of an individual's root profile, root biomass, and the depth to which the soil profile is explored by roots. The shape of an individual's rooting profile is determined by two traits, R_1 and R_2, the depth to which a soil profile is explored is determined by the trait R_m. Root biomass is influenced by a trait which determines the proportion of photosynthetically gained carbon allocated to roots, A_r (Fig. 3.2a, Table 3.3). Thus, the depth to which a plant can exploit soil water resources and root biomass directly affect modelled photosynthesis. This framework allows multiple rooting strategies to emerge and provides a flexible framework to examine the effects of constraints on plant rooting depth on plant community assembly and the positions of biome boundaries in environmental space.

4.2.2 Study area

Our study area comprises of sites in Brazil and Venezuela north of 23°S which are classified as either forest or savanna (Table 4.1). The area has a spatial extent of more than 10,000,000 km^2. Vegetation ranges from semi-arid savanna to tropical forest. It includes the Amazon rainforest and the Cerrado. The Amazon rainforest accounts for about 50% of the remaining global extent of tropical forest (Pan *et al.*, 2011) and is considered to be the most species-rich forest globally (ter Steege *et al.*, 2013). The Cerrado is listed as one of 25 global biodiversity hotspots (Myers *et al.*, 2000). The climate of the study area is classified as tropical wet, tropical monsoon, and tropical wet and dry based on the Köppen (1936) scheme (Peel *et al.*, 2007). Precipitation across the study area varies between ca. 500-3500 mm yr^{-1} with some areas experiencing a prolonged dry season (New *et al.*, 2002).

In general, the soils of the study area are extremely low in plant available nutrients (Quesada *et al.*, 2012), with oxisols being the most common soil type (Walter & Breckle, 1986). They can be of variable depth (Walter & Breckle, 1986; Batjes, 2009), contain high concentrations of aluminium (Walter & Breckle, 1986) and have lateritic layers present at varying depths (Walter & Breckle, 1986; Macedo & Bryant, 1987). In many areas the seasonal water table can approach the soil surface (Macedo & Bryant, 1987; Fan *et al.*, 2013). The depths to which tropical deciduous and evergreen trees root are extremely variable (Nepstad *et al.*, 1994) and have been observed to reach maximum depths of up to 18 m for tropical forest trees and 68 m for tropical savanna trees (Canadell *et al.*, 1996).

4.2.3 aDGVM2 simulations

The simulation experiment explored the effect of plant rooting depth, fire and precipitation on emergent vegetation. We set tree maximum rooting depth to 2.0, 4.0, 6.0, 8.0 or 10.0 m; grass maximum rooting depth was fixed at 1m. We simulated each maximum rooting depth treatment with fire and without fire (10 treatments). These 10 treatments were repeated for each 0.5° pixel of the study area thereby covering the rainfall gradient of 500-3500 mm yr^{-1}. Simulations were run for 900 years. A spin-up of 760 years was run with CO_2 concentrations fixed at a pre-industrial (1860) level of 286 p.p.m. to allow vegetation to reach equilibrium. CO_2 was then increased to the 2000 level of 368 p.p.m. following Meinshausen *et al.* (2011). Spinning-up the model using pre-industrial CO_2 concentrations excludes the possibly confounding effects of CO_2 fertilisation on emergent vegetation. CRU database monthly mean temperature and precipitation data for 20th century (1961-1990) conditions were used as model forcing data (New *et al.*, 2002). For precipitation we used the New *et al.* (2002) data and a stochastic generator to produce daily rainfall (Scheiter & Higgins, 2009). The model was initialised with 50% trees and 50% grasses to avoid making prior assumptions about initial vegetation; following initialisation this ratio changes based on the relative success of these plant types. Investigation of altitude effects on vegetation is beyond the scope of this study, we therefore exclude sites above 1000 m elevation.

4.2.4 Contemporary biome maps

To assess the distribution and accuracy of modelled biome distributions we compare our simulation results to a suite of contemporary biome maps. We classified both simulation output (see section "Biome Classification") and the biome

maps as either savanna or forest. Table 4.1 lists the various products used in our analysis as well as the schemes used to reclassify these maps into forest or savanna. R (R Core Team, 2014) packages 'maptools' (Bivand & Lewin-Koh, 2014) and 'raster' (Hijmans, 2014) were used to read spatial shapefiles, reclassify and rasterize maps to the same spatial resolution and extent as aDGVM2 output.

TABLE 4.1: Data products used for biome distribution comparisons as well as the reclassification used to create savanna and forest biome maps from each product for the study area.

	Vegetation Type Reclassification	
Data Set	**Savanna**	**Forest**
WWF Biome Map Olson *et al.* (2001)	Tropical and subtropical grasslands, savannas, and shrublands.	Tropical and subtropical moist broadleaf and dry broadleaf forest
MODIS landcover Friedl *et al.* (2010)	Woody savannas Savannas Grasslands	Evergreen broadleaf forest Deciduous broadleaf forest Mixed forest
Hickler 2006 Biome Map Hickler *et al.* (2006) (adapted from Hexeltine and Prentice 1996)	Xeric woodland/shrub Moist savannas Dry savannas Tall grassland Dry grassland	Tropical rain forest Tropical deciduous forest Tropical seasonal forest
Buitenwerf Phenology Classifier Buitenwerf *et al.* (2015)	Minimum NDVI values below 0.6	Minimum NDVI values above 0.6
Lehmann Savanna Map Lehmann *et al.* (2014)	Savanna	Non-savanna

4.2.5 Ecosystem physical properties

Baccini *et al.*'s (2012) biomass data were aggregated to 0.5° resolution and used to compare modelled above ground biomass to satellite derived biomass. Tree cover data for the year 2010, from the MODIS vegetation continuous fields product (Friedl *et al.*, 2010) were reprojected to the 0.5° resolution using the MODIS Reprojection Tool (Dwyer & Schmidt, 2006) and compared with simulated tree cover. To assess modelled tree height against satellite derived tree height we compared Simard *et al.* (2011) data with model output. These data were aggregated to the same resolution as simulation data giving an average tree height.

4.2.6 Trait diversity

Trait diversity was calculated as the sum of the normalised Euclidean distance between individuals divided by the total number of individuals. Distances are calculated using the following traits: phenology trigger (P_S), evergreen (P_E), specific leaf area (A_{SL}), carbon allocation to roots (A_R), carbon allocation to leaves (A_L), carbon allocation to stem (A_S), carbon allocation to bark (A_B), carbon allocation to reproduction (A_P), carbon allocation to storage (A_T), allocation from storage to stem (A_{TS}), allocation from storage to leaf (A_{TL}), stem allometric traits (b_1 and b_2), and maximum rooting depth (R_m). See Table 3.3 for a complete listing of traits.

4.2.7 Biome classification

The biome classification scheme used tree basal area and grass biomass; a savanna has modelled tree basal area less than 14 m^2 ha^{-1} and modelled grass biomass more than 500 kg ha^{-1}; a forest has a modelled tree basal area greater than or equal to 14 m^2 ha^{-1}, irrespective of modelled grass biomass.

4.3 Results

4.3.1 Savanna probability is mediated by fire, constraints on plant rooting depth and precipitation

We used a logistic regression to estimate the probability of savanna occurrence as a function of precipitation for each soil and fire treatment. We found that at the

highest levels of precipitation the vegetation state is forest irrespective of rooting depth or fire. However, the probability of savanna increased with decreasing precipitation, decreasing depth to which trees can root and with fire turned on (Fig. 4.2).

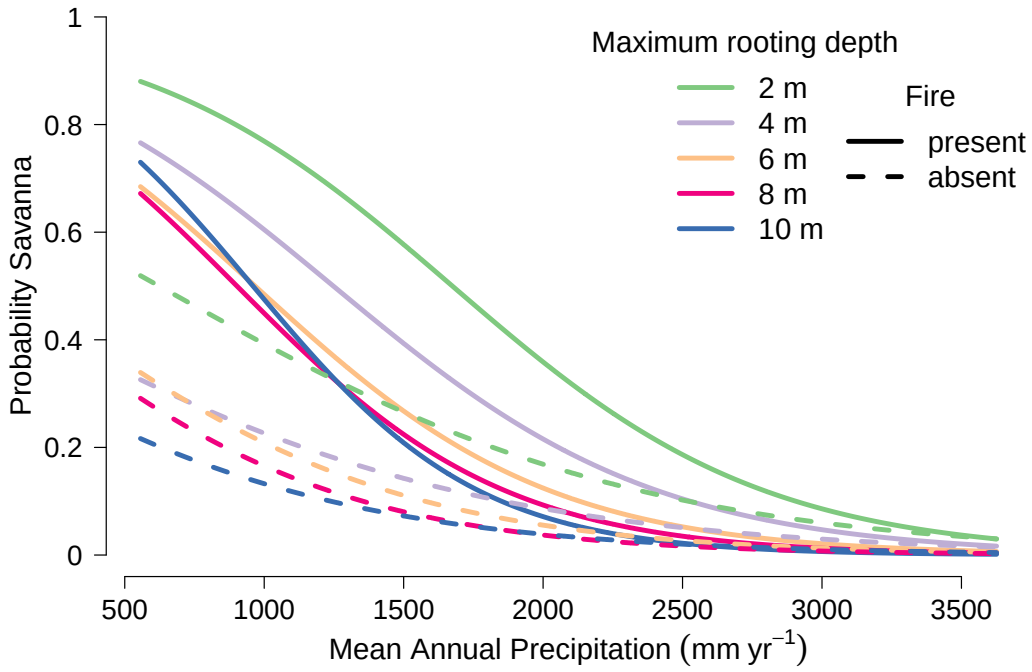

FIGURE 4.2: The probability of occurrence of a savanna biome state with respect to precipitation, fire and depth to which trees can root. Different colours represent different depths to which trees can root. Curves are fitted logistic regression models to simulated data.

4.3.2 Trait dynamics – fire, rooting depth and precipitation interactions

Constraints on plant rooting depth and fire affected the trait composition and diversity of modelled plant communities (Fig. 4.3). The proportion of evergreen trees increases as precipitation increases, this change is mediated by the depth to which plants can root (Fig. 4.3a). Where precipitation exceeds *ca.* 2500 mm yr^{-1},

simulated communities are almost entirely dominated by evergreen individuals. Where precipitation is below 2500 mm yr^{-1}, the emergence of deciduousness is dependent on rooting depth. Access to deeper soil layers increases the total amount soil water available to plants which allows increased evergreen dominance. By reducing the total amount of water available, shallower rooting depths facilitate the co-existence of evergreen and deciduous individuals.

Emerging from our results is a clear relationship between deciduousness and P_{50} (Fig. 4.3a, b). At low levels of precipitation drought tolerant evergreen and drought avoiding deciduous individuals emerge from the model. Drought tolerance is evidenced by the more negative P_{50} values exhibited in simulations where evergreen trees dominate (Fig. 4.3b); drought tolerant evergreen dominance is associated with deeper rooting depths (Fig. 4.3a) and a lower probability of simulating a savanna (Fig. 4.2). Less negative P_{50} values at low precipitation are associated with increases in the proportion of deciduousness (Fig. 4.3a), shallower rooting depths and higher probabilities of simulating a savanna (Fig. 4.2). In general, as precipitation increases P_{50} becomes less negative indicating reduced water stress.

Phenolological triggers determine the environmental cues plants use to initiate leaf flush or abscission. In aDGVM2, plants respond to either light or water triggers (see Appendix B). We find that tree community phenology changes in response to precipitation and constraints on rooting depth. At low precipitation tree community phenology is predominantly water triggered. As precipitation increases a more even mixture of water and light triggered phenologies is simulated (Fig. 4.3c). Plant phenology is affected by constraints on plant rooting depth; at drier sites, reductions in the depth to which plants can root decrease the

proportion of individuals in the modelled community which have a light responsive phenological trigger (Fig. 4.3c).

In simulations without fire, tree trait diversity increases from low to high precipitation (Fig. 4.3d). At the highest levels of precipitation reductions in the depth to which trees can root reduce trait diversity. The highest trait diversity was simulated where precipitation is highest. At low to intermediate levels of precipitation the presence of fire increases simulated trait diversity to levels approaching those simulated at high precipitation.

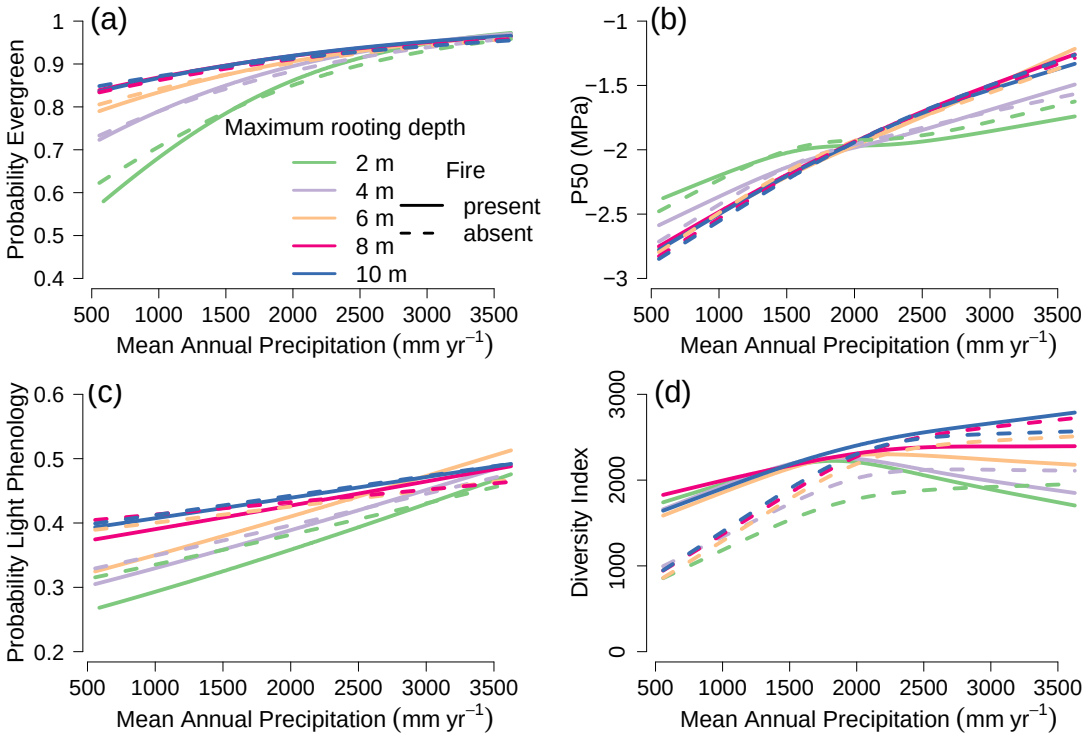

FIGURE 4.3: Tree trait and diversity responses to fire and depth to which trees can root across a precipitation gradient. (a) Shown is the proportion of evergreen trees, (b) P_{50}, (c) phenology trigger, and (d) trait diversity index. Curves are fit using logistic regression (a & c) and splines (b & d).

4.3.3 Spatially variable constraints on plant rooting

We investigated whether interactions between the depth to which trees can root, fire and precipitation can reconcile differences between observed and simulated biome distributions in South America. We did this by identifying the plant rooting depth which minimised the absolute deviance between simulated above ground live biomass and satellite derived biomass estimates (Baccini *et al.*, 2012) in simulations with fire. In simulations where trees can root to a maximum depth of 10 m we find that emergent average maximum rooting depth of trees across the study area shows predominantly shallow rooting in aseasonal high precipitation areas (Fig. A.4a). In seasonal areas of intermediate precipitation trees root to greater depth. The effects of constraining tree rooting depth are greatest where the rooting depth that minimised the deviation between modelled biomass and Baccini biomass is shallower than the simulated emergent average rooting depth (see Fig. Fig. A.4b for the extent and spatial distribution of these differences). Our simulation results show that constraints on tree rooting depth are required to explain biomass patterns and vegetation state in Cerrado areas of south eastern Brazil (Fig. A.4b).

Comparison of biomass, where the depth to which plants could root was optimised to match the Baccini's biomass data, showed an excellent fit (R^2=0.86, Fig. 4.4), with a mean difference of -3.86 t biomass ha^{-1} and a standard deviation of 38.23 t biomass ha^{-1} (Fig. A.1). Although our optimisation was based on biomass, we find that these data also provide a good fit to both satellite derived tree cover (R^2=0.58) (Friedl *et al.*, 2010) and tree height (R^2=0.52) data (Simard *et al.*, 2011). Comparison of satellite derived and simulated tree cover data showed a mean

difference of 7.81 % and standard deviation of 19.86 % (Fig. A.3). Tree height comparison gave a mean difference in tree height of 1.70 m and a standard deviation of 8.34 m (Fig. A.2). These findings indicate strong linkages between biomass, tree cover and tree height.

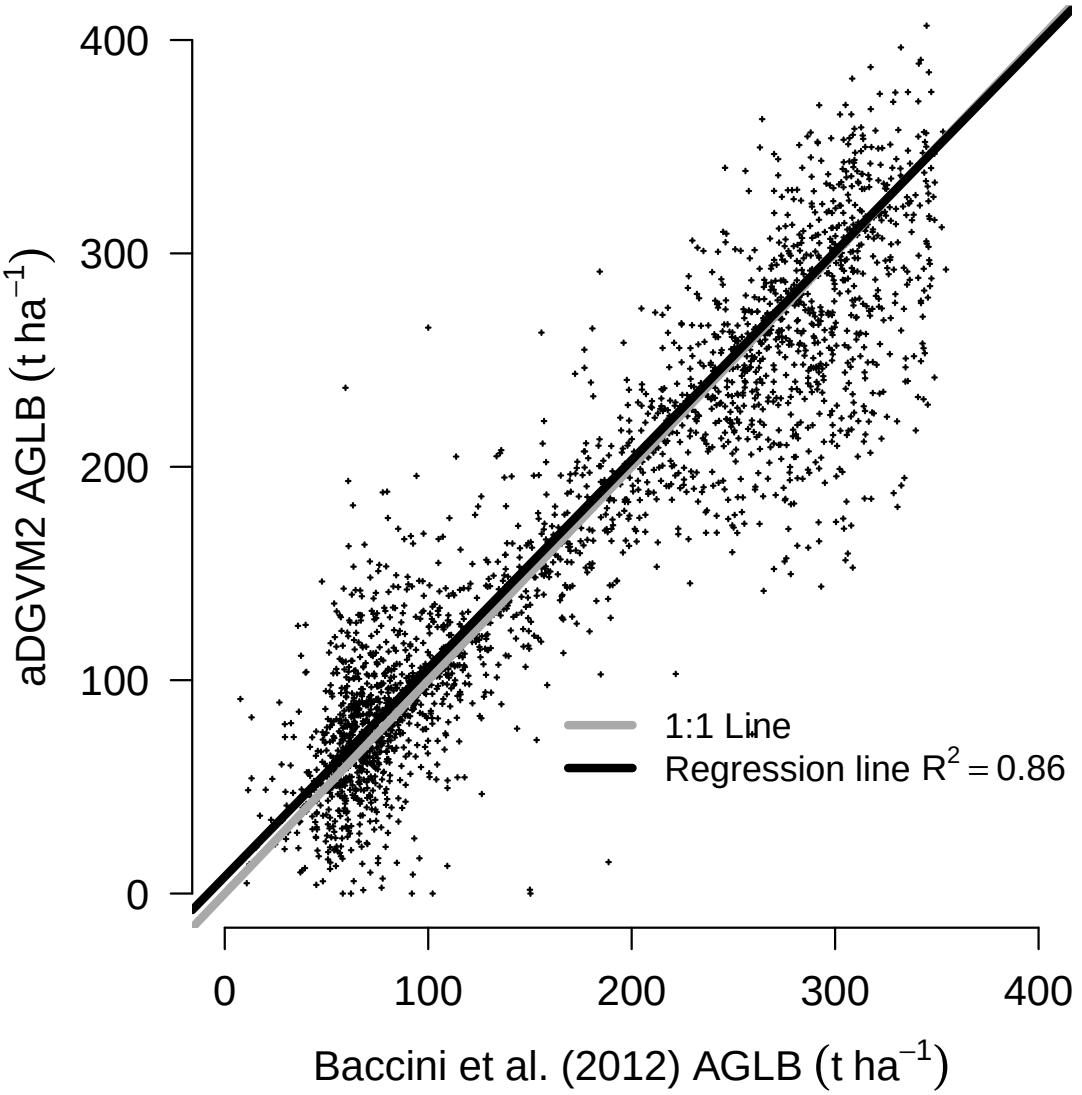

FIGURE 4.4: aDGVM2 above ground live biomass (AGLB) plotted against Baccini *et al.*'s (2012) (AGLB). Displayed AGLB was found by identifying the plant rooting depth which minimised the absolute deviance between simulated AGLB and satellite derived biomass estimates (Baccini *et al.*, 2012) in simulations with fire. Points show values for individual sites in a 0.5° x 0.5° grid of the study area.

Simulated vegetation was classified into savanna and forest and compared with a suite of contemporary biome maps (Fig. 4.5). We found the best agreement between simulated and observed biome distributions in simulations with fire and

where the depth to which plants could root was optimised to match the Baccini biomass data (Fig. 4.5). With these simulations the percentage of correctly classified grid-cells was 82%, 84%, 82%, 87% and 85% when compared to the Lehmann, WWF, Hickler, MODIS and Buitenwerf biome maps, respectively. The worst agreement was found with 10 m soil and no fire: 69%, 73%, 72%, 60%, 63%. The agreements between the WWF and other contemporary biome maps ranged from 82% to 91%.

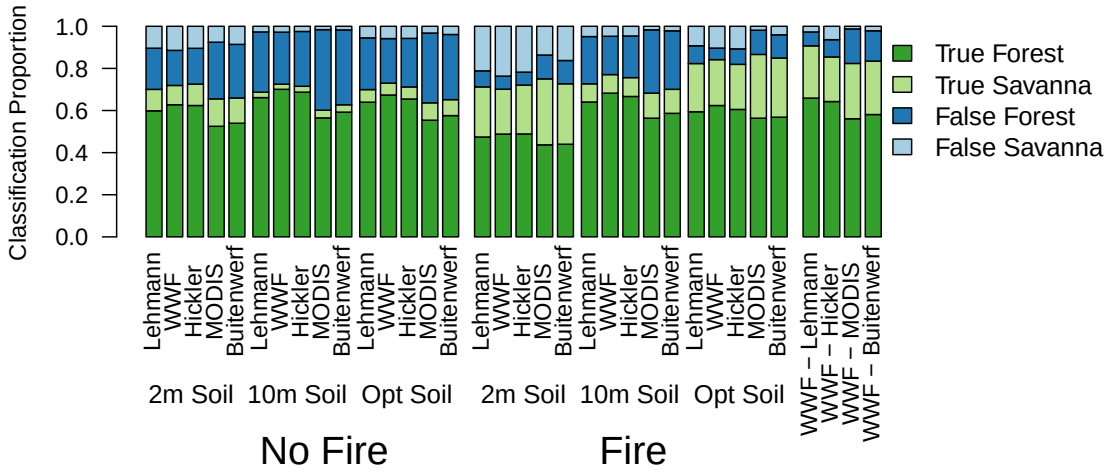

FIGURE 4.5: The proportion of correctly classified biome states compared across multiple contemporary biome maps. Simulations results are shown for treatments where plant rooting was restricted to 2 m and 10 m of soil both with and without fire. Shown also are results for simulations where the constraints on plant rooting were spatially variable, both with and without fire. For comparison we also compare the agreement between different biome maps. True Forest = forest biome in simulations and map, True Savanna = savanna biome in simulations and map, False Forest = forest biome in simulations and savanna in map, False Savanna = savanna biome in simulations and forest in map.

aDGVM2 predicts a geographic patterning of several plant traits (Fig. 4.6). The average tree community P_{50} values in south eastern Brazil are the least negative in our study area (Fig. 4.6c) owing to the coexistence of evergreen and deciduous trees. Evergreen trees in this area are associated with highly negative P_{50} values (Fig. 4.6a) allowing a high level of drought tolerance. Deciduous trees exhibit

less negative P_{50} values and avoid drought via leaf abscission. The coordination of evergreenness with highly negative P_{50} values and deciduousness with less negative P_{50} values was not prescribed *a priori* but rather emerged as a result of selection within the model. The mixture of these two strategies led to less negative P_{50} values on average than in surrounding areas dominated by evergreen trees (Fig. 4.6a). In the model, we linked specific leaf area (SLA) to P_{50} (Eqs. 3.47, 3.49 & 3.48) such that less negative P_{50} leads to higher SLA values (Fig. 4.6b). In south eastern Brazil most trees used water as a phenological trigger (Fig. 4.6d). At higher precipitation predominantly evergreen vegetation emerges (Fig. 4.6c). The evergreen forest regions in south eastern Amazonia areas were associated with P_{50} values indicative of a high level of drought tolerance (Fig. 4.6c), low SLA (Fig. 4.6b) and increasing dominance of the light phenological trigger (Fig. 4.6d). In north western Amazonia where precipitation is higher, P_{50} and SLA increase, as does the dominance of the light phenological trigger.

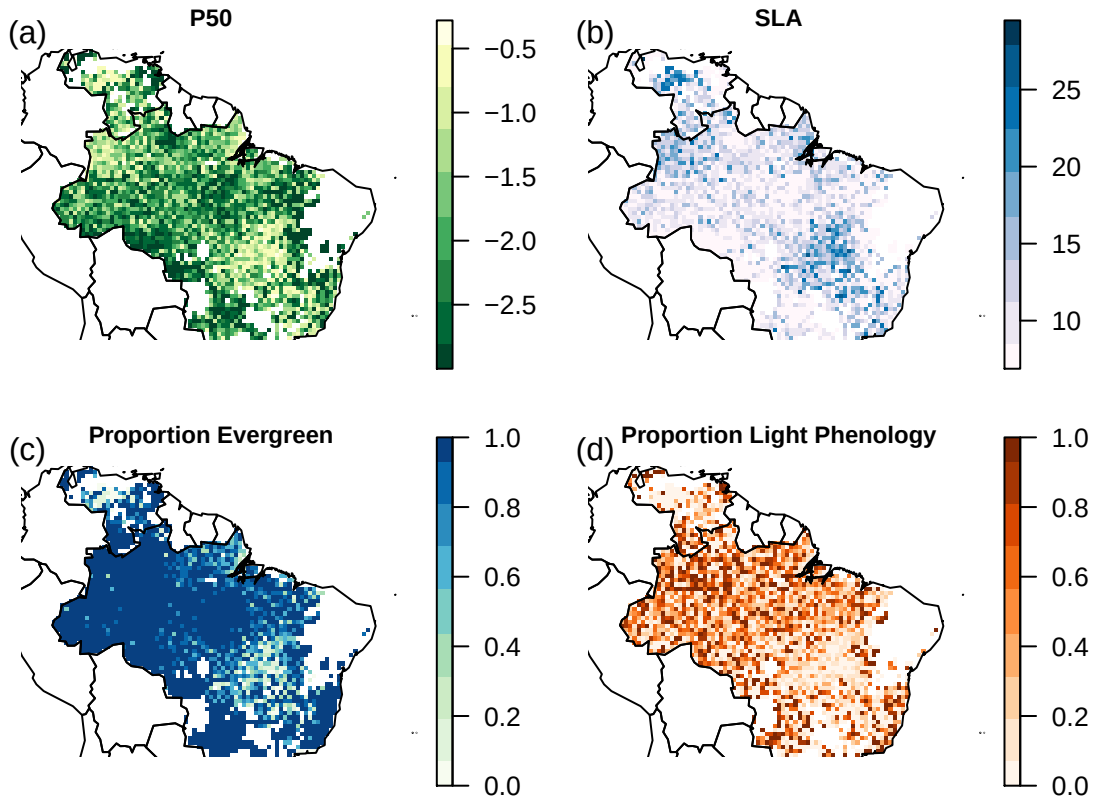

FIGURE 4.6: Simulated traits of trees. (a) P_{50}, i.e. the soil matric potential at which a 50% loss of conductance is reached (MPa). (b) Specific leaf area (m^2kg^{-1}). (c) The proportion of evergreen trees in the population. (d) The proportion of the population of trees with a light as opposed to a soil moisture phenological trigger. These simulations use the spatially variable plant rooting depth where depth is optimised to minimise the difference between simulated and Baccini biomass (Fig. 4.4). For (a) and (b) the plotted values are the mean values of all simulated trees at that location.

4.4 Discussion

4.4.1 The loaded die – drivers of shifting biome probabilities

The extent to which we can use biophysical principles to predict vegetation state is an issue fundamental to biogeography and global change biology. Previous

studies have suggested that biome boundaries in the tropics can only be explained by considering the role of fire (Bond *et al.*, 2005; Staver *et al.*, 2011*a*,*b*; Higgins & Scheiter, 2012; Scheiter *et al.*, 2012; Moncrieff *et al.*, 2014*b*). These studies argue that vegetation state is not deterministically defined by climate alone because fire and initial conditions determine vegetation state; that is, they illustrate that knowing the climate is insufficient for predicting vegetation state. Advocates of this view maintain that across large areas of the tropics both forest and savanna vegetation states are possible where fire-vegetation feedbacks play a decisive role in maintaining the stability of these states (Hirota *et al.*, 2011; Staver *et al.*, 2011*b*; Higgins *et al.*, 2012; Scheiter *et al.*, 2012). These studies have neglected the potential role of constraints on plant rooting depth. Veenendaal *et al.* (2015) and Lloyd *et al.* (2015) show that consideration of the interactions between precipitation, evaporative deficit, soil water storage capacity and nutrient status reduces the need to invoke fire to explain where forest and savanna occur. Although we cannot yet simulate the feedbacks between vegetation state and nutrient dynamics invoked by Veenendaal *et al.* (2015) and Lloyd *et al.* (2015) we show clearly that constraints on plant rooting depth, fire and precipitation affect the probability of savanna and forest occurrence (Fig. 4.2). These effects alter the probabilities of savanna and forest states in ways suggested by Walker & Noy-Meir (1982): deep rooting opportunities promote tree growth and more wooded vegetation states whereas shallow rooting zones favour less wooded vegetation states. Our findings therefore potentially reconcile the alternate state views (Bond *et al.*, 2005; Hirota *et al.*, 2011; Staver *et al.*, 2011*a*,*b*; Higgins & Scheiter, 2012; Scheiter *et al.*, 2012; Moncrieff *et al.*, 2014*b*) with those of Lloyd *et al.* (2015) and Veenendaal *et al.* (2015). We show that, while sites where multiple vegetation states are possible are common, increased information on edaphic and climate controls can allow us

to reduce the predicted extent of such multi-state zones.

4.4.2 Edaphic data – the simplest way to improve predictive plant biogeogrpahy

Biogoegraphers endeavour to improve understanding of factors determining the distribution of vegetation formations. This requires careful consideration of plant water availability which is inextricably linked to the volume of soil explored and explorable by plant roots. This volume can be limited by physical constraints such as soil depth, the presence of hard lateritic layers, high aluminium concentrations (Cole, 1982; Huntley, 1982; Walter & Breckle, 1986) or water logging (Macedo & Bryant, 1987).

Our emergent rooting depth patterns (Fig. A.4a) are consistent with rooting depth predictions (Kleidon & Heimann, 1998; Schenk & Jackson, 2002*b*) and the areas of forest reliant on water from deep soil layers, we additionally predict the presence of a constraint on rooting depth in south eastern Brazil (Fig. A.4b). Macedo & Bryant (1987) found lateritic layers close to the soil surface and to depths of ca. 4 m in Carrado soil profiles, indeed impermeable lateritic layers at depths of 1-2 m are a common feature of seasonally wet-dry climates (Oliveras & Malhi, 2016).

We show that the depth to which plants can root, fire and precipitation, interactively affect the process of modelled plant community assembly and the spatial distribution of trait states. Although the role of fire and precipitation in mediating biome distributions is well established both empirically (Walter & Breckle, 1986) and in models (Bond *et al.*, 2005), the role of soil depth and rooting constraints is poorly understood empirically and seldom considered by DGVMs. Typically, DGVMs assume globally constant soil and rooting depths, usually not more than

2-3 m, and fixed root profile distributions, see Kleidon & Heimann (1998) for an exception and Ostle *et al.* (2009) for a comprehensive review. Even though we ignore nutrient availability in this study, simply considering constraints on plant rooting and plant hydraulics allowed dramatic improvements on previous studies. In contrast to the fixed-trait and fixed rooting PFT models, our simulations reveal that the mean emergent trait values of plant communities change in response to precipitation, fire and constraints on plant rooting. Our study suggests that it is both possible and necessary to move away from static PFT models which are pervasive in vegetation modelling.

4.4.3 Conclusions

We illustrate that edaphic conditions together with fire and climate influence the location of biome boundaries in South America. However, areas where edaphic effects result in azonal vegetation are not limited to savanna-forest boundaries in South America; pedobiomes occupy vast areas of the planet (Walter & Breckle, 1986). Our study suggests that better understanding of the current distribution of vegetation can be achieved by considering the depth to which plants root and plant hydraulics. Accurately predicting current vegetation formations is a necessary precursor for accurately predicting future vegetation formations. It is unfortunately now clear that we need to dramatically improve our capacity to predict how vegetation may shift as our climate changes (Bonan, 2008; Smith *et al.*, 2016). We show that an individual-based modelling approach that allows functional diversity to evolve within simulations is a plausible and powerful route to such improvements. We however further argue that considering how constraints on plant rooting and plant hydraulics affect spatial and temporal water availability

will further improve the accuracy with which we can predict how vegetation will respond to changing climates.

Chapter 5

Functional trait diversity affects Amazonian forest stability, productivity and resistance.

Liam Langan, Simon Scheiter, Mirjam Pfeiffer, Camille Gaillard, Carola Martens, Dushyant Kumar and Steven I. Higgins [*] [†]

5.1 Introduction

The Amazon is one of the Earth's major terrestrial reservoirs of carbon and biodiversity. How it responds to climate and atmospheric changes anticipated over the next decades will have major implications for Earth system functioning and for human well-being. Previous attempts to forecast the fate of the Amazon have

[*]This chapter has been or will be submitted to the journal *Science* as 'Langan *et al.* Functional trait diversity affects Amazonian forest stability, productivity and resistance.'

[†]Author contributions: L.L. designed and performed the study. L.L. analysed results with assistance from S.H.. L.L. and S.H. wrote the manuscript with contributions from S.S. and M.P.. C.G., C.M. and D.K. approved the manuscript.

highlighted three major uncertainties, each of which having the potential to affect the trajectory of the Amazon's response to climate change.

First, CO_2 fertilisation of plant growth is incorporated into vegetation models via the Farquhar equations which govern photosynthesis (Farquhar *et al.*, 1980) whereby plant growth is equal to photosynthetically acquired carbon minus respiration costs. In modelling studies, whether future biomass stored within Amazon rainforests collapses or increases depends strongly on whether CO_2 fertilisation of plant growth is allowed or not, i.e. whether CO_2 is increased in-line with a particular climate change scenario or held fixed (Cox *et al.*, 2004; Rammig *et al.*, 2010; Hickler *et al.*, 2015). Empirical evidence suggests that increased CO_2 can indeed fertilise tree growth (Ainsworth & Long, 2005). However, whether such empirical findings are scalable from the seedlings and small trees tested to mature individuals, transferable to tropical systems, would remain continuous through time, or increase the long term carbon storage in tropical forests via changes in plant longevity is uncertain (Körner, 2009, 2017). Satellite derived estimates of CO_2 fertilisation are much lower than those predicted by vegetation models (Smith *et al.*, 2016). Indeed, whether increasing CO_2 results in a fertilisation of plant growth will depend on interactions between biochemical (nutrients) and biophysical (water, temperature) limitations (Smith *et al.*, 2016).

Second, across Amazonia, where future precipitation projections agree, reductions in precipitation and a general increase in dry spell frequency are predicted (Magrin *et al.*, 2014). Changes to the amount and temporal distribution of precipitation will put large areas of tropical forest at risk of drought stress (Magrin *et al.*, 2014). Experiments within tropical forests have shown significant decreases in living biomass in response to drought (Brando *et al.*, 2008; da Costa *et al.*, 2010).

Drought induced tree mortality will affect the global carbon budget and potentially affect continental scale precipitation patterns via land-atmosphere feedbacks (Zemp *et al.*, 2017). However, many vegetation models under-predict observed biomass loss when drought is simulated and show low sensitivity to changes in water availability (Galbraith *et al.*, 2010; Powell *et al.*, 2013). Therefore, to be able to unravel the interactions between biochemical and biophysical processes and predict the future of tropical rainforests, improving the representation of plant hydraulics and responses to reductions in water availability is crucial (McDowell *et al.*, 2008; Hickler *et al.*, 2006; Xu *et al.*, 2013; Langan *et al.*, 2017).

Third, the linkages between biodiversity and ecosystem services have broad global consequences for human well-being (Perrings *et al.*, 2011). However the rate with which our understanding of these linkages is increasing pales in comparison to the current rapid loss of biodiversity globally (CBD, 2006). Improved understanding of these linkages can facilitate policy and sustainable development plans (Midgley, 2012). The Amazon is hyperdiverse (ter Steege *et al.*, 2000). Experimental work on non-woody (grassland) systems has shown that diversity can increase average plot biomass, biomass stability and buffer against ecosystem shocks (Tilman *et al.*, 1997, 2006; Isbell *et al.*, 2015), but see (Huston, 1997). Whether such diversity effects occur in tropical forest systems remains unclear. Evidence suggests that diversity can influence tropical forest above ground biomass both positively and negatively (Poorter *et al.*, 2015), show no apparent signal (Finegan *et al.*, 2015), and increase the resistance of tropical forests (Sakschewski *et al.*, 2016). However, the extent to which diversity may buffer tropical forest responses to drought and a changing climate is largely uncertain.

5.2 Materials and methods

5.2.1 aDGVM2 drought simulation protocol

For drought experiments we followed the individual site protocols given by (Brando *et al.*, 2008) for the Tapajos national forest (TNF) site and (da Costa *et al.*, 2010) for the Caxiuana national forest (CAX) site. Soil texture and depth values were site specific. Both sites were simulated with a soil depth of 10m (Fisher *et al.*, 2007). For TNF, precipitation was reduced by 34% (Brando *et al.*, 2008) for 4 years, at CAX, precipitation was reduced by 50% (da Costa *et al.*, 2010) for 7 years. For each site the drought experiment was replicated 96 times using different random initialisations of the model. For these simulations the trait values of individuals in the initial population were randomly drawn from a uniform distribution for each trait. The trait-values of seeds produced by individuals with a particular species label are a determined by crossing parent trait values with those of a randomly chosen individual of the same species. In aDGVM2 a "species" is a group of plants which are reproductively isolated from other species. The trait values of seeds are further altered by mutation. We refer to this set-up as the "full-model".

aDGVM2 drought-diversity simulation protocol

To test the effects diversity has on the response of vegetation to drought we ran simulations where the model was initialised with different numbers of species (1, 2, ..., 12, 16, 32, 48, 64, 80 and 96), each species number treatment was replicated 96 times giving a total of 1728 simulation runs for each site. The species used for these treatments were derived from the simulations using the full model (see above). The species which were frequency dominant in the year before drought

treatments were applied were identified, the mean trait values for each frequency dominant species were used to generate a species trait-pool to initialise the model for the drought-diversity simulation experiments. For these experiments each species had fixed, but different, trait values. Mutation and crossover were turned off (see (Langan *et al.*, 2017) for a model description). For each of the 96 replicates for each diversity treatment, species were randomly drawn without replacement from the trait-pool.

Calculating diversity relationships

To examine potential relationships between diversity, ecosystem properties and drought responses we identified how many species (unique trait combinations) were co-existing in the year before drought treatments were applied (species richness pre-drought) with one pre-drought species richness value for each of the 1728 simulation runs. We refer to this below as "full-data".

Calculating functional diversity from drought-diversity simulations

To reduce the dimensionality of data generated in the drought-diversity simulations we used the 'Clara' function in package 'Cluster' (Maechler *et al.*, 2017) to extract 96 trait clusters for each of the 1728 simulation runs. The mean trait values of each returned cluster for each simulation were used to conducted a principal component analysis (R Core Team, 2017) (traits were scaled and centred) in order to select the most relevant traits for further analysis, we thus selected the eight plant traits which had the highest loadings on the first two principal component axes (Swenson, 2014). These traits were related to plant allocation of carbon to various plant organs, leaf habit, phenological strategy, rooting strategy, and were

as follows: proportion of carbon gained allocated to storage (A-Stor), proportion of carbon gained allocated to stem growth (A-Stem), proportion of carbon gained allocated to leaf growth (A-Leaf), proportion of carbon gained allocated to root growth (A-Root), specific leaf area (SLA), a trait which defines whether an individual is evergreen or deciduous (Eg), a trait which defines whether plant phenology is triggered by changes in light or changes in water availability (Phenology), and a trait which defines the maximum depth to which a plant can root (Root-D). A further principal component analysis we conducted on this subset of data (traits were scaled and centred), Fig. 5.4 was produced using these data and a customised version of the code from package 'ggbiplot' (Vu, 2011). These data were also used to calculate diversity indices using the 'dbFD' function in the R package 'FD' (Laliberté *et al.*, 2014). Diversity indices were only calculated if there were more than two species present, i.e. two entries with trait values which differed for any trait (n=1402 for TNF and n=1520 for CAX) (we refer to this below as "full-data"), trait values were standardised by the dbFD function, the number of principal component axes to use as traits for diversity calculations was fixed at 2 to avoid issues calculating convex hull volumes and allow better comparison of indices between simulation runs (Laliberté & Legendre, 2010; Laliberté *et al.*, 2014).

5.2.2 Plotting species richness, functional diversity, pre-drought biomass, biomass loss, biomass stability, transpiration, transpiration stability and functional diversity

Curves in figures 5.1 C and 5.2 A, B, C and D are smoothed splines (R Core Team, 2017) fit to the "full data". Curves in figures 5.1 D and Fig. 5.3 A are smoothed

splines fit to the mean value for each pre-drought level of species richness. All smoothed splines fit to data (Fig. 5.1 C and D; Fig. 5.2 A, B, C and D; Fig. 5.3 A) were fit using three degrees of freedom (knots).

5.2.3 aDGVM2 simulation protocol Amazonian climate change scenarios

Simulations were run using aDGVM2 (Scheiter *et al.*, 2013; Langan *et al.*, 2017). Simulations were run for 1000 years. A spin-up of 760 years was run with CO_2 concentrations fixed at a pre-industrial (1860) level of 286 p.p.m. to allow vegetation to reach equilibrium. CO_2 was then increased to levels given for RCP 4.5 and 8.5 following (Meinshausen *et al.*, 2011). Spinning-up the model using pre-industrial CO_2 concentrations excludes the possibly confounding effects of CO_2 fertilisation on emergent vegetation. CRU database monthly mean temperature and precipitation data for 20th century (1961-1990) conditions were used as model forcing data (New *et al.*, 2002). For precipitation we used the (New *et al.*, 2002) data and a stochastic generator to produce daily rainfall (Scheiter & Higgins, 2009), these data were scaled using anomalies generated for RCP 4.5 and 8.5 following (Meinshausen *et al.*, 2011).

Calculating functional diversity for climate change simulations

The calculation of functional diversity indices for the Amazon climate change simulations followed the same protocol as the drought-diversity simulations except 50 clusters were drawn for each site in each climate change scenario and the traits used were those already selected from the drought-diversity analysis. Fig. 5 was produced by conducting a principal component analysis on this subset of

data using a customised version of the code from package 'ggbiplot' (Vu, 2011). Functional diversity indices were generated using these subset data for every simulated pixel in each climate change scenario both before RCP scenario forcing was applied and in the last simulated year. We constructed a simple linear model (R Core Team, 2017) to examine the dependency of the percentage of biomass loss in each scenario on various predictor variables. Each climate change scenario was modelled separately and predictor variables were retained which had a p-value less than 0.05. Interactions were ignored in order to produce the most parsimonious model. Functional diversity indices were included as predictor variables to analyse how biomass changes between the years 1990 & 2100 depend on the standing biomass in 1990, the precipitation in 1990, the temperature in 1990, the change in precipitation in 2100 from 1990 levels, the change in temperature from 1990 levels, as well as the functional richness, evenness, divergence and dispersion in 1990.

5.3 Results and discussion

In this study we use aDGVM2 (Scheiter *et al.*, 2013; Langan *et al.*, 2017), a state of the art dynamic global vegetation model (DGVM), to examine potential interactions between changes in precipitation regime, CO_2 concentration, drought and diversity in the Amazon basin. aDGVM2 is individual based allowing drought and fire impacts to be conditioned on the phenotypic properties of the individual. Further, a plants longevity, competitive ability and ultimately its relative reproductive success is determined by its trait values, the trait values of competitors and how these are influenced by, and interact with, the abiotic environment. Essentially the process of community assembly, as constrained by natural selection,

is modelled. The trait and functional diversity which emerges from our simulations are the result of this process. The model has previously been shown to predict current biome and biomass distributions of the Amazon basin well (Langan *et al.*, 2017).

To examine whether the model can mimic observed tropical forest drought responses we set up a model experiment that mimics the through-fall exclusion experiments run at Tapajos (TNF) (Brando *et al.*, 2008) and Caxiuana (CAX) (da Costa *et al.*, 2010) national forest sites. In our simulation experiments rainfall was reduced by 50% for 7 and years for the TNF site (da Costa *et al.*, 2010) and 34% for 4 years at the CAX site (Brando *et al.*, 2008). The amount and duration of precipitation reductions mimic those applied in (Brando *et al.*, 2008) and (da Costa *et al.*, 2010) rather than following the simulation protocol of previous modelling studies (Galbraith *et al.*, 2010; Powell *et al.*, 2013). For each site the drought experiment was replicated 96 times. Each replicate was randomly initialised with a community of plants whose traits were randomly drawn from a uniform distribution, mutation and cross-over of plant traits were allowed.

Climate change is predicted to increase the frequency and intensity of drought across much of Amazonia (Magrin *et al.*, 2014), widespread forest mortality is expected (McDowell & Allen, 2015). Studies exploring how the vulnerability of plants to drought is mediated by traits and trait strategies are providing us with crucial new insights (Skelton *et al.*, 2015). Xylem cavitation resistance has been shown to be central trait involved in plant hydraulic strategies (Larter *et al.*, 2017; Brodribb, 2017). Many DGVMs cannot yet simulate plant responses to drought

accurately (Galbraith *et al.*, 2010; Powell *et al.*, 2013; McDowell *et al.*, 2013*b*) possibly owing to the simplified representation of water stress commonly used (Powell *et al.*, 2013). In aDGVM2 plant hydraulics are represented using an implementation of the cohesion-tension theory of sapwood ascent whereby plant trait values define the rate at which water can be conducted as well as xylem resistance to cavitation (Langan *et al.*, 2017). Previous simulations conducted using aDGVM2 (Langan *et al.*, 2017) showed that across South America traits associated with plant hydraulics responded strongly to precipitation gradients and changes in the rooting depth available to plants. Further, selection within the model led to the emergence of whole plant hydraulic strategies via coordination between plant hydraulic and phenological traits. Replicating drought experiments with this implementation of plant hydraulics revealed that the model was able to reproduce both the level of biomass loss and the rate of biomass loss well at both experimental sites (Fig. 5.1 A, B).

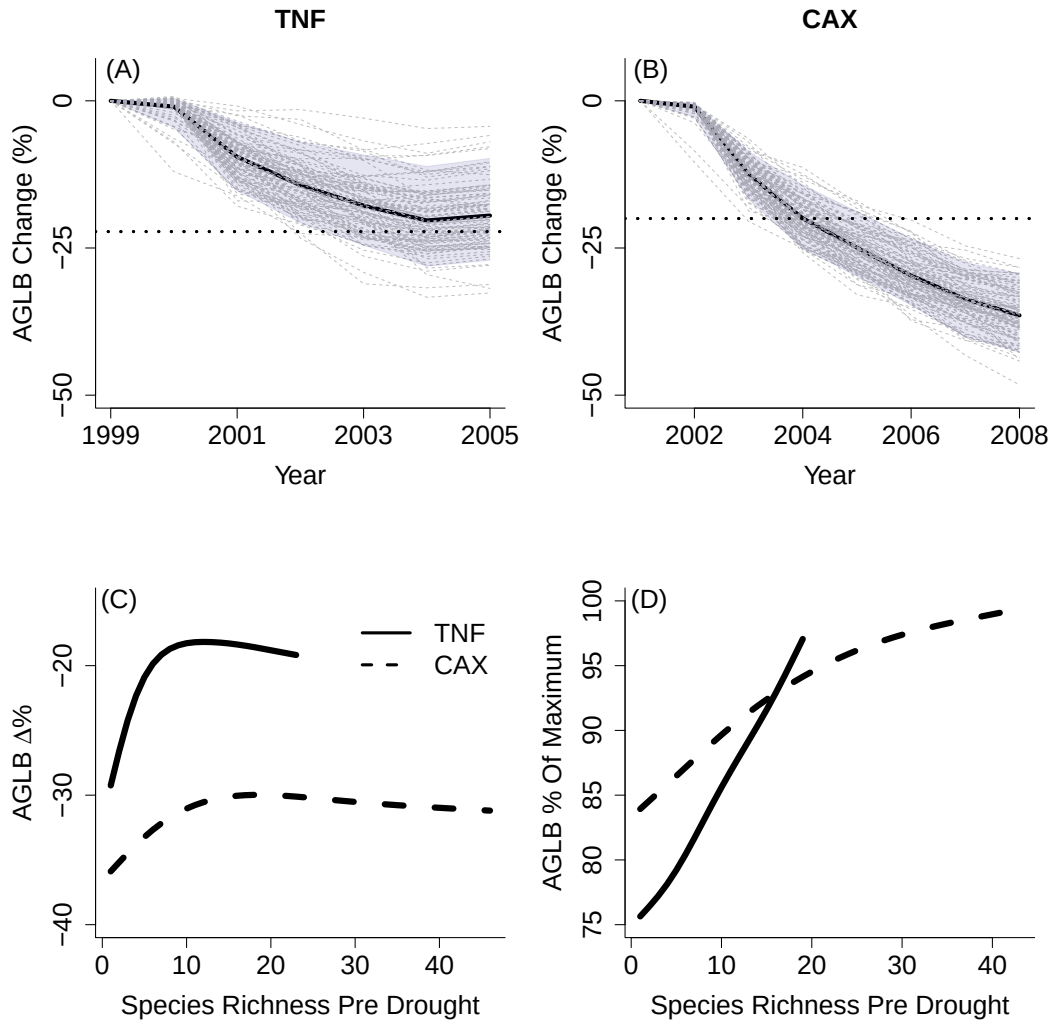

FIGURE 5.1: **Drought-diversity dynamics**: Drought simulation experiments for TNF (A) and CAX (B) sites showing the simulated drought response for the full model with 96 replicates. The thick black line shows the mean percentage reduction in biomass. The horizontal dashed lines show observed percentage biomass reductions. (C) shows the post drought percentage biomass loss against pre-drought species richness. For this experiment the model was initialised with (1, 2, ..., 12, 16, 32, 48, 64, 80 and 96) species. Each of these 96 species were the frequency dominant species in (A) and (B). Each species number treatment was replicated 96 times. (D) shows the pre-drought percentage of maximum biomass against pre-drought species richness. In (C) and (D) the lines are smoothed splines fit to the full data in (C) and the mean for each species richness level (D). In (D) the maximum biomass is taken as being the maximum of the pre-drought species richness means.

Whether higher diversity begets higher ecosystem stability has interested ecologists since at least the middle of the 20th century (Odum, 1953; Elton, 1958)

yet the debate continues. In the face of climate change and current rapid loss of species globally it is imperative to disentangle diversity-stability relationships (McCann, 2000). We investigated whether diversity affects biomass response to drought by conducting simulations initialised with different numbers of species. In total 96 species were created by assigning the mean trait values of the frequency dominant species in each of the 96 replicates conducted for Fig. 5.1 A, B (see Materials and methods). For both sites, there where no two species that possessed identical trait values. These drought-diversity simulations revealed that pre and post drought biomass were conditional on pre-drought species richness (i.e. the number of functionally unique species which were present in simulations the year before drought was applied). Empirical work has shown that higher diversity can increase resilience to drought (Tilman *et al.*, 2006) as well as biomass stored (Tilman *et al.*, 1997) in grassland experiments, our results echo these findings for tropical forest whereby sites with lower species richness exhibited more dramatic reductions of biomass following drought (Fig. 5.1 C) and lower pre drought biomass (Fig. 5.1 D). At higher levels of species richness drought induced biomass loss was remarkably similar (Fig. 1 C) indicative of a resilience tipping point, i.e. a level of species richness below which resilience to drought is reduced non-linearly (Willis *et al.*, 2018) (Fig. 5.1 C). However, while higher diversity led to increased pre drought biomass storage and increased drought resilience, high diversity sites exhibited lower stability in biomass in the 100 years before drought was applied (Fig. 5.2 C). This result is in contradiction with the higher stability found by Tilman *et al.* (2006) but in keeping with theoretical predictions of May (1973). Interestingly, while higher diversity sites exhibited lower temporal stability in biomass they showed higher temporal stability in transpiration (Fig. 5.2 D).

Both forest biomass and transpiration are coupled to the atmosphere and thus climate systems. Biomass is coupled via the carbon extracted from the atmosphere and stored as living and dead biomass. Transpiration is coupled via the direct exchange of moisture with the atmosphere. These ecosystem components are also coupled at differing rates; carbon storage is related to forest age and potential longevity while the transpiration stream interacts continuously with the atmosphere and can affect local to continental scale precipitation patterns (Zemp *et al.*, 2017).

Species in our simulations were all functionally unique. Examining the components of functional diversity for our simulations revealed that, while functional richness is relatively similar across species richness levels, functional evenness increases with species richness (Fig. 5.2 A, B). High functional evenness implies a more even distribution of the density with which trait-space is occupied (Villéger *et al.*, 2008) and potentially a more complete utilisation of resources which can increase productivity (Mason *et al.*, 2005). Indeed, our simulations reveal that sites with higher pre drought species richness transpired higher amounts of water (Fig. 5.3 A). Additionally, functional divergence, the mean distance of a species to the centroid of trait space (Laliberté & Legendre, 2010), shows an increasing trend which plateaus at approximately the same level of pre-drought species richness as the percentage biomass lost following drought treatments (compare Fig. 5.1 C and Fig. 5.2 A, B). To rule out the sampling effect (Maréchaux & Chave, 2017), i.e. the increased probability of drawing the most productive species in samples which draw a high number of species (Huston, 1997), as a driver of our diversity relationships we identified the species which produced the highest biomass when simulated in single species treatments (mono-culture). The highest biomass produced at both sites was in mono-culture simulations. At CAX the three highest

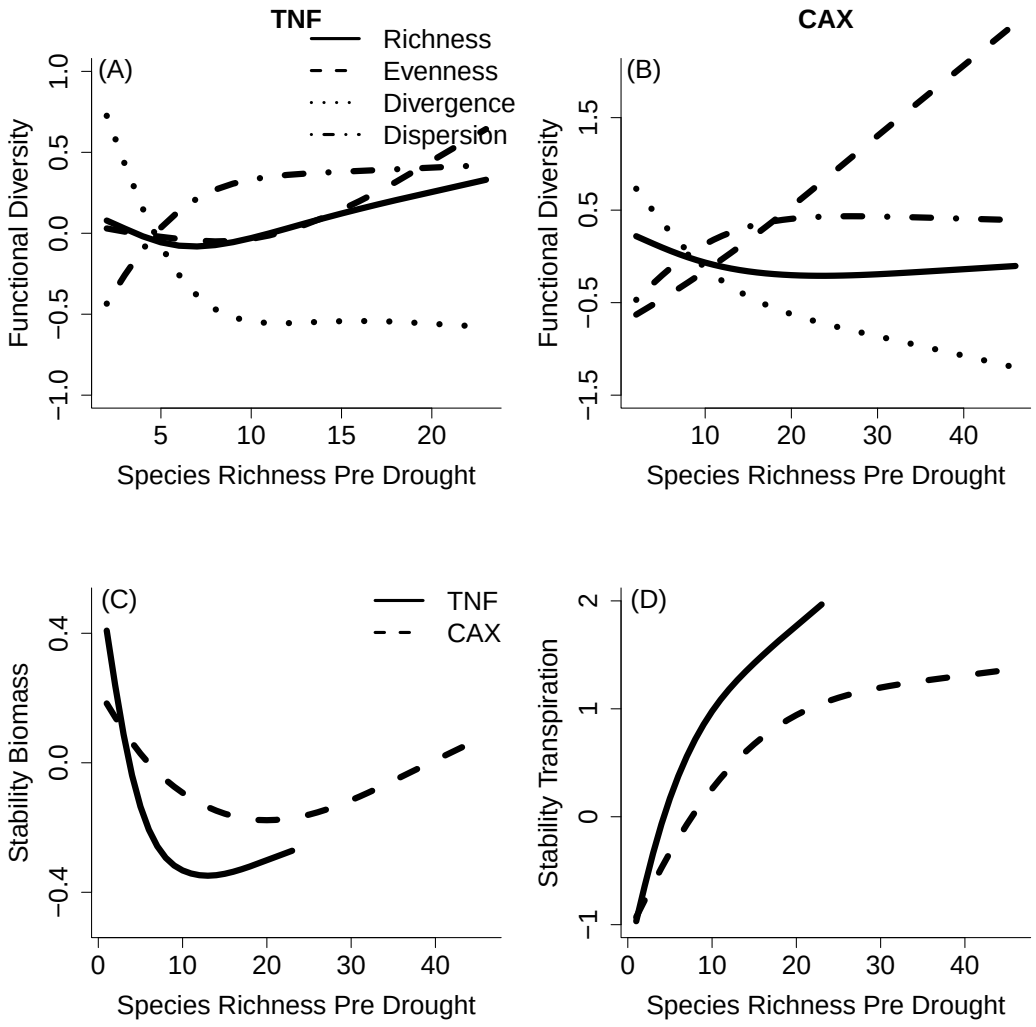

FIGURE 5.2: **Functional diversity components and Ecosystem stability**: Shown are normalised components of functional diversity, biomass stability and transpiration stability plotted again the number of species present before drought treatments were applied for (A) function diversity Tapajos national forest (TNF), (B) functional diversity Caxiuana national forest (CAX), (C) biomass stability calculated as the mean biomass in the 100 years before drought divided by the standard deviation of biomass in the 100 years before drought and (D) transpiration stability calculated as the mean transpiration in the 100 years before drought divided by the standard deviation in transpiration in the 100 years before drought. Lines are smoothed splines fit to the full data.

biomass values produced across all simulations were in mono-culture. At TNF the second highest biomass produced was in a simulation with a pre-drought

species richness of 12. For both sites these species were deciduous, had high specific leaf area and relatively shallow roots. In our simulations where all species were drawn for every replicate we identified the relative abundance and percentage contribution to total biomass of these species. At TNF and CAX these species were not present in the pre-drought species pool in ca. (21%) and (14%, 3%, 5%) of simulations. These species displayed an average relative frequency of ca. (0.5%) and (0.8%, 2.4%, 1.1%) (Fig. 5.3 B) and accounted for an average percentage of total biomass of (0.4%) and (0.5%, 3%, 0.7%) for TNF and CAX respectively. Thus, rather than dominating high diversity simulations, the species which produced the highest biomass in mono-culture where either completely out competed or held at low frequency and did not contribute substantially to plot biomass. This result is unsurprising given that the unit of currency in nature, and in our model, is not biomass production but relative reproductive success. Our modelling paradigm is constructed so that trade-offs between traits prohibit the emergence of Darwinian daemons, i.e. individuals which maximise all components of fitness (Scheiter *et al.*, 2013). Such trade-offs require for example that higher allocation to stems reduces allocation to one or more other plant compartments. To explore further the assembly of communities in trait-space we examined the density with which trait-space is filled at low species richness and high species richness (Fig. 5.4). In high species richness simulations, the density in trait-space of a number of plant-strategies increases: (1) evergreen drought tolerant species which exhibit low specific leaf area, deep rooting and lower allocation to stems and leaves; (2) deciduous drought avoiding species which exhibit high specific leaf area, shallow rooting, lower allocation to stems and leaves while allocating more to storage. The increased density of these strategies is similar at

both sites. Thus, the exploration of diversity relationships revealed that the functional trait composition of high species richness communities differs to that of low species richness communities in our simulations, i.e. while the community possesses an almost identical distribution of trait ranges, the relative abundance of trait-combinations changes considerably.

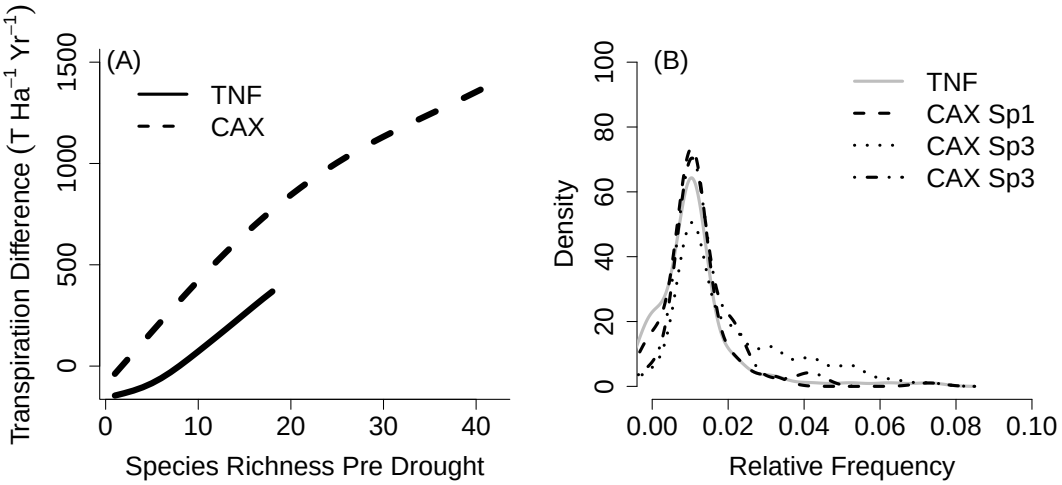

FIGURE 5.3: **Transpiration and frequency of biomass dominants:** (A) Difference between the mean transpiration for each level of species richness and that for the mean transpiration for simulations where one species was present before drought was applied. (B) The relative frequency of the species which produced the highest biomass in mono-culture in simulations initialised with 96 species in the species-pool. At TNF only one species produced more biomass in mono-culture than poly-culture simulations. At CAX the first three highest biomass values produced were in mono-culture.

The ability of the model to mimic the drought experiments (Fig. 5.1) and to explain 70% of the variance in vegetation biomass and to correctly predict the biome state of more than 80% of simulated grid cells in the Amazon study region (Langan *et al.*, 2017), suggest that the model provides a reasonable representation of the dynamics and distribution of vegetation within the study region. This good performance motivated us to explore future scenarios of vegetation development under the IPCC's RCP scenarios (Meinshausen *et al.*, 2011). We used the RCP 4.5

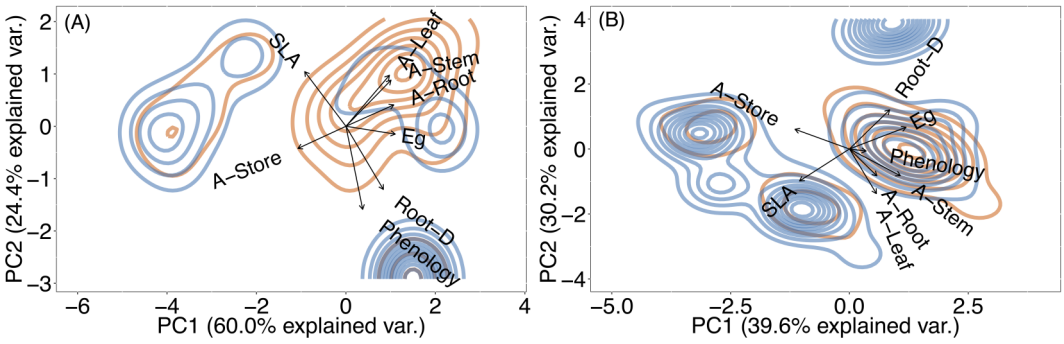

FIGURE 5.4: **Contours of the density of pre-drought trait space**: (A) TNF, (B) CAX. Orange indicates the density with which trait-space was filled when the species richness before drought treatments was low. Blue indicates the density with which trait-space was filled when the species richness before drought was high. For each site the boundary between low and high was chosen to correspond to the tipping point in Fig. 5.1C, TNF with a species richness of 10 and CAX with a species richness of 15.

and 8.5 climate forcing with and without a CO_2 impact on plants. For simulations without a CO_2 impact on plants we held CO_2 levels constant at 380 ppm, for simulations with a CO_2 impact we increased CO_2 as prescribed by the RCP scenario. Simulations were run without imposing constraints on diversity. These simulations revealed the sensitivity of modelled biomass to CO_2 (Fig. 5.5). In simulations where both CO_2 and climate varied, biomass increased by ca. 10-15% by 2100 (Fig. 5.5 A, B, C). However, in simulations where only climate forcing was applied, there was a reduction in total biomass stored, ca. 18% with RCP 4.5 and ca. 38% with RCP 8.5 (Fig. 5.5 A, D, E). In the absence of CO_2 fertilised plant growth, forest biomass loss is widespread while savanna biomass increase is negligible (Fig. 5.5 A, D, E). The effect of CO_2 fertilisation of plant growth has previously been shown to mitigate the risk of Amazon forest die-back (Rammig *et al.*, 2010). However, our results reveal that, with an improved representation of the biophysical interactions between CO_2, plant growth and plant responses to changes in water status, even with increasing CO_2 there are large areas of Amazonia where biomass is reduced by up to 40% (Fig. 5.5 A, B, C), these reductions

are associated with reductions in precipitation. These losses are however counterbalanced by increases in biomass in savanna biomes associated with increased precipitation.

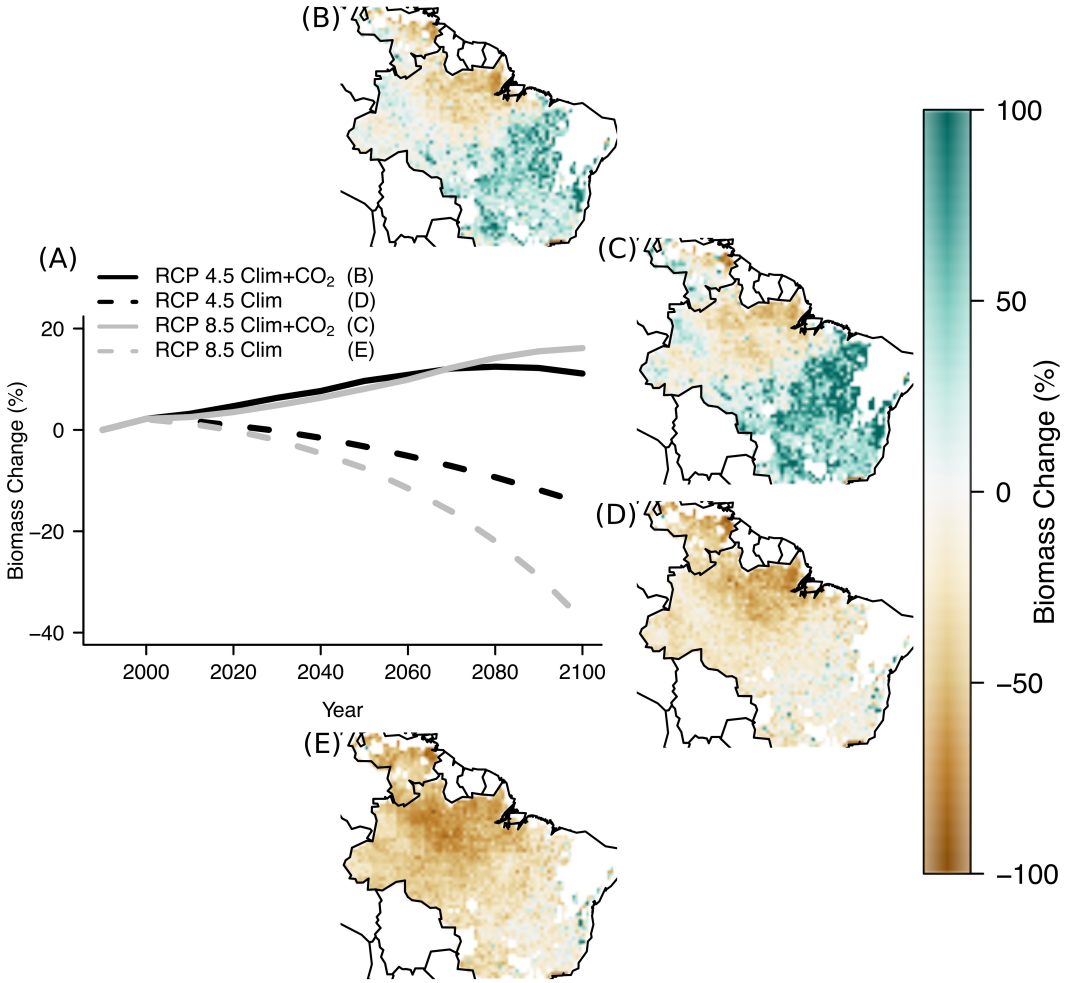

FIGURE 5.5: **Amazonian biomass trajectories:** (A) Percentage change in the total biomass stored in the study region. Maps show the spatial distribution of changes, (B) RCP 4.5 with increasing CO_2, (C) RCP 8.5 with increasing CO_2, (D) RCP 4.5 with fixed CO_2, (E) RCP 8.5 with fixed CO_2.

Examination of the components of functional diversity for these climate change simulations revealed that sites with higher functional diversity show a lower reduction in biomass (Fig. 5.6). Here, in agreement with the drought experiments (Fig. 5.2), we find that increased functional evenness and decreased functional divergence reduces the reduction in biomass (Fig. 5.6 and Tab.5.1). However, we

only find significant positive diversity effects when CO_2 fertilises plant growth. The absence of CO_2 fertilised plant growth increases the water stress of plants caused by climate change and overrides any diversity bestowed resistance. When plant growth is not fertilised by increasing CO_2 we find that diversity components show non-significant or negative effects with minute effect sizes. Further, across all RCP scenarios, our results show substantial changes in the density with which Amazonian trait-space is filled (Fig. 5.7).

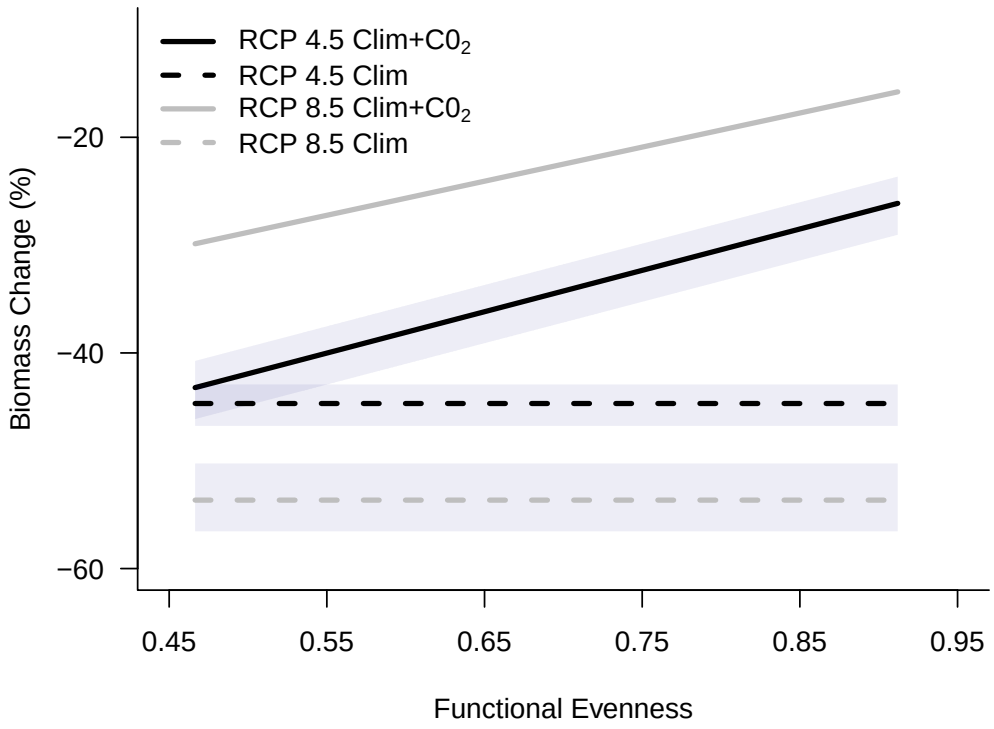

FIGURE 5.6: **Diversity mediated changes in future biomass:** lines show the effect of functional evenness on biomass change for each scenario (lines are predicted percentage biomass change for each simulation run, see Table 5.1). The coefficients for each predicted change model (Table 5.1) were: Standing biomass = mean for study area in year 2000; Precipitation = mean for study area in year 2000; Precipitation anomaly = 50% reduction; Temperature = mean for study area in year 2000; Temperature anomaly = mean for study area in year 2100 for each RCP scenario. Quantiles show the additional effect of functional divergence.

TABLE 5.1: Regression relationship fit to the percentage change in biomass between 1990 and 2100. All coefficients were normalised and significant with a p-value less than 0.05.

	RCP 4.5 Clim increasing CO_2	RCP 4.5 Clim fixed CO_2	RCP 8.5 Clim increasing CO_2	RCP 8.5 Clim fixed CO_2
Coefficients	Estimate	Estimate	Estimate	Estimate
Intercept	-46.420	-40.926	-60.043	-23.671
Standing biomass	-118.978	-44.121	-128.890	-34.195
Precipitation	75.254	36.794	83.934	27.990
Precipitation anomaly	88.052	60.355	125.211	58.746
Temperature	20.579	-	20.908	-38.878
Temperature anomaly	-22.265	-15.477	-21.743	-29.727
Functional richness	-	-	-	-
Functional evenness	17.092	-	14.091	-
Functional divergence	-5.399	-3.849	-	6.299
Functional dispersion	-	-	-	-
R^2	0.67	0.57	0.70	0.65

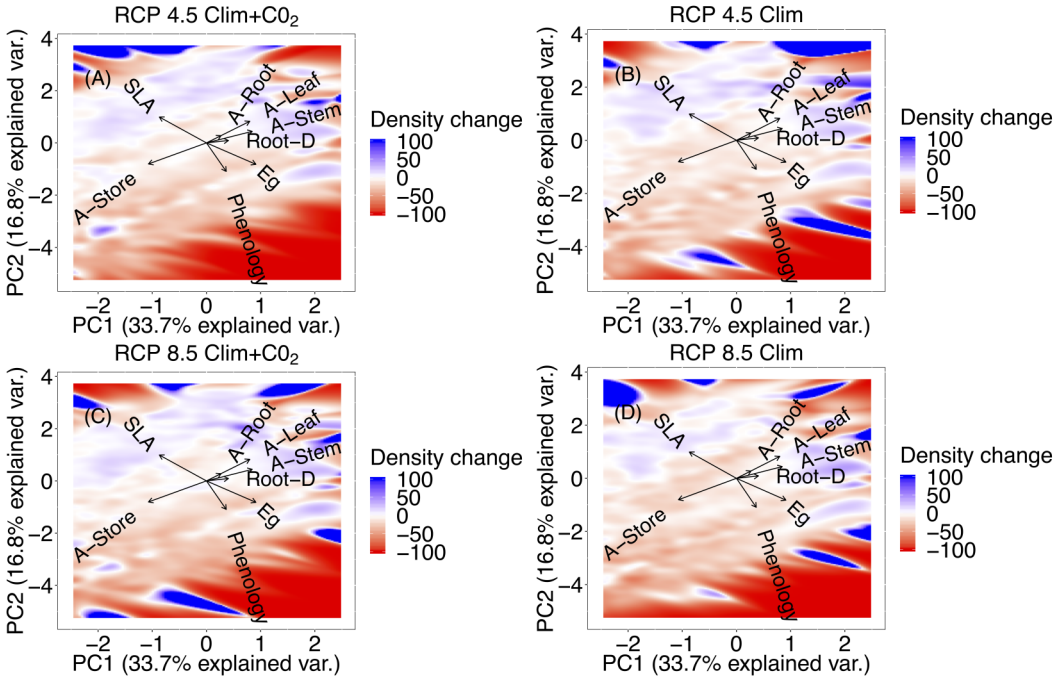

FIGURE 5.7: **Changes in the density of occupied trait space for the Amazon with different RCP scenarios**: Red indicates a reduction in the density with which trait-space was filled in the year 2100 relative to the density in the year 2000. Blue indicates an increase in the density with which trait-space was filled in the year 2100 relative to the density in the year 2000.

In conclusion, our results suggest that functional diversity plays a significant role

in tropical forest systems with effects which can lead to higher stability in transpiration, increased water-use completeness, increased biomass storage and increased resistance to drought and climate change. However we urgently need to improve our understanding of how interactions between biochemical (CO_2 and nutrients) and biophysical (precipitation changes and plant water availability) processes affect plant dynamics as these play an overwhelming role in determining the future of these forests.

Chapter 6

Synthesis

6.1 Overview

In this thesis I have described the progression of the development of a "next generation DGVM". To successfully construct this model required improvement in the representation of and interactions between processes associated with both the biological and physical sciences, yet, at the onset, the route to achieve the goal of a working trait based vegetation model was uncertain. The development process however highlighted key disparities between modelled and natural dynamics which required improvement. Thus, vastly increasing the complexity with which we model the interface of the natural and physical world by interweaving processes related to the fields of evolutionary ecology, community ecology, co-existence theory, soil science, soil hydrology, and plant hydraulics, rather than leading to unintelligibly complicated results, allowed the identification of a relatively simple set of key results. I will highlight these key results in the following sections.

6.1.1 Improving biological process representation

In Chapter 2 limitations of many contemporary DGVMs were reviewed and discussed. The case was made that many of these limitations could be addressed by improving the representation of biological processes via improved integration of concepts from community assembly and co-existence theory. We tested this assertion with a less developed version of aDGVM2. We demonstrated that an approach where the process of natural selection is modelled at the individual level, where individual fitness is determined by the values of multiple traits, and trade-offs between them, can indeed allow diverse communities of plants emerge from the modelling framework (Fig. 2.5). We showed that the position of the emergent communities in trait space differed along abiotic gradients and that, although emergent communities were clustered about one area in trait space, a certain level of trait diversity was present which contrasts with the fixed trait PFT paradigm of many contemporary DGVMs (Fig. 2.5A).

The diversity we see in the world around us is intrinsically linked to the mechanisms which allow co-existence of species, indeed, in its simplest form, co-existence of two species through time can only be stable if both species have identical fitness. There exist multiple mechanisms through which species can attain equal fitness and co-existence can occur (May & McLean, 2007). Within the aDGVM2 framework we included a light competition sub-module which allowed there to be explicit spatial heterogeneity in light competition and thus the availability of light as a resource. Temporal variability in the availability of light and water can allow co-existence, such variability in aDGVM2 can be due to input data, continually changing phenotypic properties of individuals within a population through time affecting light and water availability, or both. Trade-offs

between traits such as those associated in increased competitive ability for water and light versus those associated with colonisation such as allocation to reproduction or seed size can also allow co-existence (May & McLean, 2007). Indeed, in aDGVM2 we additionally showed that, in simulations where reproductive isolation was simulated, communities emerged which were composed of multiple co-existing clusters in trait-space (Fig. 2.5B). Why simulating more than one reproductively isolated species would lead to multiple co-existing clusters is intriguing. It is certainly not impossible for a single interbreeding population to differentiate across a fitness landscape (Wolf *et al.*, 2004). Indeed, such differentiation is the precursor of sympatric speciation. It is likely that reproductive isolation between populations simply increases the probability or chance that multiple peaks in the fitness landscape will be found. Indeed, the simulated trait values of co-existing strategies emerging from aDGVM2 were often multimodal (Fig. 2.6B) and indicate that multiple life-history strategies can emerge from the model dynamics. Importantly however, the ability of vegetation to respond to climate change will depend on its adaptive potential whereby adaptive potential is generally related to diversity (Kuparinen *et al.*, 2010), thus, to improve confidence in our ability with aDGVM2 to make predictions about vegetations' response to change it is necessary that modelled genetic (trait) and demographic processes be benchmarked against existing quantitative genetic models and where possible, empirical data. Further, as highlighted in Chapters 1 and 2, the modelled process of natural selection can only generate appropriately evolved or filtered communities if the direction and strength of selection on traits is appropriate. This represents the key difficulty with "tuning" aDGVM2. The direction that selection should push a trait can often be assessed based on observations. Within

aDGVM2, the direction selection will push a trait given a certain set of assumptions can often be assessed via thought experiments as highlighted in relation to water availability as a function of root fractions (Chapter 1). The strength of selection on particular traits of living organisms, under differing abiotic and biotic conditions, is however largely unknown (Hoekstra *et al.*, 2001). Selection strength on a particular trait depends on the extent to which a particular value moderates the fitness of an individual under a particular set of abiotic and biotic conditions. Hence, to successfully model the assembly of a community via natural selection as well as the response of communities to changing abiotic conditions requires: the accurate representation of abiotic conditions to determine resource amounts through time; the accurate representation of plant resource acquisition as mediated by a plants trait values, trade-offs between traits (e.g. water uptake and transport), and resource availability; the accurate representation of biotic conditions since competition between individuals for resources mediates the amount of resource available through time.

6.1.2 Selection for improved hydraulic status

The availability of water to plants is one of the biggest constraints on plant performance globally, yet, the most frequently employed representation of plant water availability within vegetation models appeared overly simplified and logically incompatible with the aDGVM2 modelling paradigm. Across Amazonia, where future precipitation projections agree, reductions in precipitation and a general increase in dry spell frequency are predicted (Magrin *et al.*, 2014). Changes to the amount and temporal distribution of precipitation will put large areas of tropical forest at risk of drought stress (Magrin *et al.*, 2014). Experiments within tropical

forests have shown significant decreases in living biomass in response to drought (Brando *et al.*, 2008; da Costa *et al.*, 2010). Drought induced tree mortality will affect the global carbon budget and potentially affect continental scale precipitation patterns via land-atmosphere feedbacks (Zemp *et al.*, 2017). However, simulated plant responses to drought certainly appeared to bare little resemblance to observed plant responses in the majority of DGVMs tested (Galbraith *et al.*, 2010; Powell *et al.*, 2013).

I tested various aspects of the newly developed integration between biotic and abiotic water dynamics (Chapters 2 and 3) in Chapters 4 and 5. In Chapter 4 I additionally tested the effect of the volume of soil available to plant roots can have on simulated plant communities. While the focus of Chapter 4 was the examination of the interactive effects climate, soils and fire play in mediating savanna and forest biome boundaries in tropical South America, these simulations also served to test the newly designed sub-modules for soil and plant hydraulics in aDGVM2.

From the physical perspective I demonstrated in Chapter 4 that, in addition to fire and precipitation, edaphic constraints on the volume of soil explorable by plant roots (e.g. by shallow soils, lateritic layers, anoxic conditions due to water logging, toxicity resulting from heavy metal concentrations (Cole, 1982; Huntley, 1982; Walter & Breckle, 1986; Macedo & Bryant, 1987; Buisson *et al.*; Bowman & Perry, 2017) can affect the process of plant community assembly, alter the mean values of multiple traits in communities, and the trait diversity of communities (Fig. 4.3). Further, such constraints can also alter the probability of a particular biome being simulated (Fig. 4.2). That changes in the volume of soil explorable by plant roots alone can alter the probability of simulating a biome, the highest level of organisation used to categorise vegetation into distinct groups

(Moncrieff, 2014), by ca. 35% highlights the strong importance of considering the role of interactions between plants and edaphic conditions in mediating observed biome distributions. It is also possible to re-interpret these results from a somewhat more biological perspective. The effects of functional diversity on ecosystem function and properties is a hotly debated topic (Loreau *et al.*, 2001). In Chapter 4, rather than changing the characteristics of simulated soil profiles I constrained the potential values of a trait which defines the maximum rooting depth of plants between different bounds (0-2m, 0-4m, 0-6m, 0-8m, and 0-10m), essentially I constrained the potential variability in this maximum rooting depth trait. Thus I would argue that this experiment also highlights the effect of allowing increased levels of diversity in this rooting trait on the evolution and assembly of plant communities. That is, given a fixed soil depth, say 10m, higher diversity in rooting depth can also alter the probability of simulating a particular biome state and multiple, unlinked, emergent traits of plant communities. Indeed, as Chapin (2002) points out, the invasion or evolution of deep rooting strategies, in areas where limiting resources are available at depth, is expected to have large impacts on ecosystems and their properties. The results presented in Chapter 4 suggests that an individual-based modelling approach that allows functional diversity to evolve within simulations is a plausible and powerful route to improve our capacity to predict how vegetation may shift as our climate changes. That a better understanding of the current distribution of vegetation can be achieved by considering the depth to which plants can and do root and plant hydraulics. Additionally, consideration of how constraints on plant rooting and plant hydraulics affect spatial and temporal water availability will further improve the accuracy with which we can predict how vegetation will respond to changing climates.

6.1.3 Co-selection and the emergence of ecological strategies

Chapter 4 details the response of emergent trait values to constraints on rooting depth, fire, and precipitation. That is, I showed that evergreenness, the matric potential at 50% loss of conductivity (P_{50}), and phenological triggers change based on the maximum allowed rooting depth, fire and precipitation (Fig. 4.3 & 4.6). Observed plant responses to changes in abiotic conditions generally involve a number of traits with natural selection acting on the individual to produce coordination of traits (Garnier *et al.*, 2015; Díaz *et al.*, 2016). Such coordinated combinations of traits are commonly referred to as "ecological strategies" (Garnier *et al.*, 2015). In Chapter 4 I show that natural selection within the model does indeed lead to coordination of trait values and the emergence of a number of ecological strategies e.g. in south-eastern Brazil the model predicts co-existence of both evergreen and deciduous strategies. In this region evergreen trees are associated with highly negative P_{50} (low SLA and high wood density) values and a rain responsive phenological trigger indicative of a drought tolerating strategy. Likewise, deciduous trees exhibit less negative P_{50} (high SLA and low wood density) and a rain phenological trigger indicative of a strategy which avoids drought. This coordination between three traits was not prescribed but rather emerged from the model dynamic. That natural selection within the model would lead to coordination of multiple traits to produce two of the most commonly observed plant strategies adept to dealing with conditions of water scarcity (Hoffmann *et al.*, 2011; Markesteijn *et al.*, 2011) supports the idea that the set up of the suite of hydraulic traits and trade-offs upon which natural selection acts within the model is appropriate to reproduce observed ecological strategies. Further investigation of emergent ecological strategies at both the site level (Fig. 5.4) and across the entire study region (Fig. 5.7) reveals coordination between further plant traits

and emergent trade-off axes, these axes can be associated with ecological strategies and can be generalised as follows. The first strategy axis (Figs. 5.4 & 5.7) represents deciduous vs. evergreen strategies. Here deciduous strategies tend to exhibit higher SLA (shorter longevity leaves), allocate relatively more to storage and less to roots, leaves, and stems, root to shallower depths, and generally have a phenological trigger which responds to water. Givnish (2002) highlighted that if we are to improve our understanding of the fitness benefit of deciduous vs. evegreen strategies we need to include within our models differential allocation to photosynthetic vs. non photosynthetic tissue, rooting depths and allocation, xylem traits. Doing this within aDGVM2 has shown that, not only does our broad distribution of evergreen and deciduous strategies match observed patterns well but also that many of the traits highlighted by Givnish are indeed important in determining deciduous and evergreen ecological strategies.

The second strategy axis can be viewed to mainly represent variability in slow vs fast growing strategies (Westoby *et al.*, 2002) or similarly the stress tolerant vs. competitive strategies of Grime (1988). Fast growing strategies tend toward higher SLA (less negative P_{50} and lower wood density), higher allocation to leaves and stems, and shallower rooting. Here, fast growth is achieved via increased allocation to stem and leaves, a reduced carbon cost for any stem volume since high SLA is linked to lower wood density and less negative P_{50} values which implies a lower level of drought tolerance but higher water transport efficiency. Tolerant, or slow growing, strategies emerge as having low SLA and thus a high level of drought tolerance, high wood density and root to greater depths. Such slow vs. fast, or tolerant vs. competitor strategies represent further major axes of ecological strategy variation (Westoby *et al.*, 2002).

It has been proposed that ecosystem properties such as productivity, functioning,

stability, resistance and resilience "vary in concert" (Grime & Pierce, 2012) with variation in ecological strategies and their associated trait suites and thus such trait-suites which compose ecological strategies are of critical importance for both plant fitness and ecosystem function and integrity (Grime & Pierce, 2012). Indeed, the linkages between biodiversity and ecosystem services have broad global consequences for human well-being (Perrings *et al.*, 2011).

6.1.4 Ecological strategy diversity moderates the productivity, stability, and resistance of the Amazon

I explore this proposition in Chapter 5 whereby I examine potential interactions between plant functional trait diversity, changes in precipitation regime, CO_2 concentration, and drought in the Amazon basin. Climate change is predicted to increase the frequency and intensity of drought across much of Amazonia (Magrin *et al.*, 2014), widespread forest mortality is expected (McDowell & Allen, 2015). Studies exploring how the vulnerability of plants to drought is mediated by traits and trait strategies are providing us with crucial new insights (Skelton *et al.*, 2015). Xylem cavitation resistance has been shown to be a central trait involved in plant hydraulic strategies (Larter *et al.*, 2017; Brodribb, 2017). Worryingly however, many DGVMs cannot yet simulate plant response to drought accurately (Galbraith *et al.*, 2010; Powell *et al.*, 2013; McDowell *et al.*, 2013*b*) possibly owing to the simplified representation of water stress commonly used (Powell *et al.*, 2013). I worry greatly about the future, my feeling is that globally, "the" most catastrophic effect that climate change will have on terrestrial vegetation is to increase water stress. Yet vegetation models and the land surface schemes in Earth system models do not appear capable of matching observed responses of

vegetation to water stress. I wonder to what extent climate change predictions would differ from current predictions if vegetation responded to changes in water availability to a similar extent to observed responses?

To examine whether aDGVM2, with its improved representation of plant hydraulics and soil hydrology, can mimic observed tropical forest drought responses we set up a model experiment that mimics the through-fall exclusion experiments run at Tapajos (TNF) (Brando *et al.*, 2008) and Caxiuana (CAX) (da Costa *et al.*, 2010) national forest sites. These simulations revealed that the model was able to reproduce both the level of biomass loss and the rate of biomass loss well at both experimental sites (Fig. 5.1 A, B). I further investigated whether diversity affects biomass response to drought by conducting simulations initialised with different numbers of species.

Empirical work has shown that higher diversity can increase resilience to drought (Tilman *et al.*, 2006) as well as biomass stored (Tilman *et al.*, 1997) in grassland experiments, my results echo these findings for tropical forest whereby sites with lower species richness exhibited more dramatic reductions of biomass following drought (Fig. 5.1 C) and lower pre drought biomass (Fig. 5.1 D). At higher levels of species richness drought induced biomass loss was remarkably similar (Fig. 5.1 C) potentially indicative of a resilience tipping point, i.e. a level of species richness below which resilience to drought is reduced non-linearly (Willis *et al.*, 2018). Higher diversity sites also exhibited higher temporal stability in transpiration (Fig. 5.2 D).

Species in our simulations were all functionally unique. Examining the components of functional diversity for our simulations revealed that, while functional richness is relatively similar across species richness levels, functional evenness

increases with species richness (Fig. 5.2 A, B). High functional evenness implies a more even distribution of the density with which trait-space is occupied (Villéger *et al.*, 2008), increased niche differentiation (Kraft *et al.*, 2008), and potentially a more complete utilisation of resources which can increase productivity (Mason *et al.*, 2005). Indeed, our simulations reveal that sites with higher pre drought species richness transpired higher amounts of water (Fig. 5.3 A). Further, as highlighted in the previous section, Fig. 5.4 demonstrates a high level of ecological strategy differentiation with strategies separating across multiple traits. This differentiation results in niche differentiation, e.g. evergreen drought tolerant and deciduous drought avoiding strategies separating out into different rooting niches. Additionally, Fig. 5.4 also highlights how the density with which trait-space is filled at low species richness and high species richness. In high species richness simulations, the density in trait-space of a number of plant ecological strategies increases, i.e. there is a more even distribution of density across ecological strategy space. Thus, the exploration of diversity relationships revealed that the functional trait composition of high species richness communities differs to that of low species richness communities in our simulations, i.e. while the community possesses an almost identical distribution of trait ranges, the relative abundance of trait-combinations changes considerably.

To explore the potential effect of diversity on forest response to climate change I simulated future scenarios of vegetation development under the IPCC's RCP scenarios (Meinshausen et al., 2011) using climate forcing from scenarios RCP 4.5 and 8.5 both with and without a CO_2 impact on plants to explore uncertainty associated with CO_2 fertilisation of plant growth (Körner, 2009; Smith *et al.*, 2016).

In simulations where both CO_2 and climate varied, biomass increased by ca. 10-15% by 2100 (Fig. 5.5 A, B, C). However, in simulations where only climate forcing was applied, there was a reduction in total biomass stored, ca. 18% with RCP 4.5 and ca. 38% with RCP 8.5 (Fig. 5.5 A, D, E). In the absence of CO_2 fertilised plant growth, forest biomass loss is widespread while savanna biomass increase is negligible (Fig. 5.5 A, D, E). The effect of CO_2 fertilisation of plant growth has previously been shown to mitigate the risk of Amazon forest die-back (Rammig *et al.*, 2010). However, our results reveal that, with an improved representation of the biophysical interactions between CO_2, plant growth and plant responses to changes in water status, even with increasing CO_2 there are large areas of Amazonia where biomass is reduced by up to 40% (Fig. 5.5 A, B, C).

Functional diversity components for these climate change simulations revealed that sites with higher functional diversity show a lower reduction in biomass (Fig. 5.6). Here, in agreement with the drought experiments (Fig. 5.2), we find that increased functional evenness and decreased functional divergence reduces the reduction in biomass (Fig. 5.6 and Tab. 5.1). However, we only find significant positive diversity effects when CO_2 fertilises plant growth. The absence of CO_2 fertilised plant growth increases the water stress of plants caused by climate change and overrides any diversity bestowed resistance. When plant growth is not fertilised by increasing CO_2 we find that diversity components show non-significant or negative effects with minute effect sizes. Further, across all RCP scenarios, our results show substantial changes in the density with which Amazonian trait-space is filled (Fig. 5.7).

These results suggest that conservation of functional diversity and diversity of ecological strategy is crucial since such diversity can mediate tropical forest stability, productivity and resistance to both drought and climate change. However

we urgently need to improve our understand of how interactions between biochemical (CO_2 and nutrients) and biophysical (precipitation changes and plant water availability) processes affect plant dynamics as these play an overwhelming role in determining the future of these forests.

6.2 Moving beyond now

6.2.1 Moving forward by going backwards - addressing soil-plant-water dynamics

There is an incredibly remarkable convergence in the calculations employed to represent water availability across all vegetation models with which I am familiar (apart from ED2 (Medvigy *et al.*, 2009) and that of Hickler *et al.* (2006)). Sometimes however evolution, even the evolutionary development of vegetation models, converges on an answer that is not as fit as it could be. It is apparent that DGVMs and ESMs do not appropriately represent observed vegetation responses to changes in water availability well (although see ED2 (Medvigy *et al.*, 2009)). This low predictive ability should have led to the "hypothesis" (a model itself or the representation of the interactions between plants, soil and water) being rubbished and replaced with an hypothesis with higher utility. One where simulated and observed responses of plants to changes in water availability match more closely.

The current performance of DGVMs and land surface schemes of ESMs is dependent on historical contingency. That is, features are usually added to a model successively and not frequently removed or reviewed. Models are then re-tuned

once additional features are added in order to appropriately approximate multiple benchmarks. The representation of plant water availability in vegetation models must have one of the initial core features added in the developmental history of any model. The lack of progress with simulated plant responses to changes in water availability is perhaps the result of the aforementioned historical contingency. Re-doing plant-soil-water dynamics, an initial core feature, would also require that all model components which were developed subsequently, which contain components which would be affected by changes in plant-soil-water dynamics, be re-done. This would be a monumentally difficult task. Yet, I believe, this to be "the" most essential work which needs to be carried out and crucially significant in order to improve our ability to predict the future of the Earth system as our climate changes. Indeed, the results presented in Chapter 5 corroborate this contention. While I have shown with much personal excitement the potential for diversity to mediate forest responses to climate change, the effect size of functional evenness is ca. 5-9 times lower than that of changes in precipitation (Tab. 5.1). Further, I demonstrated that diversity increases resilience to drought. Therefore, in order to be able to represent diversity's ability to mitigate drought, one needs to have simulated vegetation which exhibits a drought response in the first place. Thus, I believe wholeheartedly that to make progress in vegetation modelling and Earth system modelling and increase our ability to predict the future requires going back to the start of the model development chain to address deficiencies in plant-soil-water relationships.

6.2.2 The missing part of Grime's triangle - improving the representation of r-selected ecological strategies

Trade-offs between growth allocated to reproduction and allocated to compartments which improve the resource capture potential of plants via reduced competition or increased uptake machinery as well as the timing of such allocation are arguably the most fundamental to the study of life history evolution (Stearns, 1976; Wenk & Falster, 2015). Indeed, Grime's (1988; 2012) competitor vs stress tolerator vs ruderal (C-S-R) scheme highlights three of the key axis of variation in plant ecological strategies. In Chapter 5 and above I have argued that two of these major axes currently emerge from aDGVM2 dynamics, i.e. competitors or fast growing strategies and tolerators or deciduous drought avoiders and evergreen drought tolerant strategies. The ability for ruderal strategies to emerge from within our modelling framework is limited.

While in aDGVM2 we allow that differential allocation to reproduction and variability in seed weight can create a diversity of life-history strategies, we do not yet allow individuals to differentiate in the timing of reproduction. For example, while the amount of growth an individual allocates to reproduction is an adaptive plant trait, the timing of this allocation is not considered, i.e. an individual allocates a fixed amount of growth to reproduction daily irrespective of ontogeny. Modelling not just the amount allocated to reproduction but also allowing that the timing of this allocation depend on ontogenic stage would unlock the ability to allow the emergence of further important life history strategies. Doing so would may allow the emergence of ruderal ecological strategies such as grass strategies with trait defined behaviour which approximates closely that of annual and perennial grasses. Such an implementation may allow selection

for a strategy which delays reproduction until "maturity" in order to improve its chances of gaining a place in the canopy such as a forest tree or escaping fire in the case of a savanna tree. Or, in the case of stand levelling fires, one might expect the emergence of r-selected strategies which complete their life cycle, or at least begin reproduction at a stage which can be readily attained between fires. Indeed, investigating the number of possible ecological strategies which may emerge under differing fire regimes could improve our understanding of successional dynamics within fire prone ecosystems as well as our ability to predict changes in these systems (Bond & Keeley, 2005).

6.2.3 Relative reproductive success, climate change, and ecological success

In the introduction I highlighted the potential drawbacks of assigning a fitness criterion based on biomass production or NPP versus one based on the production of reproductive biomass. The positive effects of biodiversity on the production of biomass (Tilman *et al.*, 1996) have been criticised as potentially representing the sampling effect (Huston, 1997), i.e. sampling a higher number of species from a species pool increases the likelihood of including the most productive species in an experimental plot. To investigate whether such sampling effects could be responsible for the positive relationships we found between diversity and productivity in Chapter 5 I identified the species which produced the highest above ground biomass in mono-culture and examined their performance in terms of both frequency and contribution to total simulated biomass when grown together will all other species. The results showed that the species which

produced the largest amounts of above ground biomass where often driven to extinction when grown together with all other species and that, when present, they existed in low frequency and contributed little to total plot biomass. This finding appears to preclude the sampling effect as the cause of simulated diversity-productivity relationships to an extent. Or, at least leads me to suppose that the most productive species (ecological strategy) in mono-culture are not necessarily the most productive species (ecological strategy) in poly-culture, i.e. the trait-suite which leads to the highest productivity in mono-culture differs to that which leads to the highest productivity in poly-culture. More importantly however this re-highlights the point I made in the introduction, it is relative reproductive success (and chance) which determines which individuals "make it" in a community, this success is not necessarily related to biomass production. Relative reproductive success is however a moving window and the success of an ecological strategy is determined by the relative importance of having traits adept to deal with stress, disturbance, and competition (Grime & Pierce, 2012). Climate change will however alter the current balance between stress, disturbance, and competition and thus re-shuffle selection strength for ecological strategies in novel ways. An interesting avenue for further research would be to investigate the fitness landscape associated with varying levels of stress, disturbance and competition, to identify combinations and strengths which may lead to rapid changes in the fitness landscape, to identify feedbacks and interactions between abiotic changes and the biotic environment, and to isolate combinations and strengths of change which may lead to non-linear changes in selection strength for different ecological strategies.

6.2.4 Re-assembly speed and direction

As our climate changes the selection strength for different ecological strategies will change. Statistical models have predicted large changes in trait values (e.g. reductions in specific leaf area) across Amazonia (Madani *et al.*, 2018) as a result of climate change. However, whether such predicted changes happen at all (Falster & Westoby, 2003) as well the length of time such changes will take will depend on the interplay between trade-offs associated with different ecological strategies, the rates of birth, growth and death of individuals in a forest stand, the presence of particular ecological strategies within a stand (or ability to disperse into it) as well as their relative frequency and relative fitness at various ontogenic stages relative to competitors (Bertrand *et al.*, 2016; Alexander *et al.*, 2018). aDGVM2 represents all of the aforementioned dependencies within the modelling framework, thus a very brave investigator could disentangle the relative importance of all of these various factors in determining the outcome of the process of community assembly or re-assembly under various abiotic conditions. Doing so would allow comparison of their relative importance with current ecological thinking and experimental results. Such comparisons could both highlight areas where our modelling approach is deficient and increase the confidence with which we can make predictions about the future.

Madani et al. (2018) predict an approximate 15-30% change by 2070 in SLA across Amazonia whereas with the simulations presented in Chapter 5 for RCP 4.5 and increasing CO_2, our mean predicted change in SLA between the year 2000 and 2100 with aDGVM2 is ca. 0.23%. This mean change being close to zero is however an artefact of the fact that the areas where precipitation increases are mostly savanna biome states where deciduous and evergreen strategies co-exist. The

combination of increased precipitation and increasing CO_2 pushes these sites towards increased evergreen dominance and lower SLA. In contrast, across large areas of tropical rainforest we predict an approximate increase in SLA of 5-10%. Not only is this percentage change much lower than that of Madani *et al.* (2018), it is (mostly) in the opposite direction and associated with an increase in the abundance of deciduous ecological strategies. Noteworthy is that the reduced SLA prediction of Madani *et al.* (2018) could be seen as an increase in the proportion of forest trees which adopt a stress (drought) tolerant strategy. Essentially we are making the same prediction, an increase in the proportion of ecological strategies which can endure drought stress. While Fauset *et al.* (2012) have shown that prolonged drought in Ghanan tropical forests has resulted in an increases in dominance of deciduous species, time (and data) will ultimately show us which direction climate change will alter the fitness landscape across ecological strategy space in Amazonia. Whether climate change results in increases in drought tolerators which are evergreen or tolerators which are deciduous may potentially have implications for the Earth system dynamics via changes in the magnitude and timing of moisture recycling with the atmosphere, albedo, as well as influencing competitive dynamics via differences in the extent and timing of light competitive interactions within plant communities. Further, while statistical models can make predictions for what a new optimum strategy may be as climate changes these, predicted changes do not account for how successional and demographic processes may result in temporal mismatches between the trait values expressed by communities and the new climate defined "optimum" values. Quantifying the determinants of such mismatches is crucial to understand the impacts of climate change (Bertrand *et al.*, 2016).

6.2.5 De-prioritise plant traits - concentrate on interactions between CO_2 fertilisation of plant growth and water limitation

Finally, as highlighted in Chapter 5, the future biomass storage potential of the Amazon rainforest, and by extension many areas of the world, will be dependent on interactions between biochemical (nutrients) and biophysical (water, temperature) limitations (Krebs, 2014; Smith *et al.*, 2016). Other modelling studies have also shown that whether simulated Amazonian biomass collapses or increases in future change scenarios depends strongly on whether CO_2 fertilisation of plant growth is allowed or not, i.e. whether CO_2 is increased in-line with a particular climate change scenario or held fixed (Cox *et al.*, 2004; Rammig *et al.*, 2010).

Empirical evidence suggests that increased CO_2 can indeed fertilise tree growth (Ainsworth & Long, 2005) yet, satellite derived estimates of CO_2 fertilisation are much lower than those predicted by vegetation models (Smith *et al.*, 2016). Extremely high priority for future empirical, modelling, and particularly experimental research needs to set on elucidating how interactions between biochemical (CO_2 and nutrients) and biophysical (precipitation changes and plant water availability) processes affect plant dynamics. These interactions will play an overwhelming role in determining the future of much of Earth's vegetation.

Appendix A

Appendix A – Biomass, tree height, tree cover and rooting depth plots.

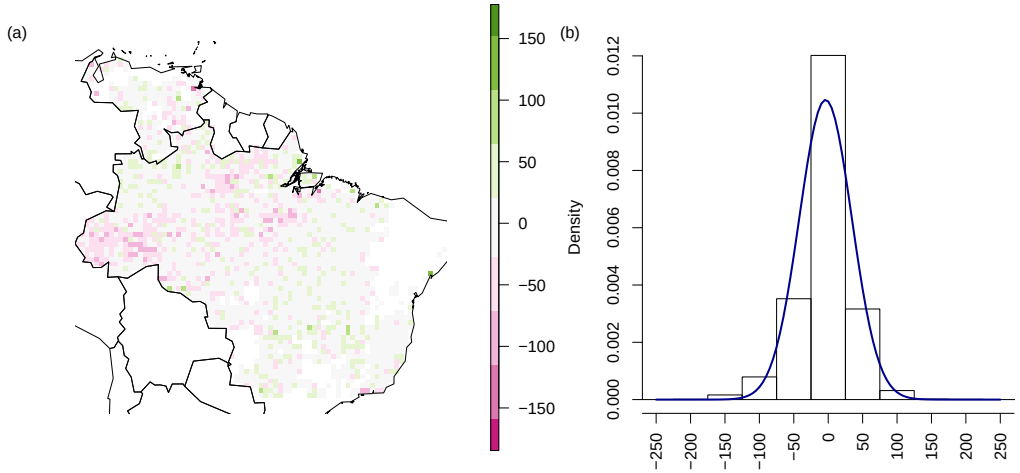

FIGURE A.1: Difference between aDGVM2 soil depth optimised biomass with fire turned on & Baccini *et al.*'s (2012) above ground live biomass (AGLB). (a) Difference in AGLB t Ha^{-1} (b) Histogram of differences with a mean and standard deviation of (-3.86, 38.23).

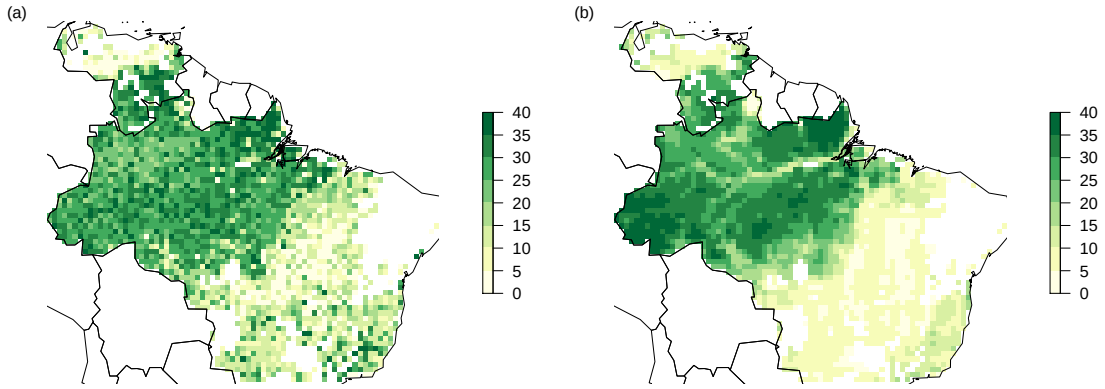

FIGURE A.2: Simulated and satellite derived tree height in meters. (a) aDGVM2 tree height with optimised soil depth and fire turned on, (b) Simard *et al.* (2011) tree height.

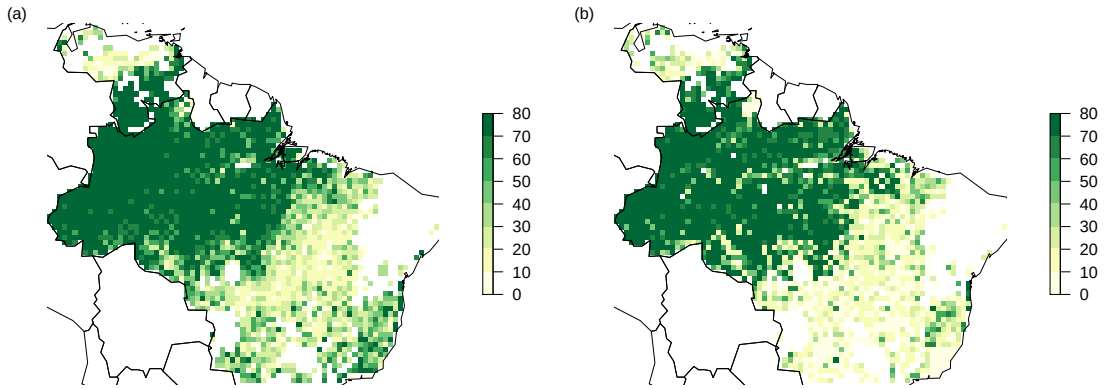

FIGURE A.3: Simulated and satellite derived tree cover percent. (a) aDGVM2 percentage tree cover of trees taller than 5 m with optimised soil depth and fire turned on, (b) MODIS percentage tree cover.

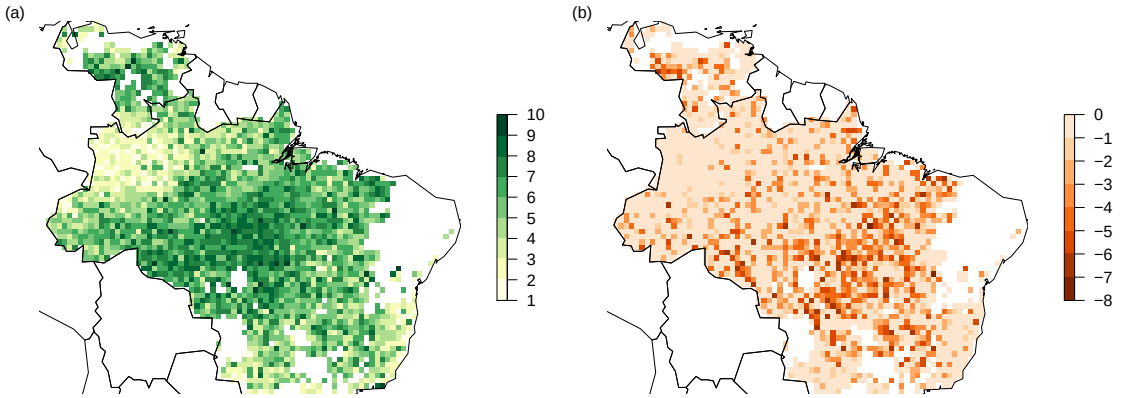

FIGURE A.4: Tree rooting depth in meters. (a) Shown is the emergent average rooting depth of trees in simulations with fire and a fixed soil depth of 10 m, (b) shows the reduction in depth between the biomass optimised soil depth and the average depth to which plants root in (a).

Bibliography

Ackerly, D. D., Schwilk, D. W. & Webb, C. O. 2006 Niche evolution and adaptive radiation: testing the order of trait divergence. *Ecology*, **87**(sp7), S50–S61.

Ainsworth, E. A. & Long, S. P. 2005 What have we learned from 15 years of free-air CO_2 enrichment (FACE)? A meta-analytic review of the responses of photosynthesis, canopy properties and plant production to rising CO_2. *New Phytologist*, **165**(2), 351–372.

Alexander, J. M., Chalmandrier, L., Lenoir, J., Burgess, T. I., Essl, F., Haider, S., Kueffer, C., McDougall, K., Milbau, A., Nuñez, M. A., Pauchard, A., Rabitsch, W., Rew, L. J., Sanders, N. J. & Pellissier, L. 2018 Lags in the response of mountain plant communities to climate change. *Global change biology*, **24**(2), 563–579.

Allen, R. G., Pereira, L. S., Raes, D. & Smith, M. 1998 *Crop evapotranspiration: Guidelines for computing crop water requirements*. Irrigation & Drainage, Paper 56, FAO, Rome, Italy.

Anderegg, W. R. L., Konings, A. G., Trugman, A. T., Yu, K., Bowling, D. R., Gabbitas, R., Karp, D. S., Pacala, S., Sperry, J. S., Sulman, B. N. & Zenes, N. 2018 Hydraulic diversity of forests regulates ecosystem resilience during drought. *Nature*, **561**(7724), 538–541.

Angert, A. L., Huxman, T. E., Chesson, P. & Venable, D. L. 2009 Functional tradeoffs determine species coexistence via the storage effect. *Proceedings of the National Academy of Sciences*, **106**(28), 11641–11645.

Arora, V. K. 2003 Simulating energy and carbon fluxes over winter wheat using coupled land surface and terrestrial ecosystem models. *Agricultural and Forest Meteorology*, **118**, 21–47.

Arora, V. K. & Boer, G. J. 2006 Simulating competition and coexistence between plant functional types in a dynamic vegetation model. *Earth Interactions*, **10**, 179–197.

Baccini, A., Goetz, S. J., Walker, W. S., Laporte, N. T., Sun, M., Sulla-Menashe, D., Hackler, J., Beck, P. S. A., Dubayah, R., Friedl, M. A., Samanta, S. & Houghton, R. A. 2012 Estimated carbon dioxide emissions from tropical deforestation improved by carbon-density maps. *Nature Climate Change*, **2**(3), 182–185.

Ball, J. T., Woodrow, I. E. & Berry, J. A. 1987 Progress in Photosynthesis Research. pp. 221–224. Nijhoff, Dordrecht.

Banin, L., Feldpausch, T. R., Phillips, O. L. *et al.* 2012 What controls tropical forest architecture? Testing environmental, structural and floristic drivers. *Global Ecology and Biogeography*, **21**(12), 1179–1190.

Batjes, N. H. 2009 Harmonized soil profile data for applications at global and continental scales: updates to the WISE database. *Soil Use and Management*, **25**(2), 124–127.

Baudena, M., Dekker, S. C., van Bodegom, P. M., Cuesta, B., Higgins, S. I., Lehsten, V., Reick, C. H., Rietkerk, M., Scheiter, S., Yin, Z., Zavala, M. A. & Brovkin, V. 2015 Forests, savannas, and grasslands: bridging the knowledge

gap between ecology and Dynamic Global Vegetation Models. *Biogeosciences*, **12**(6), 1833–1848.

Bertrand, R., Riofrío-Dillon, G., Lenoir, J., Drapier, J., Ruffray, P. d., Gégout, J.-C. & Loreau, M. 2016 Ecological constraints increase the climatic debt in forests. *Nature Communications*, **7**, 12643.

Bivand, R. & Lewin-Koh, N. 2014 *maptools: Tools for reading and handling spatial objects*. R package version 0.8-30.

Bonan, G. B. 2008 Forests and Climate Change: Forcings, Feedbacks, and the Climate Benefits of Forests. *Science*, **320**(5882), 1444–1449.

Bond, W. J. & Keeley, J. E. 2005 Fire as a global 'herbivore': the ecology and evolution of flammable ecosystems. *Trends in Ecology & Evolution*, **20**(7), 387–394.

Bond, W. J. & Midgley, G. F. 2012 Carbon dioxide and the uneasy interactions of trees and savannah grasses. *Philosophical Transactions of the Royal Society B-Biological Sciences*, **367**(1588), 601–612.

Bond, W. J., Woodward, F. I. & Midgley, G. F. 2005 The global distribution of ecosystems in a world without fire. *New Phytologist*, **165**(2), 525–538.

Bondeau, A., Smith, P. C., Zaehle, S., Schaphoff, S., Lucht, W., Cramer, W., Gerten, D., Lotze-Campen, H., Muller, C., Reichstein, M. & Smith, B. 2007 Modelling the role of agriculture for the 20th century global terrestrial carbon balance RID G-2180-2011 RID B-8221-2008. *Global Change Biology*, **13**(3), 679–706.

Boone, A., Habets, F., Noilhan, J. *et al.* 2004 The Rhône-Aggregation Land Surface Scheme Intercomparison Project: An Overview. *Journal of Climate*, **17**(1), 187–208.

Bowman, D. M. J. S. & Perry, G. L. W. 2017 Soil or fire: what causes treeless sedgelands in Tasmanian wet forests? *Plant and Soil*, pp. 1–18.

Boyce, C. K. & Lee, J.-E. 2010 An exceptional role for flowering plant physiology in the expansion of tropical rainforests and biodiversity. *Proceedings of the Royal Society of London B: Biological Sciences*, p. rspb20100485.

Brando, P. M., Nepstad, D. C., Davidson, E. A., Trumbore, S. E., Ray, D. & Camargo, P. 2008 Drought effects on litterfall, wood production and belowground carbon cycling in an Amazon forest: results of a throughfall reduction experiment. *Philosophical Transactions of the Royal Society of London B: Biological Sciences*, **363**(1498), 1839–1848.

Brodribb, T. J. 2017 Progressing from 'functional' to mechanistic traits. *New Phytologist*, **215**(1), 9–11.

Brovkin, V., Raddatz, T., Reick, C. H., Claussen, M. & Gayler, V. 2009 Global biogeophysical interactions between forest and climate. *Geophysical Research Letters*, **36**(7).

Buis, G. M., Blair, J. M., Burkepile, D. E., Burns, C. E., Chamberlain, A. J., Chapman, P. L., Collins, S. L., Fynn, R. W. S., Govender, N., Kirkman, K. P., Smith, M. D. & Knapp, A. K. 2009 Controls of Aboveground Net Primary Production in Mesic Savanna Grasslands: An Inter-Hemispheric Comparison. *Ecosystems*, **12**(6), 982–995.

Buisson, E., Stradic, S. L., Silveira, F. A. O., Durigan, G., Overbeck, G. E., Fidelis, A., Fernandes, G. W., Bond, W. J., Hermann, J.-M., Mahy, G., Alvarado, S. T., Zaloumis, N. P. & Veldman, J. W. Resilience and restoration of tropical and subtropical grasslands, savannas, and grassy woodlands. *Biological Reviews*, **0**(0).

Buitenwerf, R., Rose, L. & Higgins, S. I. 2015 Three decades of multi-dimensional change in global leaf phenology. *Nature Climate Change*, **5**(4), 364–368.

Bykova, O., Chuine, I., Morin, X. & Higgins, S. I. 2012 Temperature dependence of the reproduction niche and its relevance for plant species distributions. *Journal of Biogeography*, **12**(39), 2191–2200.

Canadell, J., Jackson, R. B., Ehleringer, J. B., Mooney, H. A., Sala, O. E. & Schulze, E.-D. 1996 Maximum rooting depth of vegetation types at the global scale. *Oecologia*, **108**(4), 583–595.

CBD 2006 Global Biodiversity Outlook 2. Tech. rep., Secretariat of the Convention on Biological Diversity, Montreal.

Chapin, F. S. 2002 *Principles of terrestrial ecosystem ecology*. New York ; London: Springer.

Chave, J., Coomes, D., Jansen, S., Lewis, S. L., Swenson, N. G. & Zanne, A. E. 2009 Towards a worldwide wood economics spectrum. *Ecology Letters*, **12**(4), 351–366.

Chesson, P. 2000 Mechanisms of Maintenance of Species Diversity. *Annual Review of Ecology and Systematics*, **31**(1), 343–366.

Clapp, R. B. & Hornberger, G. M. 1978 Empirical equations for some soil hydraulic properties. *Water Resources Research*, **14**(4), 601–604.

Clark, J. S., Bell, D. M., Chu, C., Courbaud, B., Dietze, M. C., Hersh, M. H., HilleRisLambers, J., Ibasez, I., LaDeau, S., McMahon, S. M., Metcalf, J., Mohan, J., Moran, E., Pangle, L., Pearson, S., Salk, C., Shen, Z., Valle, D. & Wyckoff, P. 2010 High-dimensional coexistence based on individual variation: a synthesis of evidence. *Ecological Monographs*, **80**(4), 569–608.

Clark, J. S., Bell, D. M., Hersh, M. H., Kwit, M. C., Moran, E., Salk, C., Stine, A., Valle, D. & Zhu, K. 2011*a* Individual-scale variation, species-scale differences: inference needed to understand diversity. *Ecology Letters*, **14**(12), 1273–1287.

Clark, J. S., Bell, D. M., Hersh, M. H. & Nichols, L. 2011*b* Climate change vulnerability of forest biodiversity: climate and competition tracking of demographic rates. *Global Change Biology*, **17**(5), 1834–1849.

Clark, J. S. & Gelfand, A. E. 2006 A future for models and data in environmental science. *Trends in Ecology & Evolution*, **21**(7), 375–380.

Clark, J. S., LaDeau, S. & Ibanez, I. 2004 Fecundity of trees and the colonization-competition hypothesis. *Ecological Monographs*, **74**(3), 415–442.

Cole, M. M. 1982 The Influence of Soils, Geomorphology and Geology on the Distribution of Plant Communities in Savanna Ecosystems. In *Ecology of Tropical Savannas* (eds B. J. Huntley & B. H. Walker), no. 42 in Ecological Studies, pp. 145–174. Springer Berlin Heidelberg.

Collatz, G., Ribas-Carbo, M. & Berry, J. 1992 Coupled Photosynthesis-Stomatal Conductance Model for Leaves of C_4 Plants. *Functional Plant Biol.*, **19**(5), 519–538.

Collatz, G. J., Ball, J. T., Grivet, C. & Berry, J. A. 1991 Physiological and environmental regulation of stomatal conductance, photosynthesis and transpiration: a model that includes a laminar boundary layer. *Agriculture and Forest Meteorology*, **54**, 107–136.

Cox, P. M. 2001 Description of the TRIFFID dynamic global vegetation model. Technical report Note 24, Bracknell, UK: Hadley Centre.

Cox, P. M., Betts, R. A., Collins, M., Harris, P. P., Huntingford, C. & Jones, C. D. 2004 Amazonian forest dieback under climate-carbon cycle projections for the 21st century. *Theoretical and Applied Climatology*, **78**(1), 137–156.

Cox, P. M., Betts, R. A., Jones, C. D., Spall, S. A. & Totterdell, I. J. 2000 Acceleration of global warming due to carbon-cycle feedbacks in a coupled climate model. *Nature*, **408**(6809), 184–187.

Craine, J. M., Ocheltree, T. W., Nippert, J. B., Towne, E. G., Skibbe, A. M., Kembel, S. W. & Fargione, J. E. 2013 Global diversity of drought tolerance and grassland climate-change resilience. *Nature Climate Change*, **3**(1), 63–67.

Cramer, W., Bondeau, A., Woodward, F. I., Prentice, I. C., Betts, R. A., Brovkin, V., Cox, P. M., Fisher, V., Foley, J. A., Friend, A. D., Kucharik, C., Lomas, M. R., Ramankutty, N., Sitch, S., Smith, B., White, A. & Young-Molling, C. 2001 Global response of terrestrial ecosystem structure and function to CO_2 and climate change: results from six dynamic global vegetation models. *Global Change Biology*, **7**(4), 357–373.

Crisp, M. D., Arroyo, M. T. K., Cook, L. G., Gandolfo, M. A., Jordan, G. J., McGlone, M. S., Weston, P. H., Westoby, M., Wilf, P. & Linder, H. P. 2009 Phylogenetic biome conservatism on a global scale. *Nature*, **458**(7239), 754–756.

da Costa, A. C. L., Galbraith, D., Almeida, S., Portela, B. T. T., da Costa, M., Silva Junior, J. d. A., Braga, A. P., de Gonçalves, P. H. L., de Oliveira, A. A. R., Fisher, R., Phillips, O. L., Metcalfe, D. B., Levy, P. & Meir, P. 2010 Effect of 7 yr of experimental drought on vegetation dynamics and biomass storage of an eastern Amazonian rainforest. *The New phytologist*, **187**(3), 579–591.

Darwin, C. 1972 *The origin of species*. Book, Whole. London: Dent.

DeAngelis, D. L. & Mooij, W. M. 2005 Individual-based modeling of ecological and evolutionary processes. *Annual Review of Ecology Evolution and Systematics*, **36**, 147–168.

Denslow, J. S. 1987 Tropical Rainforest Gaps and Tree Species Diversity. *Annual Review of Ecology and Systematics*, **18**, 431–451.

Diaz, S. & Cabido, M. 1997 Plant functional types and ecosystem function in relation to global change. *Journal of Vegetation Science*, **8**(4), 463–474.

Dwyer, J. & Schmidt, G. 2006 The MODIS Reprojection Tool. In *Earth Science Satellite Remote Sensing: Vol. 2: Data, Computational Processing, and Tools* (eds J. J. Qu, W. Gao, M. Kafatos, R. E. Murphy & V. V. Salomonson), pp. 162–177. Berlin, Heidelberg: Springer Berlin Heidelberg.

Díaz, S., Kattge, J., Cornelissen, J. H. C. *et al.* 2016 The global spectrum of plant form and function. *Nature*, **529**(7585), 167–171.

Ehleringer, J. R., Cerling, T. E. & Helliker, B. R. 1997 C_4 photosynthesis, atmospheric CO_2 and climate. *Oecologia*, **112**(3), 285–299.

Eiten, G. 1972 The cerrado vegetation of Brazil. *The Botanical Review*, **38**(2), 201–341.

Eiten, G. 1982 Brazilian "Savannas". In *Ecology of Tropical Savannas* (eds B. J. Huntley & B. H. Walker), no. 42 in Ecological Studies, pp. 25–47. Springer Berlin Heidelberg.

Elton, C. 1958 *The Ecology of Invasions by Animals and Plants*. University of Chicago Press.

Enquist, B. J. 2002 Universal scaling in tree and vascular plant allometry: Toward a general quantitative theory linking plant form and function from cells

to ecosystems. *Tree Physiology*, **22**(15-16), 1045–1064. 2142.

Falster, D. S., Braennstroem, A., Westoby, M. & Dieckmann, U. 2017 Multitrait successional forest dynamics enable diverse competitive coexistence. *Proceedings of the National Academy of Sciences*, **114**(13), E2719–E2728.

Falster, D. S. & Westoby, M. 2003 Plant height and evolutionary games. *Trends in Ecology & Evolution*, **18**(7), 337–343.

Fan, Y., Li, H. & Miguez-Macho, G. 2013 Global Patterns of Groundwater Table Depth. *Science*, **339**(6122), 940–943.

Farquhar, G. D., Caemmerer, S. V. & Berry, J. A. 1980 A biochemical-model of photosynthetic CO_2 assimilation in leaves of C_3 species. *Planta*, **149**(1), 78–90.

Fauset, S., Baker, T. R., Lewis, S. L., Feldpausch, T. R., Affum-Baffoe, K., Foli, E. G., Hamer, K. C. & Swaine, M. D. 2012 Drought-induced shifts in the floristic and functional composition of tropical forests in Ghana. *Ecology Letters*, **15**(10), 1120–1129.

Finegan, B., Peña-Claros, M., de Oliveira, A., Ascarrunz, N., Bret-Harte, M. S., Carreño-Rocabado, G., Casanoves, F., Díaz, S., Eguiguren Velepucha, P., Fernandez, F., Licona, J. C., Lorenzo, L., Salgado Negret, B., Vaz, M. & Poorter, L. 2015 Does functional trait diversity predict above-ground biomass and productivity of tropical forests? Testing three alternative hypotheses. *Journal of Ecology*, **103**(1), 191–201.

Fisher, R. 1930 *The genetical theory of natural selection*. The Clarendon Press.

Fisher, R., McDowell, N., Purves, D., Moorcroft, P., Sitch, S., Cox, P., Huntingford, C., Meir, P. & Woodward, F. I. 2010 Assessing uncertainties in a second-generation dynamic vegetation model caused by ecological scale limitations.

New Phytologist, **187**(3), 666–681.

Fisher, R. A., Koven, C. D., Anderegg, W. R. L. *et al.* 2018 Vegetation demographics in Earth System Models: A review of progress and priorities. *Global Change Biology*, **24**(1), 35–54.

Fisher, R. A., Williams, M., Da Costa, A. L., Malhi, Y., Da Costa, R. F., Almeida, S. & Meir, P. 2007 The response of an Eastern Amazonian rain forest to drought stress: results and modelling analyses from a throughfall exclusion experiment. *Global Change Biology*, **13**(11), 2361–2378.

Flato, G., Marotzke, J., Abiodun, B., Braconnot, P., Chou, S. C., Collins, W., Cox, P., Driouech, F., Emori, S., Eyring, V. & others 2013 *Evaluation of climate models*. Cambridge University Press.

Freckleton, R. P. & Watkinson, A. R. 2000 On detecting and measuring competition in spatially structured plant communities. *Ecology Letters*, **3**(5), 423–432.

Friedl, M., Sulla-Menashe, D., Tan, B., Schneider, A., Ramankutty, N., Sibley, A. & Huang, X. 2010 *MODIS Collection 5 global land cover: Algorithm refinements and characterization of new datasets, 2001-2012, Collection 5.1 IGBP Land Cover, Boston University, Boston, MA, USA.*

Friedlingstein, P., Joel, G., Field, C. B. & Fung, I. Y. 1999 Toward an allocation scheme for global terrestrial carbon models. *Global Change Biology*, **5**(7), 755–770.

Galbraith, D., Levy, P. E., Sitch, S., Huntingford, C., Cox, P., Williams, M. & Meir, P. 2010 Multiple mechanisms of Amazonian forest biomass losses in three dynamic global vegetation models under climate change. *New Phytologist*, **187**(3), 647–665.

Garnier, E., Navas, M.-L. & Grigulis, K. 2015 *Plant Functional Diversity: Organism traits, community structure, and ecosystem properties*. Oxford, New York: Oxford University Press.

Gignoux, J., Clobert, J. & Menaut, J.-C. 1997 Alternative fire resistance strategies in savanna trees. *Oecologia*, **110**(4), 576–583.

Givnish, T. J. 2002 Adaptive significance of evergreen vs. deciduous leaves: Solving the triple paradox. *Silva Fennica*, **36**(3), 703–743.

Gotzenberger, L., de Bello, F., Brathen, K. A., Davison, J., Dubuis, A., Guisan, A., Leps, J., Lindborg, R., Moora, M., Partel, M., Pellissier, L., Pottier, J., Vittoz, P., Zobel, K. & Zobel, M. 2012 Ecological assembly rules in plant communities-approaches, patterns and prospects. *Biological Reviews*, **87**(1), 111–127.

Grime, J. P., Hodgson, J. G. & Hunt, R. 1988 *Comparative Plant Ecology: A Functional Approach to Common British Species*. Springer Netherlands.

Grime, J. P. & Pierce, S. 2012 *The evolutionary strategies that shape ecosystems*. John Wiley & Sons.

Hartig, F., Dyke, J., Hickler, T., Higgins, S. I., O'Hara, R. B., Scheiter, S. & Huth, A. 2012 Connecting dynamic vegetation models to data – an inverse perspective. *Journal of Biogeography*, **39**(12), 2240–2252.

Hawking, S. 2001 *The universe in a nutshell*. Odile Jacob.

Haxeltine, A. & Prentice, I. C. 1996 BIOME3: An equilibrium terrestrial biosphere model based on ecophysiological constraints, resource availability, and competition among plant functional types. *Global Biogeochemical Cycles*, **10**(4), 693–709.

Hickler, T., Prentice, I. C., Smith, B., Sykes, M. T. & Zaehle, S. 2006 Implementing plant hydraulic architecture within the LPJ Dynamic Global Vegetation Model.

Global Ecology and Biogeography, **15**(6), 567–577.

Hickler, T., Rammig, A. & Werner, C. 2015 Modelling CO_2 Impacts on Forest Productivity. *Current Forestry Reports*, **1**(2), 69–80.

Hickler, T., Smith, B., Sykes, M. T., Davis, M. B., Sugita, S. & Walker, K. 2004 Using a Generalized Vegetation Model to Simulate Vegetation Dynamics in Northeastern Usa. *Ecology*, **85**(2), 519–530.

Hickler, T., Vohland, K., Feehan, J., Miller, P. A., Smith, B., Costa, L., Giesecke, T., Fronzek, S., Carter, T. R., Cramer, W., Kühn, I. & Sykes, M. T. 2012 Projecting the future distribution of European potential natural vegetation zones with a generalized, tree species-based dynamic vegetation model. *Global Ecology And Biogeography*, **21**(1), 50–63.

Higgins, S. I. 2017 Ecosystem Assembly: A Mission for Terrestrial Earth System Science. *Ecosystems*, **20**(1), 69–77.

Higgins, S. I., Bond, W. J., Combrink, H., Craine, J. M., February, E. C., Govender, N., Lannas, K., Moncreiff, G. & Trollope, W. S. W. 2012 Which traits determine shifts in the abundance of tree species in a fire-prone savanna? *Journal of Ecology*, **100**(6), 1400–1410.

Higgins, S. I., Bond, W. J. & Trollope, W. S. W. 2000 Fire, resprouting and variability: a recipe for grass–tree coexistence in savanna. *Journal of Ecology*, **88**(2), 213–229.

Higgins, S. I., Bond, W. J., Trollope, W. S. W. & Williams, R. J. 2008 Physically motivated empirical models for the spread and intensity of grass fires. *International Journal of Wildland Fire*, **17**, 595–601.

Higgins, S. I. & Scheiter, S. 2012 Atmospheric CO_2 forces abrupt vegetation shifts locally, but not globally. *Nature*, **488**(7410), 209–212.

Higgins, S. I., Scheiter, S. & Sankaran, M. 2010 The stability of African savannas: insights from the indirect estimation of the parameters of a dynamic model. *Ecology*, **91**(6), 1682–1692.

Hijmans, R. J. 2014 *raster: raster: Geographic data analysis and modeling*. R package version 2.2-31.

Hirota, M., Holmgren, M., Van Nes, E. H. & Scheffer, M. 2011 Global Resilience of Tropical Forest and Savanna to Critical Transitions. *Science*, **334**(6053), 232 –235.

Hoekstra, H. E., Hoekstra, J. M., Berrigan, D., Vignieri, S. N., Hoang, A., Hill, C. E., Beerli, P. & Kingsolver, J. G. 2001 Strength and tempo of directional selection in the wild. *Proceedings of the National Academy of Sciences*, **98**(16), 9157–9160.

Hoffmann, W. A., Adasme, R., Haridasan, M., T. de Carvalho, M., Geiger, E. L., Pereira, M. A. B., Gotsch, S. G. & Franco, A. C. 2009 Tree topkill, not mortality, governs the dynamics of savanna-forest boundaries under frequent fire in central Brazil. *Ecology*, **90**(5), 1326–1337.

Hoffmann, W. A., Geiger, E. L., Gotsch, S. G., Rossatto, D. R., Silva, L. C. R., Lau, O. L., Haridasan, M. & Franco, A. C. 2012 Ecological thresholds at the savanna-forest boundary: how plant traits, resources and fire govern the distribution of tropical biomes. *Ecology Letters*, **15**(7), 759–768.

Hoffmann, W. A., Marchin, R. M., Abit, P. & Lau, O. L. 2011 Hydraulic failure and tree dieback are associated with high wood density in a temperate forest under

extreme drought. *Global Change Biology*, **17**(8), 2731–2742.

Hooper, D. U., Adair, E. C., Cardinale, B. J., Byrnes, J. E. K., Hungate, B. A., Matulich, K. L., Gonzalez, A., Duffy, J. E., Gamfeldt, L. & O'Connor, M. I. 2012 A global synthesis reveals biodiversity loss as a major driver of ecosystem change. *Nature*, **486**(7401), 105–U129.

Hooper, D. U., Chapin, F. S., Ewel, J. J., Hector, A., Inchausti, P., Lavorel, S., Lawton, J. H., Lodge, D. M., Loreau, M., Naeem, S., Schmid, B., Setälä, H., Symstad, A. J., Vandermeer, J. & Wardle, D. A. 2005 Effects of Biodiversity on Ecosystem Functioning: A Consensus of Current Knowledge. *Ecological Monographs*, **75**(1), 3–35.

Huang, Y., Chen, Y., Castro-Izaguirre, N. *et al.* 2018 Impacts of species richness on productivity in a large-scale subtropical forest experiment. *Science*, **362**(6410), 80–83.

Huntingford, C., Fisher, R. A., Mercado, L., Booth, B. B., Sitch, S., Harris, P. P., Cox, P. M., Jones, C. D., Betts, R. A., Malhi, Y., Harris, G. R., Collins, M. & Moorcroft, P. 2008 Towards quantifying uncertainty in predictions of Amazon 'dieback'. *Philosophical Transactions of the Royal Society B: Biological Sciences*, **363**(1498), 1857–1864.

Huntley, B. J. (ed.) 1982 *Ecology of tropical savannas*, vol. 42 of *Ecological studies*. Berlin [u.a.]: Springer.

Huntley, B. J. & Morris, J. W. 1982 Structure of the Nylsvley Savanna. In *Ecology of Tropical Savannas* (eds B. J. Huntley & B. H. Walker), no. 42 in Ecological Studies, pp. 433–455. Springer Berlin Heidelberg.

Huston, M. & Smith, T. 1987 Plant Succession: Life History and Competition. *The American Naturalist*, **130**(2), 168–198.

Huston, M. A. 1997 Hidden treatments in ecological experiments: re-evaluating the ecosystem function of biodiversity. *Oecologia*, **110**(4), 449–460.

Hutchinson, G. E. 1961 The paradox of the plankton. *American Naturalist*, **95**, 137–145.

Isbell, F., Craven, D., Connolly, J. *et al.* 2015 Biodiversity increases the resistance of ecosystem productivity to climate extremes. *Nature*, **526**(7574), 574–577.

Jones, C. G., Lawton, J. H. & Shachak, M. 1994 Organisms as Ecosystem Engineers. *Oikos*, **69**(3), 373–386.

Jones, H. G. 1992 *Plants and microclimate: a quantitative approach to environmental plant physiology*. 2nd edn. Cambridge University Press.

Kattge, J., Díaz, S., Lavorel, S. *et al.* 2011 TRY – a global database of plant traits. *Global Change Biology*, **17**(9), 2905–2935.

Keddy, P. A. 1992 Assembly and response rules: two goals for predictive community ecology. *Journal of Vegetation Science*, **3**(2), 157–164.

Kleidon, A. & Heimann, M. 1998 A method of determining rooting depth from a terrestrial biosphere model and its impacts on the global water and carbon cycle. *Global Change Biology*, **4**(3), 275–286.

Kleidon, A. & Mooney, H. A. 2000 A global distribution of biodiversity inferred from climatic constraints: results from a process-based modelling study. *Global Change Biology*, **6**(5), 507–523.

Kraft, N. J. B., Valencia, R. & Ackerly, D. D. 2008 Functional Traits and Niche-Based Tree Community Assembly in an Amazonian Forest. *Science*, **322**(5901), 580–582.

Krebs, C. J. 2014 *Ecology : the experimental analysis of distribution and abundance*. Harlow, Essex : Pearson, sixth edition edn.

Kuemmerle, T., Hickler, T., Olofsson, J., Schurgers, G. & Radeloff, V. C. 2012 Reconstructing range dynamics and range fragmentation of European bison for the last 8000 years. *Diversity and Distributions*, **18**(1), 47–59.

Kuparinen, A., Savolainen, O. & Schurr, F. M. 2010 Increased mortality can promote evolutionary adaptation of forest trees to climate change. *Forest Ecology and Management*, **259**(5), 1003 – 1008.

Köppen, W. 1936 *Das geographische System der Klimate*. Allgemeine Klimalehre. Borntraeger.

Körner, C. 2009 Responses of Humid Tropical Trees to Rising CO_2. *Annual Review of Ecology, Evolution, and Systematics*, **40**(1), 61–79.

Körner, C. 2017 A matter of tree longevity. *Science*, **355**(6321), 130–131.

Lacointe, A. 2000 Carbon allocation among tree organs: A review of basic processes and representation in functional-structural tree models. *Annals of Forest Science*, **57**(5), 521–533.

Laliberté, E. & Legendre, P. 2010 A distance-based framework for measuring functional diversity from multiple traits. *Ecology*, **91**, 299–305.

Laliberté, E., Legendre, P. & Shipley, B. 2014 *FD: measuring functional diversity from multiple traits, and other tools for functional ecology*.

Langan, L., Higgins, S. I. & Scheiter, S. 2017 Climate-biomes, pedo-biomes or pyro-biomes: which world view explains the tropical forest–savanna boundary in South America? *Journal of Biogeography*, **44**(10), 2319–2330.

Larcher, W. W. .-M. a. 2003 *Physiological plant ecology : ecophysiology and stress physiology of functional groups*. Berlin: Springer, 4th edn.

Larter, M., Pfautsch, S., Domec, J.-C., Trueba, S., Nagalingum, N. & Delzon, S. 2017 Aridity drove the evolution of extreme embolism resistance and the radiation of conifer genus Callitris. *The New Phytologist*, **215**(1), 97–112.

Lavorel, S., McIntyre, S., Landsberg, J. & Forbes, T. D. A. 1997 Plant functional classifications: from general groups to specific groups based on response to disturbance. *Trends in Ecology & Evolution*, **12**(12), 474 – 478.

Law, R. 1979 Optimal Life Histories Under Age-Specific Predation. *The American Naturalist*, **114**(3), 399–417.

Lehmann, C. E. R., Anderson, T. M., Sankaran, M. *et al.* 2014 Savanna Vegetation-Fire-Climate Relationships Differ Among Continents. *Science*, **343**(6170), 548–552.

Lehmann, C. E. R., Archibald, S. A., Hoffmann, W. A. & Bond, W. J. 2011 Deciphering the distribution of the savanna biome. *New Phytologist*, **191**(1), 197–209.

Linder, H. P., de Klerk, H. M., Born, J., Burgess, N. D., Fjeldsa, J. & Rahbek, C. 2012 The partitioning of Africa: statistically defined biogeographical regions in sub-Saharan Africa. *Journal of Biogeography*, **39**(7), 1189–1205.

Lloyd, J., Domingues, T. F., Schrodt, F. *et al.* 2015 Edaphic, structural and physiological contrasts across Amazon Basin forest-savanna ecotones suggest a role

for potassium as a key modulator of tropical woody vegetation structure and function. *Biogeosciences*, **12**(22), 6529–6571.

Loreau, M., Naeem, S., Inchausti, P., Bengtsson, J., Grime, J. P., Hector, A., Hooper, D. U., Huston, M. A., Raffaelli, D., Schmid, B., Tilman, D. & Wardle, D. A. 2001 Biodiversity and Ecosystem Functioning: Current Knowledge and Future Challenges. *Science*, **294**(5543), 804–808.

Losos, J. B., Leal, M., Glor, R. E., Queiroz, K. d., Hertz, P. E., Schettino, L. R., Lara, A. C., Jackman, T. R. & Larson, A. 2003 Niche lability in the evolution of a Caribbean lizard community. *Nature*, **424**(6948), 542–545.

Macedo, J. & Bryant, R. B. 1987 Morphology, Mineralogy, and Genesis of a Hydrosequence of Oxisols in Brazil. *Soil Science Society of America Journal*, **51**(3), 690–698.

Madani, N., Kimball, J. S., Ballantyne, A. P., Affleck, D. L. R., Bodegom, P. M. v., Reich, P. B., Kattge, J., Sala, A., Nazeri, M., Jones, M. O., Zhao, M. & Running, S. W. 2018 Future global productivity will be affected by plant trait response to climate. *Scientific Reports*, **8**(1), 2870.

Maechler, M., Rousseeuw, P., Struyf, A., Hubert, M. & Hornik, K. 2017 *cluster: Cluster Analysis Basics and Extensions*.

Magrin, G., Marengo, J., Boulanger, J., Buckeridge, M., Castellanos, E., Poveda, G. & others 2014 Central and South America in Climate Change 2014: Impacts, Adaptation, and Vulnerability. *Part B: Regional Aspects. Contribution of Working Group II to the Fifth Assessment Report of the Intergovernmental Panel of Climate Change (eds. Barros, VR et al.)*, pp. 1499–1566.

Markesteijn, L., Poorter, L., Paz, H., Sack, L. & Bongers, F. 2011 Ecological differentiation in xylem cavitation resistance is associated with stem and leaf structural traits. *Plant, Cell & Environment*, **34**(1), 137–148.

Marks, C. O. & Lechowicz, M. J. 2006 A holistic tree seedling model for the investigation of functional trait diversity. *Ecological Modelling*, **193**(3-4), 141–181.

Maréchaux, I. & Chave, J. 2017 An individual-based forest model to jointly simulate carbon and tree diversity in Amazonia: description and applications. *Ecological Monographs*, **87**(4), 632–664.

Mason, N. W. H., Mouillot, D., Lee, W. G. & Wilson, J. B. 2005 Functional richness, functional evenness and functional divergence: the primary components of functional diversity. *Oikos*, **111**(1), 112–118.

May, R. & McLean, A. 2007 *Theoretical Ecology: Principles and Applications*. New York, NY, USA: Oxford University Press, Inc.

May, R. M. 1973 Qualitative Stability in Model Ecosystems. *Ecology*, **54**(3), 638–641.

McCann, K. S. 2000 The diversity–stability debate. *Nature*, **405**(6783), 228–233.

McDowell, N., Pockman, W. T., Allen, C. D., Breshears, D. D., Cobb, N., Kolb, T., Plaut, J., Sperry, J., West, A., Williams, D. G. & Yepez, E. A. 2008 Mechanisms of plant survival and mortality during drought: why do some plants survive while others succumb to drought? *New Phytologist*, **178**(4), 719–739.

McDowell, N. G. & Allen, C. D. 2015 Darcy's law predicts widespread forest mortality under climate warming. *Nature Climate Change*, **5**(7), 669–672.

McDowell, N. G., Fisher, R. A., Xu, C. *et al.* 2013*a* Evaluating theories of drought-induced vegetation mortality using a multimodel–experiment framework. *New*

Phytologist, **200**(2), 304–321.

McDowell, N. G., Ryan, M. G., Zeppel, M. J. B. & Tissue, D. T. 2013*b* Feature: Improving our knowledge of drought-induced forest mortality through experiments, observations, and modeling. *New Phytologist*, **200**(2), 289–293.

Medvigy, D., Wofsy, S. C., Munger, J. W., Hollinger, D. Y. & Moorcroft, P. R. 2009 Mechanistic scaling of ecosystem function and dynamics in space and time: Ecosystem Demography model version 2. *Journal of Geophysical Research: Biogeosciences*, **114**(G1), G01 002.

Meinshausen, M., Smith, S. J., Calvin, K., Daniel, J. S., Kainuma, M. L. T., Lamarque, J.-F., Matsumoto, K., Montzka, S. A., Raper, S. C. B., Riahi, K., Thomson, A., Velders, G. J. M. & Vuuren, D. P. P. v. 2011 The RCP greenhouse gas concentrations and their extensions from 1765 to 2300. *Climatic Change*, **109**(1-2), 213–241.

Meinzer, F. C., Clearwater, M. J. & Goldstein, G. 2001 Water transport in trees: current perspectives, new insights and some controversies. *Environmental and Experimental Botany*, **45**(3), 239–262. 2072.

Midgley, G. F. 2012 Biodiversity and Ecosystem Function. *Science*, **335**(6065), 174–175.

Mokany, K., Raison, R. J. & Prokushkin, A. S. 2006 Critical analysis of root : shoot ratios in terrestrial biomes. *Global Change Biology*, **12**(1), 84–96.

Moncrieff, G. R. 2014 Contemporary and historical drivers of biome boundaries: an intercontinental comparison. PhD Thesis.

Moncrieff, G. R., Bond, W. J. & Higgins, S. I. 2016 Revising the biome concept for understanding and predicting global change impacts. *Journal of Biogeography*,

43(5), 863–873.

Moncrieff, G. R., Hickler, T. & Higgins, S. I. 2014*a* Intercontinental divergence in the climate envelope of major plant biomes. *Global Ecology and Biogeography*, pp. 324–334.

Moncrieff, G. R., Scheiter, S., Bond, W. J. & Higgins, S. I. 2014*b* Increasing atmospheric CO_2 overrides the historical legacy of multiple stable biome states in Africa. *New Phytologist*, **201**(3), 908–915.

Mullen, K., Ardia, D., Gil, D., Windover, D. & Cline, J. 2009 *DEoptim: An R Package for Global Optimization by Differential Evolution. URL http://ssrn.com/abstract=1526466*.

Myers, N., Mittermeier, R. A., Mittermeier, C. G., da Fonseca, G. A. B. & Kent, J. 2000 Biodiversity hotspots for conservation priorities. *Nature*, **403**(6772), 853–858.

Nachtergaele, F., van Velthuizen, H., Verelst, L. & Wiberg, D. 2012 Harmonised World Soil Database version 1.2, FAO, Rome and IIASA, Laxenburg, Austria.

Nepstad, D. C., de Carvalho, C. R., Davidson, E. A., Jipp, P. H., Lefebvre, P. A., Negreiros, G. H., da Silva, E. D., Stone, T. A., Trumbore, S. E. & Vieira, S. 1994 The role of deep roots in the hydrological and carbon cycles of Amazonian forests and pastures. *Nature*, **372**(6507), 666–669.

Nepstad, D. C., Tohver, I. M., Ray, D., Moutinho, P. & Cardinot, G. 2007 Mortality of large trees and lianas following experimental drought in an amazon forest. *Ecology*, **88**(9), 2259–2269.

New, M., Lister, D., Hulme, M. & Makin, I. 2002 A high-resolution data set of surface climate over global land areas. *Climate Research*, **21**(1), 1–25.

Niklas, K. 1994 *Plant Allometry: The Scaling of Form and Process*. Women in Culture and Society. University of Chicago Press.

Niklas, K. J. & Spatz, H.-C. 2010 Worldwide correlations of mechanical properties and green wood density. *American Journal of Botany*, **97**(10), 1587–1594.

Norberg, J., Swaney, D. P., Dushoff, J., Lin, J., Casagrandi, R. & Levin, S. A. 2001 Phenotypic diversity and ecosystem functioning in changing environments: A theoretical framework. *Proceedings of the National Academy of Sciences of the United States of America*, **98**(20), 11376–11381.

Odum, E. P. 1953 *Fundamentals of Ecology*. Saunders.

Ohlson, M., Brown, K. J., Birks, H. J. B., Grytnes, J.-A., Hörnberg, G., Niklasson, M., Seppä, H. & Bradshaw, R. H. W. 2011 Invasion of Norway spruce diversifies the fire regime in boreal European forests: Spruce invasion alters the fire regime. *Journal of Ecology*, pp. 395–403.

Oliveras, I. & Malhi, Y. 2016 Many shades of green: the dynamic tropical forest–savannah transition zones. *Phil. Trans. R. Soc. B*, **371**(1703), 20150308.

Olson, D. M., Dinerstein, E., Wikramanayake, E. D., Burgess, N. D., Powell, G. V. N., Underwood, E. C., D'amico, J. A., Itoua, I., Strand, H. E., Morrison, J. C., Loucks, C. J., Allnutt, T. F., Ricketts, T. H., Kura, Y., Lamoreux, J. F., Wettengel, W. W., Hedao, P. & Kassem, K. R. 2001 Terrestrial Ecoregions of the World: A New Map of Life on Earth A new global map of terrestrial ecoregions provides an innovative tool for conserving biodiversity. *BioScience*, **51**(11), 933–938.

Ostle, N. J., Smith, P., Fisher, R., Ian Woodward, F., Fisher, J. B., Smith, J. U., Galbraith, D., Levy, P., Meir, P., McNamara, N. P. & Bardgett, R. D. 2009 Integrating

plant–soil interactions into global carbon cycle models. *Journal of Ecology*, **97**(5), 851–863.

Pan, Y., Birdsey, R. A., Fang, J., Houghton, R., Kauppi, P. E., Kurz, W. A., Phillips, O. L., Shvidenko, A., Lewis, S. L., Canadell, J. G., Ciais, P., Jackson, R. B., Pacala, S. W., McGuire, A. D., Piao, S., Rautiainen, A., Sitch, S. & Hayes, D. 2011 A Large and Persistent Carbon Sink in the World's Forests. *Science*, **333**(6045), 988–993.

Pausas, J. G., Bradstock, R. A., Keith, D. A. & Keeley, J. E. 2004 Plant functional traits in relation to fire in crown-fire ecosystems. *Ecology*, **85**(4), 1085–1100.

Pausas, J. G. & Verdú, M. 2008 Fire reduces morphospace occupation in plant communities. *Ecology*, **89**(8), 2181–2186.

Pavlick, R., Drewry, D. T., Bohn, K., Reu, B. & Kleidon, A. 2013 The Jena Diversity-Dynamic Global Vegetation Model (JeDi-DGVM): a diverse approach to representing terrestrial biogeography and biogeochemistry based on plant functional trade-offs. *Biogeosciences*, **10**(6), 4137–4177.

Pearson, T. R. H., Burslem, D. F. R. P., Mullins, C. E. & Dalling, J. W. 2002 Germination Ecology of Neotropical Pioneers: Interacting Effects of Environmental Conditions and Seed Size. *Ecology*, **83**(10), 2798–2807.

Peel, M. C., Finlayson, B. L. & McMahon, T. A. 2007 Updated world map of the Köppen-Geiger climate classification. *Hydrology and Earth System Sciences*, **11**(5), 1633–1644.

Perrings, C., Duraiappah, A., Larigauderie, A. & Mooney, H. 2011 The Biodiversity and Ecosystem Services Science-Policy Interface. *Science*, **331**(6021), 1139–1140.

Poorter, L., van der Sande, M. T., Thompson, J. *et al.* 2015 Diversity enhances carbon storage in tropical forests. *Global Ecology and Biogeography*, **24**(11), 1314–1328.

Poulter, B., Hattermann, F., Hawkins, E., Zaehle, S., Sitch, S., Restrepo-Coupe, N., Heyder, U. & Cramer, W. 2010 Robust dynamics of Amazon dieback to climate change with perturbed ecosystem model parameters. *Global Change Biology*, **16**(9), 2476–2495.

Powell, T. L., Galbraith, D. R., Christoffersen, B. O., Harper, A., Imbuzeiro, H. M. A., Rowland, L., Almeida, S., Brando, P. M., da Costa, A. C. L., Costa, M. H., Levine, N. M., Malhi, Y., Saleska, S. R., Sotta, E., Williams, M., Meir, P. & Moorcroft, P. R. 2013 Confronting model predictions of carbon fluxes with measurements of Amazon forests subjected to experimental drought. *New Phytologist*, **200**(2), 350–365.

Prentice, I. C., Bondeau, A., Cramer, W., Harrison, S. P., Hickler, T., Lucht, W., Sitch, S., Smith, B. & Sykes, M. T. 2007 Dynamic Global Vegetation Modeling: Quantifying Terrestrial Ecosystem Responses to Large-Scale Environmental Change. In *Terrestrial Ecosystems in a Changing World* (eds J. G. Canadell, D. E. Pataki & L. F. Pitelka), Global Change — The IGBP Series, pp. 175–192. Springer Berlin Heidelberg.

Prentice, I. C., Harrison, S. P. & Bartlein, P. J. 2011 Global vegetation and terrestrial carbon cycle changes after the last ice age. *New Phytologist*, **189**(4), 988–998.

Price, K. V., Storn, R. M. & A, L. J. 2005 *Differential Evolution - A Practical Approach to Global Optimization*. Springer-Verlag.

Quesada, C. A., Phillips, O. L., Schwarz, M. *et al.* 2012 Basin-wide variations in Amazon forest structure and function are mediated by both soils and climate.

Biogeosciences, **9**(6), 2203–2246.

Quillet, A., Peng, C. & Garneau, M. 2010 Toward dynamic global vegetation models for simulating vegetation–climate interactions and feedbacks: recent developments, limitations, and future challenges. *Environmental Reviews*, **18**, 333–353.

R Core Team 2014 *R: A Language and Environment for Statistical Computing*. Vienna, Austria: R Foundation for Statistical Computing.

R Core Team 2017 *R: A Language and Environment for Statistical Computing*. Vienna, Austria: R Foundation for Statistical Computing.

R Development Core Team 2008 *R: A Language and Environment for Statistical Computing*. Vienna, Austria: R Foundation for Statistical Computing. ISBN 3-900051-07-0.

Raddatz, T. J., Reick, C. H., Knorr, W., Kattge, J., Roeckner, E., Schnur, R., Schnitzler, K. G., Wetzel, P. & Jungclaus, J. 2007 Will the tropical land biosphere dominate the climate-carbon cycle feedback during the twenty-first century? *Climate Dynamics*, **29**(6), 565–574.

Rammig, A., Jupp, T., Thonicke, K., Tietjen, B., Heinke, J., Ostberg, S., Lucht, W., Cramer, W. & Cox, P. 2010 Estimating the risk of Amazonian forest dieback. *New Phytologist*, **187**(3), 694–706.

Rawls, W. J., Brakensiek, D. L. & Saxtonn, K. E. 1982 Estimation of Soil Water Properties. *Transactions of the ASAE*, **25**(5), 1316–1320.

Reich, P. B., Walters, M. B. & Ellsworth, D. S. 1997 From tropics to tundra: Global convergence in plant functioning. *Proceedings of the National Academy of Sciences*, **94**(25), 13730–13734.

Reu, B., Proulx, R., Bohn, K., Dyke, J. G., Kleidon, A., Pavlick, R. & Schmidtlein, S. 2011 The role of climate and plant functional trade-offs in shaping global biome and biodiversity patterns: Climate, biome and biodiversity patterns. *Global Ecology and Biogeography*, **20**(4), 570–581.

Sakschewski, B., Bloh, W. v., Boit, A., Poorter, L., Peña-Claros, M., Heinke, J., Joshi, J. & Thonicke, K. 2016 Resilience of Amazon forests emerges from plant trait diversity. *Nature Climate Change*, **6**(11), nclimate3109.

Sakschewski, B., von Bloh, W., Boit, A., Rammig, A., Kattge, J., Poorter, L., Peñuelas, J. & Thonicke, K. 2015 Leaf and stem economics spectra drive diversity of functional plant traits in a dynamic global vegetation model. *Global Change Biology*, pp. n/a–n/a.

Saxton, K. E. & Rawls, W. J. 2006 Soil Water Characteristic Estimates by Texture and Organic Matter for Hydrologic Solutions. *Soil Science Society of America Journal*, **70**(5).

Scheiter, S. & Higgins, S. I. 2007 Partitioning of root and shoot competition and the stability of savannas. *American Naturalist*, **170**(4), 587–601.

Scheiter, S. & Higgins, S. I. 2009 Impacts of climate change on the vegetation of Africa: an adaptive dynamic vegetation modelling approach. *Global Change Biology*, **15**(9), 2224–2246.

Scheiter, S. & Higgins, S. I. 2012 How many elephants can you fit into a conservation area. *Conservation Letters*, **5**(3), 176–185.

Scheiter, S., Higgins, S. I., Osborne, C. P., Bradshaw, C., Lunt, D., Ripley, B. S., Taylor, L. L. & Beerling, D. J. 2012 Fire and fire-adapted vegetation promoted C_4 expansion in the late Miocene. *New Phytologist*, **195**(3), 653–666.

Scheiter, S., Langan, L. & Higgins, S. I. 2013 Next-generation dynamic global vegetation models: learning from community ecology. *New Phytologist*, **198**(3), 957–969.

Schenk, H. J. & Jackson, R. B. 2002*a* The global biogeography of roots. *Ecological Monographs*, **72**(3), 311–328. 2119.

Schenk, H. J. & Jackson, R. B. 2002*b* Rooting depths, lateral root spreads and below-ground/above-ground allometries of plants in water-limited ecosystems. *Journal of Ecology*, **90**(3), 480–494.

Shinozaki, K., Yoda, K., Hozumi, K. & Kira, T. 1964 A quantitative analysis of plant form;the pipe model theory,1. *Japanese Journal of Ecology*, **14**(3), 97–105.

Shipley, B. 2010 *From plant traits to vegetation structure: chance and selection in the assembly of ecological communities*. Cambridge University Press.

Shipley, B., Lechowicz, M., Wright, I. & Reich, P. 2006 Fundamental trade-offs generating the worldwide leaf economics spectrum. *Ecology*, **87**, 535–541.

Silvertown, J., McConway, K., Gowing, D., Dodd, M., Fay, M. F., Joseph, J. A. & Dolphin, K. 2006 Absence of phylogenetic signal in the niche structure of meadow plant communities. *Proceedings of the Royal Society of London B: Biological Sciences*, **273**(1582), 39–44.

Simard, M., Pinto, N., Fisher, J. B. & Baccini, A. 2011 Mapping forest canopy height globally with spaceborne lidar. *Journal of Geophysical Research: Biogeosciences*, **116**(G4).

Simon, M. F., Grether, R., de Queiroz, L. P., Skema, C., Pennington, R. T. & Hughes, C. E. 2009 Recent assembly of the Cerrado, a neotropical plant diversity hotspot, by in situ evolution of adaptations to fire. *Proceedings of the*

National Academy of Sciences of the United States of America, **106**(48), 20359–20364.

Sitch, S., Huntingford, C., Gedney, N., Levy, P. E., Lomas, M., Piao, S. L., Betts, R., Ciais, P., Cox, P., Friedlingstein, P., Jones, C. D., Prentice, I. C. & Woodward, F. I. 2008 Evaluation of the terrestrial carbon cycle, future plant geography and climate-carbon cycle feedbacks using five Dynamic Global Vegetation Models (DGVMs). *Global Change Biology*, **14**(9), 2015–2039.

Sitch, S., Smith, B., Prentice, I. C., Arneth, A., Bondeau, A., Cramer, W., Kaplan, J. O., Levis, S., Lucht, W., Sykes, M. T., Thonicke, K. & Venevsky, S. 2003 Evaluation of ecosystem dynamics, plant geography and terrestrial carbon cycling in the LPJ dynamic global vegetation model. *Global Change Biology*, **9**(2), 161–185.

Skelton, R. P., West, A. G. & Dawson, T. E. 2015 Predicting plant vulnerability to drought in biodiverse regions using functional traits. *Proceedings of the National Academy of Sciences of the United States of America*, **112**(18), 5744–5749.

Slingo, J. & Palmer, T. 2011 Uncertainty in weather and climate prediction. *Philosophical transactions. Series A, Mathematical, physical, and engineering sciences*, **369**(1956), 4751–4767.

Smith, B., Prentice, I. C. & Sykes, M. T. 2001 Representation of vegetation dynamics in the modelling of terrestrial ecosystems: comparing two contrasting approaches within European climate space. *Global Ecology and Biogeography*, **10**(6), 621–637.

Smith, W. K., Reed, S. C., Cleveland, C. C., Ballantyne, A. P., Anderegg, W. R. L., Wieder, W. R., Liu, Y. Y. & Running, S. W. 2016 Large divergence of satellite and Earth system model estimates of global terrestrial CO_2 fertilization. *Nature Climate Change*, **6**(3), 306–310.

Sperry, J. S., Adler, F. R., Campbell, G. S. & Comstock, J. P. 1998 Limitation of plant water use by rhizosphere and xylem conductance: results from a model. *Plant, Cell and Environment*, **21**(4), 347–359.

Sperry, J. S. & Love, D. M. 2015 What plant hydraulics can tell us about responses to climate-change droughts. *New Phytologist*, (1), 14–27.

Sperry, J. S., Wang, Y., Wolfe, B. T., Scott, M. D., Anderegg, W. R. L., McDowell, N. & Pockman 2016 Pragmatic hydraulic theory predicts stomatal responses to climatic water deficits. *New Phytologist*, **212**(3), 577–589.

Staver, A. C., Archibald, S. & Levin, S. 2011*a* Tree cover in sub-Saharan Africa: Rainfall and fire constrain forest and savanna as alternative stable states. *Ecology*, **92**(5), 1063–1072.

Staver, A. C., Archibald, S. & Levin, S. A. 2011*b* The Global Extent and Determinants of Savanna and Forest as Alternative Biome States. *Science*, **334**(6053), 230–232.

Stearns, S. & Hoekstra, R. 2000 *Evolution: An Introduction*. Oxford University Press.

Stearns, S. C. 1976 Life-History Tactics: A Review of the Ideas. *The Quarterly Review of Biology*, **51**(1), 3–47.

Storn, R. & Price, K. 1997 Differential evolution - A simple and efficient heuristic for global optimization over continuous spaces. *Journal of Global Optimization*, **11**(4), 341–359.

Strigul, N., Pristinski, D., Purves, D., Dushoff, J. & Pacala, S. 2008 Scaling from Trees to Forests: Tractable Macroscopic Equations for Forest Dynamics. *Ecological Monographs*, **78**, 523–545.

Swenson, N. 2014 *Functional and Phylogenetic Ecology in R*. Use R! New York: Springer-Verlag.

Swenson, N. G. & Weiser, M. D. 2010 Plant geography upon the basis of functional traits: an example from eastern North American trees. *Ecology*, **91**(8), 2234–2241.

ter Steege, H., Pitman, N. C. A., Sabatier, D. *et al.* 2013 Hyperdominance in the Amazonian Tree Flora. *Science*, **342**(6156), 1243092.

ter Steege, H., Sabatier, D., Castellanos, H., Van Andel, T., Duivenvoorden, J., Adalardo De Oliveira, A., Ek, R., Lilwah, R., Maas, P. & Mori, S. 2000 An analysis of the floristic composition and diversity of Amazonian forests including those of the Guiana Shield. *Journal of Tropical Ecology*, **16**(06), 801–828.

Thonicke, K., Spessa, A., Prentice, I. C., Harrison, S. P., Dong, L. & Carmona-Moreno, C. 2010 The influence of vegetation, fire spread and fire behaviour on biomass burning and trace gas emissions: results from a process-based model. *Biogeosciences*, **7**(6), 1991–2011.

Tilman, D. 1988 *Plant Strategies and the Dynamics and Structure of Plant Communities*. Princeton University Press.

Tilman, D., Knops, J., Wedin, D., Reich, P., Ritchie, M. & Siemann, E. 1997 The Influence of Functional Diversity and Composition on Ecosystem Processes. *Science*, **277**(5330), 1300–1302.

Tilman, D. & Pacala, S. 1993 The maintenance of species richness in plant communities. In *Species diversity in ecological communities*. University of Chicago Press.

Tilman, D., Reich, P. B. & Knops, J. M. H. 2006 Biodiversity and ecosystem stability in a decade-long grassland experiment. *Nature*, **441**(7093), 629–632.

Tilman, D., Wedin, D. & Knops, J. 1996 Productivity and sustainability influenced by biodiversity in grassland ecosystems. *Nature*, **379**(6567), 718–720.

Tyree, M. T. 1997 The Cohesion-Tension theory of sap ascent: current controversies. *Journal of Experimental Botany*, **48**(10), 1753–1765.

Valk, A. G. v. d. 1981 Succession in Wetlands: A Gleasonian Approach. *Ecology*, **62**(3), 688–696.

Veenendaal, E. M., Torello-Raventos, M., Feldpausch, T. R. *et al.* 2015 Structural, physiognomic and above-ground biomass variation in savanna–forest transition zones on three continents – how different are co-occurring savanna and forest formations? *Biogeosciences*, **12**(10), 2927–2951.

Verhoef, A. & Egea, G. 2014 Modeling plant transpiration under limited soil water: Comparison of different plant and soil hydraulic parameterizations and preliminary implications for their use in land surface models. *Agricultural and Forest Meteorology*, **191**, 22–32.

Villéger, S., Mason, N. W. H. & Mouillot, D. 2008 New Multidimensional Functional Diversity Indices for a Multifaceted Framework in Functional Ecology. *Ecology*, **89**(8), 2290–2301.

Vincent, T. L. & Brown, J. S. 2005 *Evolutionary game theory, natural selection, and Darwinian dynamics*. Cambridge University Press.

Vu, V. Q. 2011 *ggbiplot: A ggplot2 based biplot*.

Walker, B. H. & Noy-Meir, I. 1982 Aspects of the Stability and Resilience of Savanna Ecosystems. In *Ecology of Tropical Savannas* (eds B. J. Huntley & B. H.

Walker), pp. 556–590. Berlin, Heidelberg: Springer Berlin Heidelberg.

Walter, H. & Breckle, S.-W. 1986 *Ecological Systems of the Geobiosphere*. Berlin, Heidelberg: Springer Berlin Heidelberg.

Warner, R. R. & Chesson, P. L. 1985 Coexistence Mediated by Recruitment Fluctuations: A Field Guide to the Storage Effect. *The American Naturalist*, **125**(6), 769–787.

Webb, C. T., Hoeting, J. A., Ames, G. M., Pyne, M. I. & Poff, N. L. 2010 A structured and dynamic framework to advance traits-based theory and prediction in ecology. *Ecology Letters*, **13**(3), 267–283.

Weiher, E. & Keddy, P. A. 1995*a* The assembly of experimental wetland plant-communities. *OIKOS*, **73**(3), 323–335.

Weiher, E. & Keddy, P. A. 1995*b* The Assembly of Experimental Wetland Plant Communities. *Oikos*, **73**(3), 323–335.

Wenk, E. H. & Falster, D. S. 2015 Quantifying and understanding reproductive allocation schedules in plants. *Ecology and Evolution*, **5**(23), 5521–5538.

Westoby, M., Falster, D. S., Moles, A. T., Vesk, P. A. & Wright, I. J. 2002 Plant ecological strategies: Some leading dimensions of variation between species. *Annual Review of Ecology and Systematics*, **33**, 125–159.

Westoby, M. & Wright, I. J. 2006 Land-plant ecology on the basis of functional traits. *Trends in Ecology & Evolution*, **21**(5), 261–268.

Williams, M., Law, B. E., Anthoni, P. M. & Unsworth, M. H. 2001 Use of a simulation model and ecosystem flux data to examine carbon-water interactions in ponderosa pine. *Tree Physiology*, **21**(5), 287–298.

Willis, K. J., Jeffers, E. S. & Tovar, C. 2018 What makes a terrestrial ecosystem resilient? *Science*, **359**(6379), 988–989.

Wolf, J. B., Frankino, W. A. & Allen, C. 2004 Multivariate phenotypic evolution in developmental hyperspace. In *Phenotypic Integration: Studying the Ecology and Evolution of Complex Phenotypes* (eds M. Pigliucci & K. Preston), pp. 366–389. UK United Kingdom: Oxford University Press.

Woodward, F. I. & Smith, T. M. 1994 Global Photosynthesis and Stomatal Conductance: Modelling the Controls by Soil and Climate. *Advances in Botanical Research*, **20**, 1–41.

Woodward, F. I., Smith, T. M. & Emanuel, W. R. 1995 A global land primary productivity and phytogeography model. *Global Biogeochemical Cycles*, **9**(4), 471–490.

Wright, I. J., Reich, P. B., Westoby, M. *et al.* 2004 The worldwide leaf economics spectrum. *Nature*, **428**(6985), 821–827.

Xu, C., McDowell, N. G., Sevanto, S. & Fisher, R. A. 2013 Our limited ability to predict vegetation dynamics under water stress. *New Phytologist*, **200**(2), 298–300.

Zemp, D. C., Schleussner, C.-F., Barbosa, H. M. J., Hirota, M., Montade, V., Sampaio, G., Staal, A., Wang-Erlandsson, L. & Rammig, A. 2017 Self-amplified Amazon forest loss due to vegetation-atmosphere feedbacks. *Nature Communications*, **8**, 14681.